

Development of novel neurophysiological investigations for age-related muscle weakness

Stuart Maitland

Thesis submitted for the degree of Doctor of Philosophy

January 2022



Clinical and Translational Research Institute
Faculty of Medical Sciences
Translational & Clinical Research Institute
Newcastle University
Newcastle upon Tyne, UK

Supervisors
Prof. Roger Whittaker
Prof. Stuart Baker

For Freya

Acknowledgements

It would not have been possible to complete this thesis without the generous support of NIHR Newcastle Biomedical Research Centre. The funding and training support which they have provided has been invaluable in helping me develop as a clinical researcher.

I'd like to thank my supervisors, Professors Roger Whittaker & Stuart Baker, who have continually provided support to my training, and offering encouragement and patience during the most challenging of circumstances.

A whole host of other people have given their valuable time to help me, and I'd like to thank Dr Richard Dodds for his insights into the utility of grip strength, and Professor Miles Witham for specific guidance on recruitment and trials with older participants.

The investigation into ipsilateral Motor Evoked Potentials only happened thanks to the wizardly technical support of Norman Charlton, who built much of the setup used for participants. I'd also like to extend thanks to Maria Germann for helping train me in using Transcranial Magnetic Stimulation.

The investigation into Micro-EMG would not have been possible without the ongoing support of the RVI Medical Physics team led by Jim Wightman, who have constantly assessed and improved the profile of a new medical device to meet exacting safety standards. Dr Ian Schofield has been a great source of much wisdom and provided useful insights to solve all manners of computing and physics puzzles across these investigations.

Of course, none of this could have happened without the support I've received from all of friends and colleagues at ION. Just to name a few - Matthew, Beshoy, Janire, Rachael.

A particular special thankyou to my family and friends; Dad, Iain, Alison, Chris, Simon, you've all been amazing sources of support.

Amy: you've been my guiding star through the most challenging work of my life, thank you for everything that you've done for me. I don't think any of us could have predicted where we would be at the end of all this!

List of publications 2018-2022

- Waite SJ, **Maitland S**, Thomas A, Yarnall AJ. Sarcopenia and frailty in individuals with dementia: A systematic review. *Archives of Gerontology and Geriatrics* 2021;92:104268. <https://doi.org/10.1016/j.archger.2020.104268>.
- **Maitland S**, McElnay P, Brady R. AI: simply reinforcing medicine's worst biases? *BMJ Innovations* 2020;6. <https://doi.org/10.1136/bmjinnov-2019-000376>
- **Maitland S**, Baker S. Ipsilateral Motor Evoked Potentials as a Measure of the Reticulospinal Tract in Age-Related Strength Changes- *Frontiers Ageing Neuroscience*. 2021. <https://doi.org/10.3389/fnagi.2021.612352>
- Sørensen DM, Bostock H, Ballegaard M, Fuglsang-Frederiksen A, Graffe CC, Grötting A, **Maitland S**, *et al*. Assessing inter-rater reproducibility in MScanFit MUNE in a 6-subject, 12-rater "Round Robin" setup. *Neurophysiologie Clinique* 2021. <https://doi.org/10.1016/j.neucli.2021.11.002>.
- **Maitland S**, Escobedo-Cousin E, Schofield I, O'Neill A, Baker S, Whittaker R. Electrical cross-sectional imaging of human motor units in vivo. *Clinical Neurophysiology* 2022. <https://doi.org/10.1016/j.clinph.2021.12.022>.
- **Maitland S**, Baker M. Serotonin Syndrome. *BMJ Drug & Therapeutics Bulletin*. (in press)
- **Maitland S**, Hall J, McNeill A, Stenberg B, Schofield I, Whittaker RG. Ultrasound-Guided Motor Unit Scanning EMG (UltraMUSE). *Muscle and Nerve*. (in review)

Covid impact statement

COVID significantly disrupted my thesis during the crucial second year where I was hoping to gather much of my data. I was redeployed into a COVID ward locally where I continued my work as an SHO. I was fortunate to be able to conduct one investigation ahead of this in an older cohort (Chapter 3), however I was unable to collect data from older people using either the Micro-EMG device (Chapter 4) or ultrasound (Chapter 5). This is because of restrictions, disruptions to supply chains which affected electrode manufacture, and the reluctance of older people to come into the university or hospital setting to take part. Much of my data is therefore in younger people but remains applicable to a wide range of neuromuscular diseases, including sarcopenia.

Table of Contents

Acknowledgements	3
List of publications 2018-2022.....	4
Covid impact statement	5
List of Figures	9
List of Tables.....	10
1. Introduction to sarcopenia and motor changes in ageing.....	1
1.1 Introduction.....	1
1.2 Pathophysiology of sarcopenia	3
1.2.1 Central & spinal changes.....	3
1.3 Motor Unit Changes	5
1.3.1 The normal motor unit.....	5
1.3.2 Conduction velocity.....	5
1.3.3 Compound Muscle Action Potential (CMAP) studies.....	6
1.3.4 Motor Unit Number Estimation (MUNE).....	7
1.3.5 Motor Unit Number Index (MUNIX).....	8
1.3.6 Decomposition-based Quantitative EMG (DQEMG).....	9
1.4 Neuromuscular junction changes.....	9
1.4.1 Single fibre studies	9
1.4.2 DQEMG in muscle weakness.....	11
1.5 Methods of assessing motor unit internal structure.....	12
1.5.1 Scanning EMG- advantages & limitations	13
1.5.2 Ultrasound in Neurophysiology.....	13
1.6 Summary	14
2. Review of Ipsilateral MEPs (iMEPs) in health and disease	17
2.1 Abstract.....	17
2.2 Introduction.....	18
2.2.1 Proposed routes for iMEPs.....	18
2.3 How to elicit iMEPs in healthy controls.....	20
2.4 Ipsilateral MEPs in neurological disease	23
2.4.1 Persistent Mirror Movement Disorders	23
2.4.2 Stroke	25
2.4.3 Neurodevelopmental changes.....	26
2.4.4 ALS/MND.....	27
2.4.5 Strength	27
2.5 Conclusion & Recommendations	27
2.6 Tables	30
3. Ipsilateral Motor Evoked Potentials as a measure of the reticulospinal tract in age-related strength changes	33
3.1 Abstract.....	33
3.2 Introduction.....	34

3.2.1	Sarcopenia.....	34
3.2.2	The reticulospinal tract.....	35
3.2.3	Ipsilateral Motor Evoked Potentials (iMEPs).....	35
3.3	Methods.....	36
3.3.1	Subjects.....	36
3.3.2	Anthropometry and sarcopenia stratification	37
3.3.3	EMG & TMS Measurements.....	38
3.3.4	Rowing task	39
3.3.5	Data and statistical analysis	41
3.4	Results.....	42
3.4.1	Participant characteristics.....	42
3.4.2	iMEPs	43
3.4.3	Ipsilateral/Contralateral amplitude ratios	46
3.5	Discussion	47
3.5.1	Key findings	47
3.5.2	Potential pathophysiologies	48
3.5.3	Clinical implications	49
3.5.4	Methodological considerations	49
3.5.5	Future research	51
3.5.6	Conclusion.....	51
4.	Electrical cross-sectional imaging of human motor units in vivo	52
4.1	Contribution statement.....	52
4.2	Highlights	52
4.3	Abstract.....	52
4.4	Introduction.....	54
4.5	Methods.....	56
4.5.1	Probe design.....	56
4.5.2	Signal Processing.....	58
4.5.3	Muscle fibre localisation.....	59
4.5.4	Fibre data visualisation	61
4.5.5	Modelling	62
4.5.6	Human recordings	63
4.6	Results.....	64
4.6.1	Single Fibre Localisation.....	64
4.6.2	Dual Fibre resolution.....	64
4.6.3	Multiple fibre localisation.....	65
4.6.4	Experimental results	65
4.7	Discussion	69
4.7.1	Modelling studies	70
4.7.2	Human recordings	70
5.	Ultrasound-Guided Motor Unit Scanning EMG (UltraMUSE)	75
5.1	Highlights.....	75
5.2	Abstract.....	76
5.3	Introduction.....	77
5.4	Methods.....	79
5.4.1	Experimental setup.....	79
5.4.2	Procedure	80
5.4.3	Modelling motor unit dimensions	82

5.5 Results	82
5.5.1 Modelling	82
5.5.2 Practical aspects.....	83
5.5.3 Motor unit parameters.....	84
5.6 Discussion	87
5.7 Supplementary File 1- needle insertion withdrawal.mp4	90
6. General discussion	91
6.1 Overview.....	91
6.2 Summary	91
6.3 Measuring performance.....	93
6.4 Next steps	94
7. References	96

List of Figures

Figure 1.1 Diagnostic flowchart for sarcopenia.	1
Figure 1.2 Recording the median motor response (CMAP)	6
Figure 1.3 Schematic of CMAP generation	7
Figure 1.4 Normal innervation of three motor units and their consequent muscle fibres.	15
Figure 2.1 Example of MEP (left) and iMEP (right) in a healthy subject.	19
Figure 2.2 Possible mechanisms underlying mirrored activity.	24
Figure 2.3 Stylised setup diagram indicating Corticospinal tract (green) and reticulospinal tract (red)28	
Figure 3.1 Full TMS experimental paradigm.	40
Figure 3.2 (A) Scatter of the Ipsilateral-Contralateral Amplitude Ratio (ICAR) changes with age (B) Stacked histograms indicating the age distribution of participants.	43
Figure 3.3 Amplitude Ratio (ICAR) compared to muscularity in different age groups & sarcopenia. ...	46
Figure 3.4 Amplitude ratio (ICAR) compared to standardised grip strength in both age groups.	47
Figure 4.1 Overview of Micro-EMG device.	57
Figure 4.2 Overview of signal analysis pipeline.	58
Figure 4.3 Fibre localisation in space, with x and y axes defined relative to the needle electrode.	59
Figure 4.4 Simulated muscle fibre localisation accuracy across the Micro-EMG array.	64
Figure 4.5 Human recordings from the tibialis anterior muscle.	66
Figure 4.6 Relative fibre position, across all recordings, and all motor units.	67
Figure 5.1 Effect of needle path on estimated motor unit dimensions.	78
Figure 5.2 Ultrasound experimental setup diagram.	80
Figure 5.3 Needle in situ in a motor unit within tibialis anterior.	81
Figure 5.4 Motor unit territory dimensions collected from the literature.	84
Figure 5.5 Example EMG scans from healthy human TA muscle.	85

List of Tables

Table 2.1 Summary of iMEPs in healthy individuals in literature.....	30
Table 3.1 Participant characteristics.. ..	45
Table 4.1 Summary statistics for motor units across five human recordings.	68
Table 5.1 Simulated motor unit diameters measured exhaustively in every orientation	83
Table 5.2 Measured parameters of single motor unit scans.. ..	86

1. Introduction to sarcopenia and motor changes in ageing

1.1 Introduction

Sarcopenia ('poverty of flesh') is a disease representing the progressive degenerative loss of muscle mass and strength associated with ageing. While most adults lose strength with age, sarcopenia represents such a significant failure of muscle function that physical performance is affected. While sarcopenia may be secondary to systemic illness (especially inflammatory or malignant disease) or obesity (sarcopenic obesity), it may also occur without these causes. As part of the frailty syndrome, sarcopenia is a significant obstacle to the independence, quality of life, and longevity of ageing adults, who are more likely to require hospitalisation and additional care (Shafiee *et al.*, 2017; Cruz-Jentoft *et al.*, 2018). Age-related muscle weakness is the leading contributing factor to falls (Rubenstein, 2006), and 1 in 3 people over the age of 65 suffer a fall, with an economic burden to the NHS of £2.3 billion (NHS England, 2019). The main interventions for sarcopenia at present are related to adequate diet and sufficient exercise, including good quality resistance training (Morley, 2018), however ambiguity regarding operational definitions has led to inconclusive results regarding future treatment strategies.

Muscle mass has previously been the primary factor in defining sarcopenia, as it is relatively easy to measure, and clinicians are often able to identify those with subjectively low

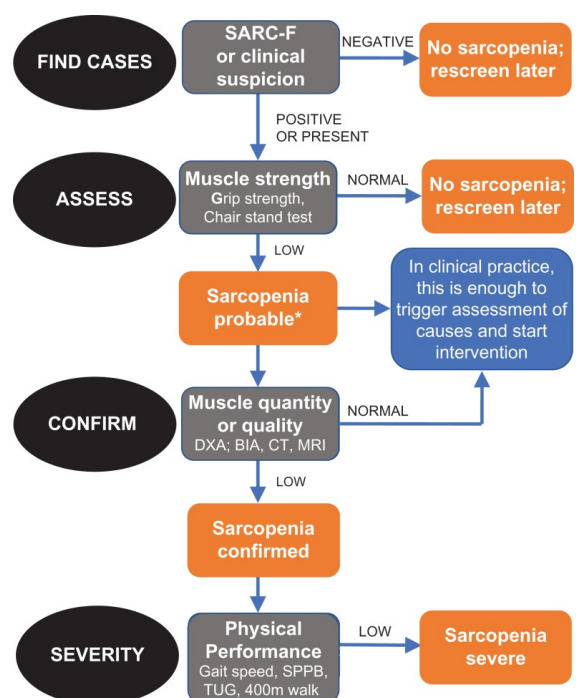


Figure 1.1 Diagnostic flowchart for sarcopenia. Reproduced from Cruz-Jentoft *et al.*, 2018. SARC-F = Sarcopenia symptomatic questionnaire. DXA=Dual energy x-ray absorptiometry. BIA= Bioimpedance analysis. SPPB = Short physical performance battery. TUG = Timed up and go.

muscle mass from a clinical examination. However, muscle mass alone is not sensitive in finding individuals with functional limitation due to sarcopenia (Hughes *et al.*, 2001). The European Working Group on Sarcopenia in Older People (EWGSOP) has therefore recently updated the definition of sarcopenia to place primacy on muscle strength and functional parameters rather than muscle bulk (Cruz-Jentoft *et al.*, 2018) (Figure 1.1); so-called muscle 'quality over quantity', or dynapenia (Clark and Manini, 2008) ('poverty of strength').

Measuring strength requires only a simple, portable, and affordable grip strength meter, but these are not common in the community or on the wards. Grip strength also holds a degree of subjectivity according to effort and fails to account for individual variations, which may affect the lifetime trajectory of strength (Dodds *et al.*, 2014). Questionnaires which assess symptoms of sarcopenia are vital for understanding the personal impact of sarcopenia on the patient but lack sensitivity to myriad other causes of weakness.

There are many current indirect measures of "muscle quality" which assess whole body performance. These include the short physical performance battery (Beaudart *et al.*, 2016) and timed up and go (Podsiadlo and Richardson, 1991). While these are easily deployed in the clinical setting, they are susceptible to limitation by factors external to muscle health, including fatigue and dyspnoea. There is a clear need for a better measure of 'muscle quality' (i.e. the relationship between muscle size and strength) in order to prognose and prevent sarcopenia in ageing adults. Part of this is understanding how the relationship between voluntary contraction and force production goes awry in sarcopenia. These can include factors ranging from central activation to the peripheral production of force.

While neurophysiological investigations are unsuitable for screening on a population level, a potential diagnostic measure must fulfil the core tenets of a clinical test as defined by the UK screening committee (UK Screening Committee, 2003). The criteria especially relevant to investigating sarcopenia include:

1. There should be a simple, safe, precise and validated test.
2. The distribution of test values in the target population should be known and a suitable cut-off level defined and agreed.
3. The test, from sample collection to delivery of results, should be acceptable to the target population.

Clinical neurophysiologists interpret the electrical signals from the nervous system in the context of neurological illness. These specialists have several tools at their disposal to interrogate the nervous system at various levels; broadly, these encompass Electroencephalography (EEG), Electromyography (EMG), Evoked Potentials (EP), and

Transcranial Magnetic Stimulation (TMS). Neurophysiological investigations are already gold-standard for diagnosing a number of neurological conditions and could fulfil these criteria if applied in the correct clinical context. This review provides background and evidence for neurophysiological approaches and their application to sarcopenia.

1.2 Pathophysiology of sarcopenia

The regulation of strength is a complex coordination of cortical, spinal, neuromuscular, and muscular factors. Changes in any part of this motor pathway may contribute to reduced muscle function, and therefore sarcopenia.

Briefly, the prefrontal cortex and basal ganglia networks are involved in motor planning and execution. Corticospinal motoneurons interface monosynaptically from the primary motor cortex to lower motor neurons at the spine. The final common pathway of movement is the motor unit, which innervates muscle tissue, with hundreds or thousands of motor units in each muscle, which enables healthy individuals to make precise and fluid movements.

Sarcopenia could occur as a result of insults at a number of levels in this system which have previously been reviewed (Clark and Manini, 2008), and include:

1. Decreased cortical excitability
2. Decreased spinal excitability
3. Decreased maximal motor unit discharge rate
4. Slowed nerve conduction velocity
5. Alterations in muscle architecture
6. Decreased muscle mass

This section will examine some of these changes and how they might be interrogated using clinical neurophysiological measures.

1.2.1 Central & spinal changes

The central coordination of movement is affected at multiple levels with ageing and has been reviewed previously (Kwon and Yoon, 2017). To summarise, age-related atrophy of the prefrontal cortex and basal ganglia may lead to impaired motor planning and coordination (Seidler *et al.*, 2010), however, sarcopenia is often seen even without any cognitive prefrontal impairment.

Two methods may be used to modulate additional force during volitional movement. Principally, recruitment of additional motor units is used to modulate force, but motor unit firing rate can also be increased to produce additional force.

There is clear evidence that maximal motor unit discharge rates are lower with ageing (Ling *et al.*, 2009). The motor unit firing characteristics also change, as there are fewer instances of doublet discharges (Klass, Baudry and Duchateau, 2008) which are thought to produce increased levels of force, and maintenance of force at high levels (Mrówczyński *et al.*, 2015). Concomitantly, the normally ordered relationship between recruitment and firing rate is disturbed (Erim *et al.*, 1999).

The central activation ratio (CAR) quantifies the proportion of muscle tissue activated via volitional contraction. This is measured by measuring the force at maximum voluntary contraction (MVC), compared to MVC with additional stimulation of peripheral motor nerves.

$$CAR = MVC \text{ force} / (MVC + \text{peripheral stimulation force})$$

Young, healthy people are able to recruit almost all of their muscle tissue, and so CAR approximates 1, whereas older adults exhibit small but significant activation deficits when peripheral stimulation is provided in high-frequency trains of pulses; no such deficit was seen in most studies providing a single pulse of peripheral stimulation (Stevens *et al.*, 2003). This is a clear indication that there is an inability for the older adult to reliably recruit their full range of motor units.

Transcranial Magnetic Stimulation (TMS) painlessly induces current within the brain using an intense transient magnetic field. This is commonly directed to the motor area to induce Motor Evoked Potentials (MEP). This is useful for measuring activation thresholds; however, TMS can activate neurons either directly or trans-synaptically, leading to increased latency variability. Transcranial Electrical Stimulation (TES) can also be used to stimulate the motor cortex with a stable latency; however, this procedure is somewhat painful and not routinely used.

Changes in the spinal cord with ageing are not well characterised in the literature, but reduced MEP amplitude has been demonstrated with age, indicating loss of around 35% of corticomotoneurons (Eisen, Entezari-Taher and Stewart, 1996). In a neurophysiological context, MEP amplitude is highly correlated with force production in corticomotoneuronal diseases, including stroke (Thickbroom *et al.*, 2002), suggesting that sarcopenia represents a similar phenotype. However, TES has not yet been performed to delineate whether these are cortical or motoneuronal losses.

Furthermore, the excitability of efferent corticospinal pathways has been shown to reduce with age, as demonstrated via TMS (Sale and Semmler, 2005). These findings are consistent with anatomical studies whereby motor neurone cell bodies in the lumbosacral

spinal cord of 47 patients of varying ages were counted post-mortem (Tomlinson and Irving, 1977). This demonstrated a stable count up until the age of 60, after which there was a gradual decline, with a profound loss of up to 50% of motor units. A comparable level of denervation to patients with spinal muscular atrophy type 3 (Günther *et al.*, 2019); who are often significantly functionally limited, or in the affected limbs of stroke (Kouzi *et al.*, 2014). The functional status of only some of these individuals was available, however, the authors describe two patients with significantly reduced motor unit counts living entirely independently prior to their deaths. This survival is likely due to the compensatory reinnervation which occurs, which would result in relative preservation of strength (Piasecki *et al.*, 2018).

1.3 Motor Unit Changes

1.3.1 The normal motor unit

The motor unit is the final common pathway of human movement, comprising a single motor neurone and all of the muscle fibres it innervates. A motor unit behaves as a single entity, with all constituent fibres firing together with each activation. Motor units are interdigitated, with as many as ten motor units innervating a single region of muscle in a glycogen depletion experiment in cats (Bodine *et al.*, 1988).

In the healthy motor unit, conduction from motor axon to all of the constituent muscle fibres happens nearly simultaneously and consistently. In neuropathies, motor neurone death is compensated by collateral sprouting of surviving motor neurones to innervate stranded muscle fibres, with imperfect neuromuscular junctions formed.

The motor unit potential (MUP) can be measured by several means. While measures such as motor unit number estimation (MUNE) have helped provide estimates of the loss of motor units, these techniques reveal little information about the internal structure of the motor unit, which may indicate early changes of de/reinnervation crucial in prognosticating neuromuscular disease. Alternative techniques including macro, multielectrode and scanning EMG all aim to produce a measure of the whole motor unit.

1.3.2 Conduction velocity

Nerve conduction studies use surface electrodes to stimulate peripheral nerves and measure response. There is a conduction latency between stimulation and response, and by stimulating at multiple points, these can be used to calculate conduction velocity between the two measured points.

The conduction velocity of electrical activity from the spinal cord through peripheral nerves reduces with age (Campbell, McComas and Petito, 1973; Palve and Palve, 2018), albeit remaining above pathological latencies (Mayer, 1963). This is thought to be due to demyelination and loss of larger axonal fibres. While total force should be mostly preserved, this process reduces the level of torque an individual can produce by limiting the ability to recruit larger motor units early in a contraction (Metter *et al.*, 1998).

1.3.3 Compound Muscle Action Potential (CMAP) studies

Surface EMG (sEMG) involves recording the cumulative motor unit activity near an electrode attached to the skin surface (Figure 1.2). Many factors can affect the reliability of

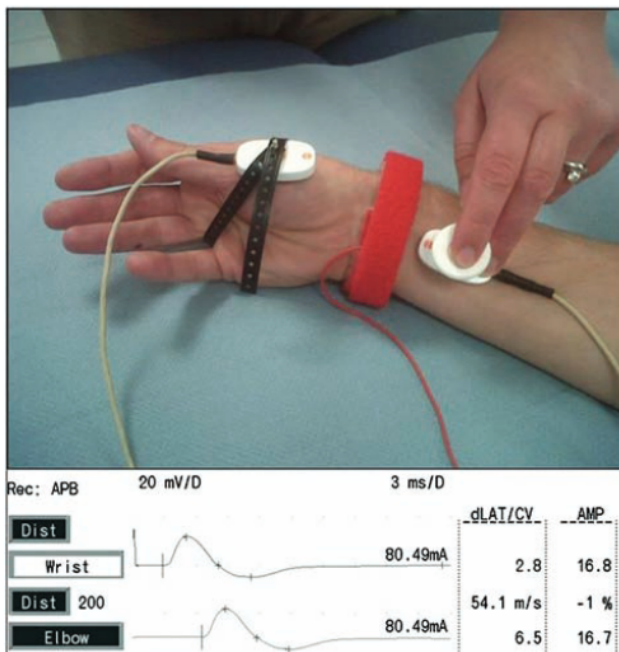


Figure 1.2 Recording the median motor response (CMAP). The nerve is being stimulated at the wrist, and the response is measured over abductor pollicis brevis. The lower traces are the resulting compound muscle action potential recorded at the wrist (top) and at the elbow (bottom). Reproduced from Whittaker 2011

this method, including crosstalk between neighbouring muscles, electrode placement position, and levels of adipose tissue between muscle and skin. The Compound Muscle Action Potential (CMAP) represents the summation of the motor action potentials within 2cm of the active electrode (Kimura, 2013) with peripheral stimulation.

CMAP is traditionally considered a proxy for denervation in processes such as ALS, however its limitation is twofold. Firstly, the CMAP amplitude may be maintained due to collateral reinnervation, but on the other hand, loss of CMAP amplitude could also reflect failure of action potential propagation along motor neurone fibres, failure of transmission at the

neuromuscular junction or primary muscle disease. Further limitations of CMAP render it inappropriate for sarcopenia in its traditional form. This is because the number of activated muscle fibres may have a significant bearing on CMAP amplitude, but equally important is the fibre density, size of muscle fibres, and action potential synchronicity. The aforementioned asynchronous nature of sarcopenic action potentials and infiltration of intramuscular fat and connective tissue may attenuate surface EMG, underestimating muscle activation (Figure 1.3) (M Piasecki *et al.*, 2016).

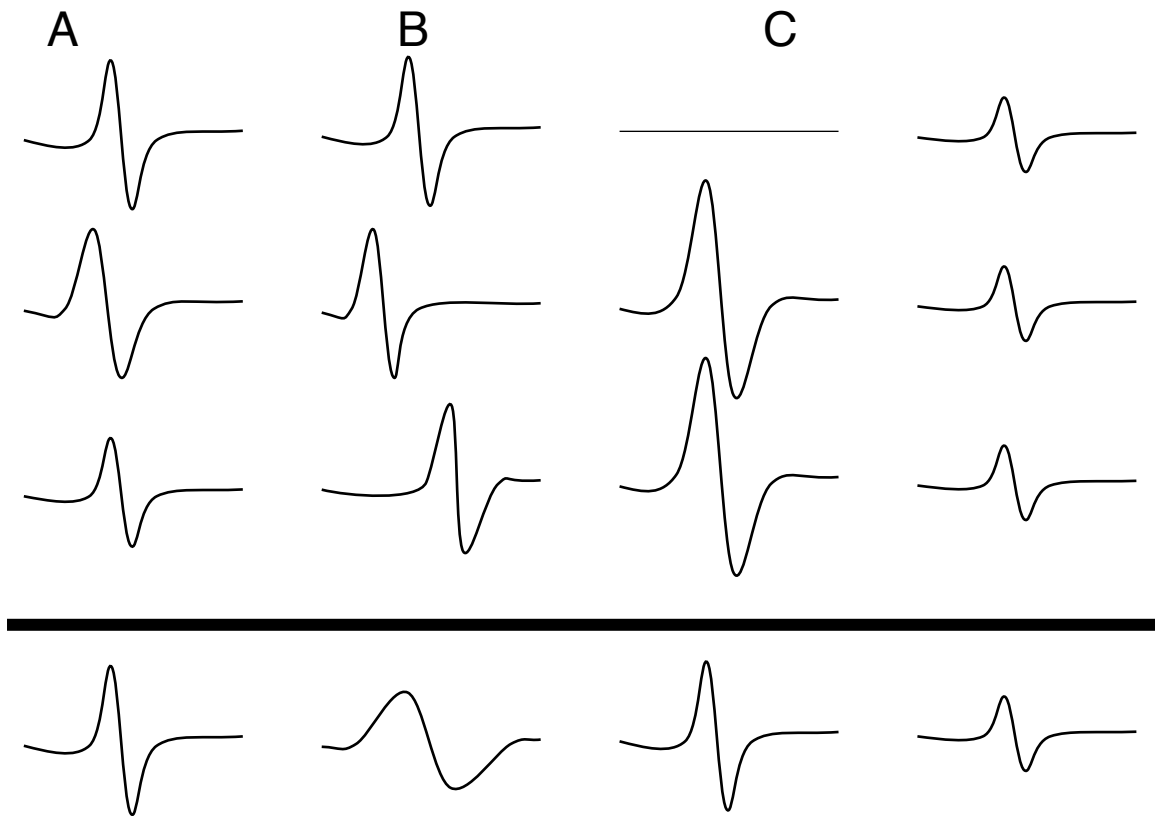


Figure 1.3 Schematic of CMAP generation, consisting of 3 Single Motor Unit Potentials (SMUPs), top, and the resulting CMAP, bottom

- A) Normal CMAP
- B) Desynchronization of SMUPs leads to reduced CMAP peak amplitude. Conduction block, demyelination
- C) Denervation of one MU, with collateral reinnervation by the other two, leads to preserved CMAP amplitude
- D) Reduced SMUP leads to reduced CMAP amplitude. Fewer fibres, smaller fibres, reduced fibre density, tissue attenuation (fat)

1.3.4 Motor Unit Number Estimation (MUNE)

Changes in CMAP at different force and stimulation levels can be measured to estimate the motor unit population. This technique is called Motor Unit Number Estimation (MUNE) and includes several different analysis methods that have evolved over years of study. One of the issues with MUNE measurements that require maximal CMAP is that the extent of the muscle must be superficial, as deeper motor units will contribute less to the CMAP. Additionally, the major nerve branch of the muscle must also be accessible for superficial peripheral stimulation. All MUNE techniques are sensitive to cross-contamination from neighbouring muscles, which means that the MUNE value may be an amalgam of multiple muscles within the detection radius of the electrode.

The first use of MUNE to estimate motor unit count through age was by McComas (McComas *et al.*, 1971). They selected the extensor digitorum brevis (EDB) muscle in the foot, which is relatively flat and lies close to the skin surface. They calculated the MUNE

value by dividing the average MU potential after incremental stimulation by the maximal CMAP from supramaximal stimulation. The authors did not include subjects older than 58, and no significant change in MUNE value was found in this group.

A follow-up study in the same hospital used the same techniques in 28 individuals aged 60-96, as well as 66 non-aged controls (Campbell, McComas and Petito, 1973). They demonstrated a drastic fall in motor unit number estimate above the age of 60 compared to controls, with some subjects demonstrating fewer than 10 MUs, compared to matched healthy controls who showed between 100-200. The combined findings of these studies concur well with anatomical studies mentioned previously.

Additionally, both studies demonstrated stable CMAP amplitudes, with increased potentials from individual motor units. This indicates that there was a loss of motor units with compensatory reinnervation, but there were few to no 'stranded' muscle fibres that failed to be reinnervated. While there is no discussion of grip strength or fatigue symptoms, the participant group selected was fit and active, suggesting that these neurogenic changes form part of normal ageing.

1.3.5 Motor Unit Number Index (MUNIX)

MUNIX is an alternative measure of MUNE that compares the power of the CMAP during supramaximal activity with the interference pattern of voluntary contraction. While it requires proprietary software, it is quick and easy to perform, and has good inter- and intra-rater agreement (Gooch *et al.*, 2014). Another value produced by MUNIX is the Motor Unit Size Index (MUSIX), which reflects the size of each SMUP.

Drey has reported two studies assessing MUNIX of the hypothenar muscle in sarcopenic patients- the first with 27 sarcopenic patients (Drey *et al.*, 2013), and the second with a further 75 (Drey *et al.*, 2014). Both compared results to age-matched healthy controls. The MUNIX value of sarcopenic patients was 25% lower than controls and demonstrated collateral reinnervation, with a strong inverse correlation between MUNIX and MUSIX; patients with fewer motor units demonstrated larger single motor units. This is somewhat unsurprising as both MUNIX is highly correlated with CMAP amplitude (Jacobsen *et al.*, 2017) and MUSIX is calculated as MUNIX/CMAP amplitude. Since the CMAP amplitude reduces with age (Dorfman and Bosley, 1979), this effect may have led the changes in this study, however these findings remain of interest. The second showed a significant association between pathological MUNIX values and the incidence of sarcopenia. While underpowered to find sub-groups, the link between MUNIX and MUSIX suggests that while

there is reinnervation of lost motor units, this is outpaced by denervation, and this net deficit leads to sarcopenia. This is consistent with animal glycogen depletion studies which demonstrate failure of reinnervation leading to weakness (Edström and Larsson, 1987).

1.3.6 Decomposition-based Quantitative EMG (DQEMG)

A further development of the MUNE technique involves using co-located surface and intramuscular EMG (iEMG) electrodes. The iEMG is used to trigger sampling of the corresponding sEMG- this is called Spike Triggered Averaging (STA-MUNE) and is one form of DQEMG. The combined signal is then decomposed into constituent motor units using signal decomposition software.

This was used to perform MUNE in young, aged, and sarcopenic individuals, which demonstrated evidence of reinnervation in healthy older people via larger MU potentials versus those with sarcopenia who had much smaller MU potentials (Piasecki *et al.*, 2018). The authors suggested that while motor unit loss is part of normal ageing, failure to reinnervate muscle fibres is the factor that distinguishes sarcopenia.

A critical limitation in MUNE performed using voluntary techniques such as MUNIX and STA-MUNE is related to motor unit recruitment. According to the size principle (Henneman, Somjen and Carpenter, 1965; Milner-Brown, Stein and Yemm, 1973), MUs are recruited in order of size. EMG becomes much more complex at higher force levels, and so both techniques are often performed at low-moderate force levels. This means that sMUPs recorded from voluntary activity may be significantly smaller than those from peripheral stimulation, which would lead to relative overestimation of MU numbers.

In normal recruitment, slow-twitch, fatigue-resistant muscle fibres are recruited before fast-twitch, fatigable fibres. Other studies have reported preferential loss of fast-twitch motor units with reinnervation by slow-twitch motor neurons earlier in the disease course of sarcopenia (Narici and Maffulli, 2010). Voluntary evoked MUNE techniques may therefore demonstrate larger sMUP at low force levels, and thus considerably underestimate motor unit numbers.

1.4 Neuromuscular junction changes

1.4.1 Single fibre studies

Single fibre EMG studies involve recording pairs of neighbouring muscle fibres within the same motor unit. Normal activation produces single fibre action potentials separated by

regular intervals. Any variability in temporal separation between consecutive activations (the Mean Consecutive Difference; MCD) is termed 'jitter', whereas differences between consecutive amplitudes is called 'jiggle' (Stålberg and Sonoo, 1994). Increased jitter is seen in several neuromuscular diseases such as myasthenia gravis, where antibodies to the postsynaptic membrane inhibit transmission. It is commonly thought that jitter increases with age (Stålberg and Trontelj, 1979); however, single fibre EMG is much less widely performed outside the ages of 15-60 due to its main indication for myasthenia gravis, which occurs in this age group, and consequently, ageing subjects are poorly represented in the literature.

Single fibre EMG can also be used to measure the density of muscle fibres within a motor unit. To perform this, the EMG needle is positioned so that the amplitude from a single fibre potential is maximal. At this position, the number of additional synchronous spikes with amplitude above $200\mu\text{V}$ and rise time less than $300\mu\text{s}$ are measured. This demonstrates how many fibres are in the neighbouring region to the principal fibre. This local measure is repeated in 20 different areas to provide a local concentration of fibres in the studied area.

We are aware of only two studies measuring normative single fibre data through the life course. This is likely because of the length of time and procedural skill involved in the measurement.

The first was a multi-centre study (Gilchrist, 1992). This study was underpowered to detect significant changes with age and is methodologically flawed in several ways. Firstly, there was no attempt to standardise investigators' techniques which may have impacted inter-centre measurements, and muscle selection was left up to individual investigators, meaning some muscles (e.g., biceps and quadriceps) were especially understudied. Exclusion criteria were not specified, and patients referred for investigation of myasthenia gravis but who were found not to have it were included. There was no follow up to ensure these symptomatic patients remained disease-free, so the data cannot be considered normative.

Despite these problems, this study demonstrates a modest relationship between jitter and age in specific muscles, namely frontalis, extensor digitorum, and orbicularis oculi. Separately, fibre density in biceps, extensor digitorum, quadriceps and tibialis anterior modestly increased with age, indicating fewer motor units innervated the fibres in that region.

Secondly, a more rigorous multi-centre study to determine jitter values using concentric needle electrodes has been performed (Stålberg *et al.*, 2016), with prospective data collection, assessment of recording quality, and specific exclusion criteria that reduced the

likelihood of accidental inclusion of those with neuromuscular disease. The investigators studied only three muscles (frontalis, orbicularis oculi and extensor digitorum). This study found a weak relationship between age and MCD, significant only in frontalis, but was underpowered for ages above 60.

If jitter is too high ($>100\mu\text{s}$), neuromuscular block can occur, with subsequent failure of contraction of the muscle fibre. Below this level, the clinical impact of jitter is uncertain, and jitter has not been shown to be anywhere near the level for neuromuscular blocking in healthy ageing subjects (Ekstedt and Stålberg, 1971). Muscle strength has been shown to reduce with increased jitter in mice (Chung *et al.*, 2018), and pathological jitter value correlates closely with clinical severity in myasthenia gravis (Konishi *et al.*, 1981). Still, no such measurements of subclinical jitter compared to muscle strength have been performed in healthy humans.

On the basis of these results, it appears that while there is a reduction in neuromuscular junction function as measured by jitter, this has been shown in animal models not to contribute to sarcopenia (Willadt, Nash and Slater, 2016). The current consensus is that while there are alterations in the structure of the neuromuscular junction, including increased fragmentation and reduced folding, these subthreshold changes are unlikely to result in the level of clinical weakness seen (Willadt, Nash and Slater, 2018).

1.4.2 DQEMG in muscle weakness

The intramuscular needle used in STA-MUNE can also be used to estimate single fibre jitter and jiggle by approximating the measure from timings of MUP segments with consistent morphology.

One study used this to compare the DQEMG in 19 patients classified according to EWGSOP criteria as pre-sarcopenic, sarcopenic, or severely sarcopenic (Gilmore *et al.*, 2017). They found progressive loss of motor units via MUNE values, but the between-group difference was not significant. There was significantly reduced neuromuscular stability as measured by jitter and jiggle in the sarcopenic groups, and one hypothesis is that this impaired stability could have reduced the size of the average SMUP, inflating the MUNE value in sarcopenic patients (Arnold and Clark, 2017); a similar problem has been reported in similar techniques applied to patients with Amyotrophic Lateral Sclerosis (Shefner *et al.*, 2004).

In contrast to motor neurone loss and denervation, neuromuscular function changes are modifiable and affected by exercise. Since exercise is the most significant modifiable factor

in preventing sarcopenia, it is reasonable to ask what impact exercise has on neuromuscular parameters. One study compared 29 world champion master athletes in their ninth decade of life with age-matched controls (Power *et al.*, 2016). They found that the retired athletes had significantly larger CMAP amplitude and significantly reduced neuromuscular jitter and jiggle.

1.5 Methods of assessing motor unit internal structure

A concentric needle EMG electrode may be inserted into muscle to sample the electrical activity from a single region of muscle fibres. Since the muscle fibres in a healthy motor unit all have similar diameters, the fibre action potentials travel at similar speeds, passing by the intramuscular EMG electrode almost simultaneously to produce a simple triphasic MUP. In neuropathies, inefficient neuromuscular connections and fibre size variability results in asynchrony of the fibre action potential, resulting in a more complex MUP with additional components.

It is well understood that the shape and characteristics of the MUP vary with even small movements of the EMG needle within the muscle. The EMG needle is targeted clinically to optimise the position of the electrode to an adjacent MUP and minimise rise time; however, the position of the needle within the motor unit territory is ill-defined. This means that the reliability of concentric needle EMG to detect neuromuscular disease is limited by the number of regions sampled within the motor unit, and early disease may not be detected by the operator, if it is confined to just a few motor units.

Single fibre EMG uses a significantly smaller recording electrode surface to record from a much narrower muscle volume ($300\mu\text{m}$). This enables a single muscle fibre action potential to be recorded. By carefully positioning the electrode, the operator can measure the number of SFAPs within the electrode recording volume as a proxy measure of muscle fibre density. As with concentric needle recordings, this technique is highly dependent upon the region of muscle sampled and operator skill.

Other attempts to measure the whole motor unit have included macro EMG (Stalberg, 1980), which involves inserting a sizeable monopolar electrode which samples from the length of the needle, triggered by a very fine single-fibre electrode located within the larger electrode in order to measure activity from a single motor unit. Macro EMG potentials are therefore considered to represent the 'whole motor unit' potential, and the macro EMG amplitude is highly correlated with motor unit size (S. Nandedkar and Stålberg, 1983; Roeleveld *et al.*, 1997).

Multielectrodes comprise a needle with many recording surfaces along their length, with electrode numbers varying from 8 to 32 (Stålberg *et al.*, 1976). By having multiple electrodes differentially recording from the muscle volume, the internal motor unit structure may be revealed at a resolution dependent upon the recording surface geometry. Challenges in electrode manufacture have limited these techniques to research environments, and multielectrodes have not yet entered routine clinical practice.

1.5.1 Scanning EMG- advantages & limitations

Scanning EMG, first described by Stalberg and Antoni in 1980, is where an EMG electrode is withdrawn in very small ($50\mu\text{m}$) increments through a motor unit to build up a continuous profile of electrical activity within a corridor of the muscle.

To perform this method, a single-fibre EMG electrode is inserted into the muscle to act as a trigger for single motor unit activity during voluntary contraction. A second concentric needle electrode is then inserted 1-3cm from the SFEMG electrode to optimise the single MU signal as triggered by the SFEMG electrode. The needle is then advanced deeper into the motor unit until a MUP is no longer recorded before being withdrawn in fixed increments.

One of the critical limitations of scanning EMG has been standardising movement increments. In early iterations, this was standardised through markings on the needle visible at the skin surface (Stalberg and Antoni, 1980) and later using a fixed stepper motor (Stålberg and Eriksson, 1987).

Using markings on the needle, visible at the skin surface is straightforward, but problematic in practice as the needle is likely to move more within the muscle than at the skin surface due to skin elasticity and stiction. Stepper motors also do not consider the stiction of muscle around the needle (although a Teflon-coated needle is recommended to minimise this) and require highly specialised equipment. Therefore, the stiction involved in both techniques introduces a non-linearity between the relative position of the needle with respect to the muscle tissue it surrounds, which may affect results by under or overestimating motor unit territory. This stiction may be different in neuromuscular diseases, which cause intramuscular fat infiltration, fibrosis or increased fibre density, which may further skew findings in disease.

1.5.2 Ultrasound in Neurophysiology

Ultrasound uses the reflection of high-frequency sound waves to determine the cross-sectional structure of tissue (B-mode) or the motion of tissue through the plane (doppler). Ultrasound is a relatively cheap and widely available imaging modality used extensively in

clinical practice to study anatomical changes in real-time. Healthy muscle is echolucent on ultrasound (Reimers *et al.*, 1993), except for the perimysium bordering muscle fascicles (Walker, 1996), while a needle may be visualised directly or by the indirect movement of the tissue as the needle displaces it. Improvements in ultrasound resolution have enabled direct visualisation of nerves (Bianchi, 2008), producing parameters to diagnose neuromuscular disease (Walker *et al.*, 2004; Padua *et al.*, 2007). In nerve, these include cross-sectional area, which increases in the median nerve in carpal tunnel syndrome (Nakamichi and Tachibana, 2000). In muscle, degenerative changes, including fat & fibrous infiltration and increased fibrous density, are demonstrated via increased echogenicity and loss of heterogeneity on imaging. This has been used to demonstrate the severity of muscle wasting on intensive care (Moukas *et al.*, 2002).

In neurophysiology, ultrasound has been used to safely target EMG of the diaphragm (Boon *et al.*, 2008; Gentile *et al.*, 2020) and to visualise fibrillations (Pillen *et al.*, 2009) and larger fasciculations in amyotrophic lateral sclerosis (Bokuda *et al.*, 2020), although operators should take care to avoid confusing movement artefacts for fibrillation (Alfen *et al.*, 2011). Further advantages of ultrasound guidance of the EMG electrode include avoiding vascular structures (especially important in those with disordered clotting) and improved accuracy when targeting deeper muscles, such as the upper leg (Boon, Smith and Harper, 2012).

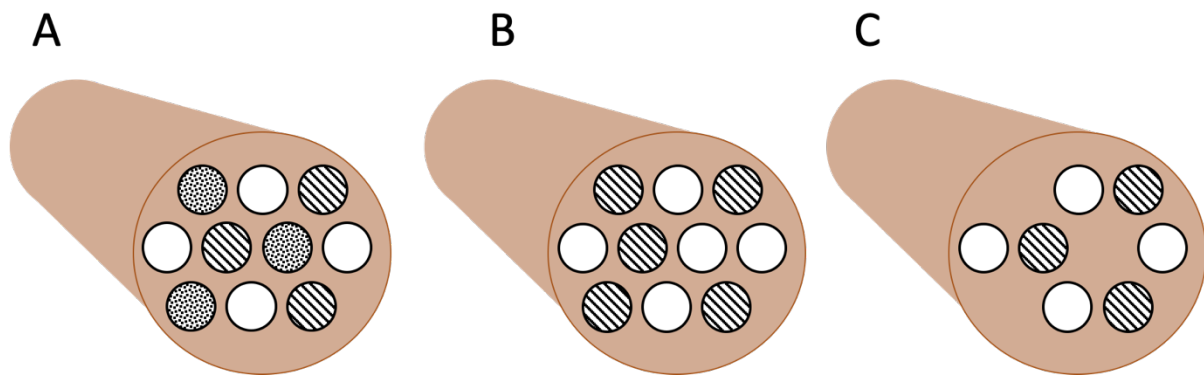
1.6 Summary

The neurophysiological evidence indicates that normal ageing is a process of neurogenic abscission, with shedding of motor units. In response, there is collateral reinnervation; however, in sarcopenia, there is evidence of a failure of reinnervation, with consequent muscle strength loss (Figure 1.4). Clinical biomarkers are required to delineate individuals with abnormal muscular micro-structure.

Factors that have been shown to reflect clinical weakness due to sarcopenia accurately include fibre density/motor unit size, muscle fibre type, and the neuromuscular stability. Taken together, these parameters could better stratify those at risk of sarcopenia prior to significant and poorly reversible functional limitation. In particular, combining the motor unit size and count provides an indication of those who are failing to reinnervate. Both DQEMG

and MUNIX can provide these values, but the latter is non-invasive and, therefore most amenable to stratify the sarcopenic phenotype.

Figure 1.4 A) Normal innervation of three motor units and their consequent muscle fibres. B) Denervation of one motor unit, with collateral reinnervation. C) Denervation without reinnervation, and consequent loss of muscle fibres.



Given the limitations associated with the existing techniques, we aimed to develop new methods of assessing neurophysiological changes in sarcopenia. Many of the chapters in this thesis have been published, or accepted for publication, at the time of thesis submission and are included with only minor changes to their appearance in press.

In this thesis, I will detail several of the experiments performed and how these can provide new insights into the neurophysiology of sarcopenia. Firstly, there was a clear need to assess the upper motor neurone changes with ageing. To this end, in chapter 2, we examine a modification of TMS to elicit ipsilateral motor evoked potentials (iMEPs). I will explain the contrast between ipsi- and contralateral MEPs and how comparing these can provide insights into the balance of neurological control between the dominant corticospinal pathway, and the more resilient, primordial reticulospinal pathway.

Taking this concept further, in chapter 3, I will demonstrate how I applied the measurement of iMEPs in younger and older adults, comparing muscle strength to the balance of control between iMEP/cMEP. The changing dynamics of muscle control with age and their effect on the iMEP/cMEP ratio supports a hypothesis of shifting balance of motor control, significantly affecting the sarcopenic phenotype. This results in individuals who have much less reticulospinal activation lacking strength compared to their peers.

Travelling orthodromically to assess the peripheral motor system and lower motor unit, I next aimed to measure the microstructure of the motor unit. We have developed a technique enabling the multielectrode measurement of single-fibre EMG potentials, across 32

electrodes on a single EMG needle (MicroEMG). This not only allows the measurement of a greater region of muscle than traditional single-fibre EMG but also enables the accurate localisation of single muscle fibres around the needle. This means that for the first time, we can perform "electro-imaging" of the motor unit to demonstrate the actual fibre density of a motor unit; a key metric for reinnervation. While covid disruptions unfortunately meant we were not able to produce measurements in older adults with sarcopenia, chapter 4 demonstrates in silico modelling to support signal processing and the first recordings of this kind in healthy human controls.

Finally, while MicroEMG demonstrates the microscopic, intra-fibre structure of the motor unit, it was also necessary to develop a technique to assess the macroscopic dimensions and internal structure of the motor unit. To do this, we updated the method of scanning EMG to utilise ultrasound targeting of an intramuscular EMG needle through the motor unit (Ultrasound guided Motor Unit Scanning EMG; UltraMUSE). By synchronising ultrasound imaging to EMG sampling, we were able to demonstrate the position of each intramuscular trace and directly measure the dimensions of a motor unit. In Chapter 5 we apply this technique again to healthy controls and model results against the extant techniques of the literature.

Ultimately, sarcopenia is a complex disorder, which results from the interaction of many different factors. By focussing on neurological factors, we can potentially seek new preventions and treatments that might help maintain older people's independence and strength. This necessitates the development of better techniques to assess the spinal pathways and motor unit.

2. Review of Ipsilateral MEPs (iMEPs) in health and disease

2.1 Abstract

iMEPs are an ipsilateral response to magnetic stimulation, not easily elicited in most individuals. It is highly likely that iMEPs are conveyed via a reticulospinal or propriospinal route and depend on suitable muscle activation through voluntary activity and high TMS intensity.

iMEPs have been used extensively in studying childhood neurodevelopment, including mirror movements, as well as disease states ranging from amyotrophic lateral sclerosis (ALS) to stroke.

This section talks through previous attempts to elicit iMEPs, their success and variability, and the link to health and disease.

2.2 Introduction

Transcranial Magnetic Stimulation (TMS) involves using an electromagnetic stimulator to activate the neurones of the brain, by inducing current with a strong and brief magnetic field. The precursor to TMS was Transcranial Electrical Stimulation (TES) (Merton and Morton, 1980). Although TES inadvertently activates sensory c-fibres of the scalp (Häkkinen *et al.*, 1995), causing some pain, it nevertheless has been used to study motor systems in healthy individuals as well as diseases such as Motor Neurone Disease, Stroke, and MS. TES has been shown to elicit fast conducting iMEPs in Mirror Movements (MM) (Farmer, Ingram and Stephens, 1990; Cohen *et al.*, 1991).

TMS was first described in 1985 by (Rouiller *et al.*, 1994), who used it to stimulate the brain and peripheral nerves. In the following years, TMS has been widely described for measuring cortical excitability, central motor conduction time, and localisation of cortical regions, including memory and motor skills. Clinically, TMS is already of utility in detecting corticospinal demyelination and spinal cord compression.

To date, most TMS studies have focussed on crossed corticospinal pathways, consistent with the Valsalva doctrine representing the predominant decussation of motor control pathways (Kuypers, 1981; Schutta, Abu-Amero and Bosley, 2010). The use of TMS to measure cortical control of ipsilateral muscles by producing ipsilateral motor evoked potentials (iMEPs) was first described by Wassermann in 1991. Since that first attempt, there has been a great deal of interest in using iMEPs to discover the “Northwest passage” of motor control via ipsilateral pathways for the rehabilitation of stroke and spinal cord injury, as iMEPs remain even when corticospinal control has been lost.

2.2.1 Proposed routes for iMEPs

2.2.1.1 Direct current spread

Before discussing direct current spread, it is important to define a “true” iMEP. While it is easily possible to simultaneously activate both hemispheres, eliciting a bilateral MEP, this is in fact producing two crossed MEPs originating from both hemispheres. By comparison, an iMEP represents activation of a single hemisphere.

Direct spread of current to the contralateral hemisphere or monosynaptic activation of uncrossed corticospinal tract fibres have been rejected as a potential route for iMEPs on three counts. Firstly, iMEPs do not increase in amplitude with more medial positioning of the TMS coil (Ziemann *et al.*, 1999). Secondly, iMEPs are produced in some hand muscles (FDI, APB, ADM, Table 2.1) but not others (opponens pollicis, finger and wrist flexors (Ziemann *et*

al., 1999)) irrespective of MEP threshold, even in TES (Wilson and Peterson, 1981). Finally, and most importantly, consistent latency differences of 4-10.5ms have been demonstrated in iMEPs, inconsistent with the duration associated with current spread (albeit with some exceptions in proximal muscles, which will be reviewed in section 2.3). The latency difference due to current spread should be close to zero representing synchronous activation of both hemispheres, [Figure 2.1](#). This latency difference is also why branching or uncrossed corticomotoneuronal axons are not considered to play a role in iMEPs.

Figure 2.1 Example of MEP (left) and iMEP (right) in a healthy subject.

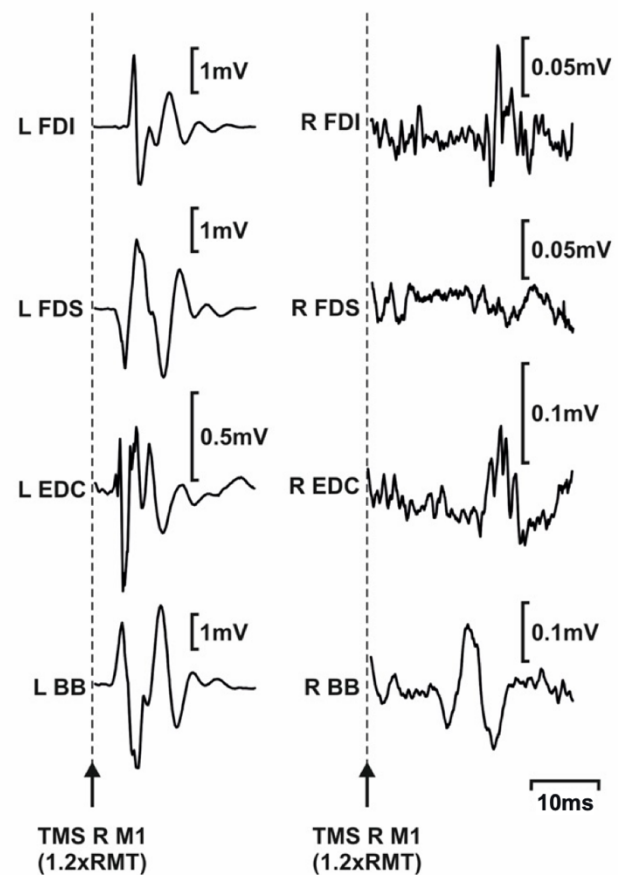
2.2.1.2 *Uncrossed/branching corticospinal pathway*

Corticospinal axonal branching would result in a latency difference between iMEP & cMEP of close to zero (Farmer, Ingram and Stephens, 1990; Carr, Harrison and Stephens, 1994). While an uncrossed pathway has been proposed as the control mechanism in patients with pathological mirror movements (Mayston, 1997), this mechanism would again be inconsistent with the significant latency difference experienced.

Recrossing of the corticospinal tract via spinal interneurons may explain the enhanced recovery of patients with

lateral corticospinal tract lesions (Nathan, 1994); however, this has not been demonstrated in healthy subjects. Neurophysiological investigations in monkeys showed negligible ipsilateral output to the upper limb (Soteropoulos, Edgley and Baker, 2011), while in humans, H-reflex/F-wave stimulation only elicits ipsilateral responses without the crossing that such a pathway would enable (Caccia *et al.*, 1973; Farmer, Ingram and Stephens, 1990; Capaday *et al.*, 1991).

2.2.1.3 *Trans-callosal pathway*



While trans-callosal projections have been proposed as one potential source for iMEPs, and sparse connections between hand areas of motor cortices have been shown (Ziemann *et al.*, 1999), patients post-hemispherectomy, or with agenesis of the corpus callosum can also produce iMEPs (Wassermann, Pascual-Leone and Hallett, 1994; Ziemann *et al.*, 1999). Furthermore, the absolute minimum transcallosal conduction time between motor cortices takes at least 7.8ms (Cracco *et al.*, 1989), and most of the latency differences described in the literature (Table 2.1) are below this threshold, with the exception of a study of Trapezius and Serratus anterior (Alexander *et al.*, 2007) which demonstrated latency differences of around 10.5ms. The reason for this prolonged difference is unclear, however the investigators rectified the MEPs, which may have affected the reliability of the latency measurement, due to the mixed inhibitory and excitatory effects of iMEPs.

2.2.1.4 Reticulospinal/Propriospinal tracts

In monkeys, significant functional recovery can occur via the rubrospinal tract (Lawrence and Kuypers, 1968); however, in humans, this is largely vestigial (Nathan and Smith, 1955). The best candidate pathways for iMEPs are corticoreticulospinal (Nathan, Smith and Deacon, 1996) or corticopropriospinal (Pierrot-Deseilligny, 1996). The evidence for the former arises from the bilateral innervation of the reticulospinal tract (Rouiller *et al.*, 1994) and the fact that the anatomical cortical location which elicits iMEPs is located lateral to the area for contralateral MEPs (Wassermann, Pascual-Leone and Hallett, 1994; Ziemann *et al.*, 1999), a feature shared by a small population of neurones with ipsilateral connections (Aizawa *et al.*, 1990) and corticobulbar connections in monkeys (Keizer and Kuypers, 1989) and in humans (Goldring and Ratcheson, 1972). Furthermore, neck angle provides input to proprio-, reticulo- and vestibulospinal neurones (Wilson and Peterson, 1981), a feature also demonstrated in iMEP facilitation (Wassermann *et al.*, 1991; Tazoe and Perez, 2014).

While around 85% of corticospinal tract fibres decussate at the medulla (Kuypers, 1981), the reticulospinal tract is organised bilaterally, with single axons innervating either side of the body (Jankowska *et al.*, 2003; Schepens and Drew, 2006; Davidson, Schieber and Buford, 2007). This organisation is consistent with the pattern of activation of iMEPs, which is also predominantly bilateral.

Given the converging information discussed here, it is highly likely that iMEPs are conveyed via a reticulospinal or propriospinal route.

2.3 How to elicit iMEPs in healthy controls

Eliciting iMEPs frequently involves using high levels of TMS output. To improve the density of magnetic field current flow within the brain, the most commonly used coils are figure-eight (Cohen and Cuffin, 1991; Basu and Turton, 1994) and double-cone (Cohen and Cuffin, 1991) shaped. The only direct comparison between the two coils is from Basu 1994, who found better success with double-cone coils, eliciting no iMEPs with the figure-eight shape. While direct activation has been rejected as a mechanism for eliciting iMEPs, a circular coil produces a much more diffuse electrical current than figure-eight or double-cone coils (Turton *et al.*, 1996). This shape should therefore be avoided to prevent inadvertent direct activation of the contra-targeted hemisphere.

The recruitment pattern of iMEPs is non-linear, in comparison to cMEPs (MacKinnon, Quartarone and Rothwell, 2004), and this can mean TMS intensities 25% or higher above the MEP threshold are often needed to elicit iMEPs. This increased intensity can result in the spread of current to the contralateral hemisphere to the one targeted (Meyer *et al.*, 1990; Basu and Turton, 1994). If this occurs, the resulting iMEP will be of similar latency to the cMEP. This potential spread means that previous investigations have recommended that ipsilateral responses <4-6ms of the cMEP should be rejected as possibly due to current spread (Farmer, Ingram and Stephens, 1990; Carr, Harrison and Stephens, 1994), although there are examples opposed to this, mostly in axial muscles (Table 2.1). These exceptions are likely to be conducted by alternative spinal pathways, including masseter, innervated by the trigeminal nerve which has bilateral cortical representation, as well as sternocleidomastoid and the diaphragm, which both are innervated by nerves originating from the cervical spinal cord with complex innervation pathways.

iMEPs are not readily produced in healthy adult subjects at rest (Bernard, Taylor and Seidler, 2011), with the possible exception of ambidextrous individuals (Netz, Lammers and Hömberg, 1997). Several techniques have been used to facilitate iMEPs, as shown in Table 2.1.

It is now clear that iMEPs depend on suitable muscle activation through voluntary activity and high TMS intensity. Wasserman 1991 used contractions of 10-100% MVC with 100% TMS intensity and found increases in amplitude of iMEP with increasing effort across limb muscles. Carr 1994 used weak contractions with low TMS intensity (30-45%) and failed to produce iMEPs except in proximal muscles (masseter, rectus abdominis). Similarly, Wassermann, Pascual-Leone and Hallett, 1994 used low MVC (around 10%) and higher TMS intensities but still only elicited iMEPs in a minority of participants.

Several studies have demonstrated the cortical motor representation of iMEPs, demonstrating regions from which iMEPs can be elicited that were spatially distinct (and often lateral) to contralateral representations (Wassermann, Pascual-Leone and Hallett, 1994; Werhahn *et al.*, 1994; Ziemann *et al.*, 1999). Using paired-pulse TMS, iMEPs have been shown to be subject to intracortical inhibition (McCambridge, Stinear and Byblow, 2016), suggesting that iMEPs are modulated by intracortical inhibitory networks.

The TMS coil may be held in various positions above the head in order to produce different activation effects. These are described in terms of the location of the focus of the magnetic field, positioned above the area intended to be activated (e.g. primary motor area) and the orientation of the TMS coil. In a figure-eight coil, this is described as the anatomical direction along the axis of the coil's field. For example, a coil which is positioned parallel to the posteroanterior axis is also described as being posteroanterior (PA), while an orientation parallel to an axis running from the lateral edge of the head (mastoid process) to the centre of the anterior surface is termed lateromedial (LM).

A PA coil orientation produces contralateral MEPs 0-3ms later than LM (Sakai *et al.*, 1997). This is thought to be due to LM orientation activating corticospinal fibres directly, whereas PA activates trans-synaptically. An LM orientation is thought to preferentially produce D and early I waves (Alagona *et al.*, 2001).

Furthermore, iMEPs have been shown to completely disappear when changing coil position from PA to LM (Ziemann *et al.*, 1999; Tazoe and Perez, 2014), or be produced more sporadically albeit with similar amplitude (Christova *et al.*, 2006). This could indicate that trans-synaptic activation is necessary for the production of iMEPs; however, these theoretical explanations are yet to be confirmed experimentally.

One reliable method of achieving reliable iMEP activation involves bilateral movements. Škarabot *et al.*, 2016 showed facilitation of iMEPs with unilateral antagonistic co-activation, but not isometric abduction of the first dorsal interosseus (1DI) muscle. Both Basu 1994 and Bawa *et al.*, 2004 used bilateral homonymous movements of limbs to elicit iMEPs at muscles throughout the body. Kuppuswamy *et al.*, 2008 showed increased iMEP activation of knee extensors using bilateral homonymous movements compared to unilateral movement, while Maitland and Baker, 2021 (detailed in Chapter 3) used bilateral phasic homonymous movements to elicit iMEPs in biceps.

By contrast, Tazoe and Perez, 2014 showed reduced iMEP activation of biceps brachii during homonymous movements and increased iMEP activation during heteronymous movements, compared with unilateral movements. This pattern of heteronymous facilitation

was supported by Bawa *et al.*, 2004 who showed facilitation of iMEPs via activation of contralateral arm abduction.

Bawa *et al.*, 2004 also demonstrated a proximal to distal gradient in iMEP: cMEP amplitude ratio. iMEPs have been demonstrated frequently in proximal muscles such as biceps and deltoid and distal hand muscles such as 1DI (Basu 1994, Bernard 2011, Wasserman 1994). Other muscles studied with iMEPs include lingual muscles (Muellbacher, Artner and Mamoli, 1999), masseter (Carr, Harrison and Stephens, 1994) and diaphragm (Khedr and Trakhan, 2001).

Ipsilateral MEPs are defined as those having a peak-to-peak amplitude of at least $15\mu V$ (Wassermann *et al.*, 1992; Bernard, Taylor and Seidler, 2011). Since iMEPs are best elicited during voluntary muscle activation, their small amplitude can be difficult to delineate from the non-linear summation of rectified voluntary EMG (Baker and Lemon, 1995, 1998). When processing iMEP data, it is therefore important to leave traces unrectified (Ziemann *et al.*, 1999; Bawa *et al.*, 2004).

The number of iMEPs to average to cancel out background activity and demonstrate iMEP activity will vary between muscles and tasks; however, the previously described studies average between 5-10 stimuli. An alternative method to quantify iMEP activity has been proposed by Ziemann *et al.*, 1999, who measure the ΔEMG peak as:

$$(iMEP - prestimulus EMG) \times iMEP \text{ duration}$$

2.4 Ipsilateral MEPs in neurological disease

Historically, the description of iMEPs in patients with certain neurological disorders resulted from the observation that some patients develop re-emergent mirror movements (MM). However, MM does not equate to producing iMEPs. For example, whilst MM are recognised in patients with Parkinson's disease (Cincotta *et al.*, 2006; Spagnolo *et al.*, 2013), studies in these patients have consistently shown that MM are not associated with iMEPs (Tassinari *et al.*, 2003).

2.4.1 Persistent Mirror Movement Disorders

iMEPs have been used to delineate clinical differences in spinal pathways between health and disease states, including patients with Klippel-Feil and Kallmann syndrome. Given that the bilaterally organised reticulospinal tract has been implicated in iMEPs, MM (in

which unilateral movement “leaks” to the other side of the body) remain an intriguing phenomenon to study motor control.

A significant part of the early literature using TMS in MM utilises circular coils and demonstrate ipsilateral responses with minimal latency difference to contralateral responses. These include in a subject with Klippel-Feil (Farmer, Ingram and Stephens, 1990), as well as in other congenital & acquired causes of MM (Britton, Meyer and Benecke, 1991; Capaday *et al.*, 1991; Cohen *et al.*, 1991). As discussed earlier, the non-focal nature of circular coils makes these results more challenging to interpret, although two of these papers (Farmer, Ingram and Stephens, 1990; Cohen *et al.*, 1991) failed to demonstrate iMEPs in controls using the same technique, limiting the likelihood of direct activation of the contra-targeted hemisphere. Furthermore, Britton 1991 demonstrated sensitivity to coil orientation in 2/3 subjects suggesting abnormal projection of corticomotoneuronal pathways.

Despite these limitations, later studies utilising a focal figure-eight coil were supportive of the early results and also demonstrated ipsilateral responses with minimal latency differences in patients with Kallman syndrome & gene carriers (Danek, Heye and Schroedter, 1992; Mayston, 1997) and other patients with congenital MM (Cincotta *et al.*,

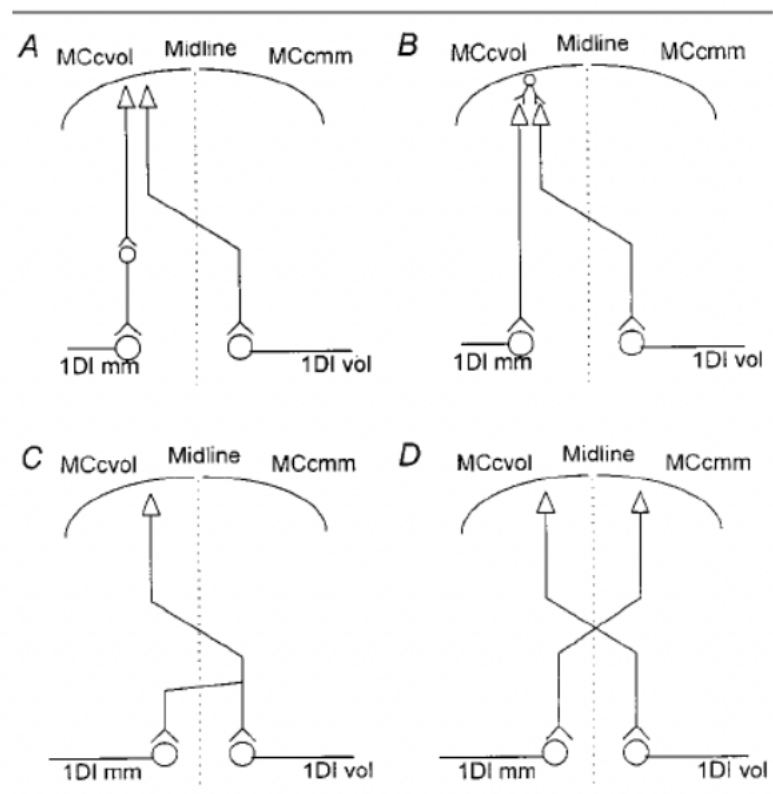


Figure 2.2 Possible mechanisms underlying mirrored activity (reproduced from Mayston *et al.* 1999). Activity in normally occurring ipsilateral corticospinal projection from the motor cortex contralateral to the voluntarily activated hand (MCcvol) (A), or shared synaptic input to pyramidal cortical cells situated in the MCcvol that project to contralateral and ipsilateral motoneuron pools of homologous muscle pairs (B), or activity in ipsilateral axon collateral caused by branching of the normally occurring crossed corticospinal projection from the MCcvol (C). (D) Simultaneous activity in crossed corticospinal projection from motor cortex contralateral to voluntarily activated hand (MCcvol) and from motor cortex contralateral to mirror movement hand (MCcmm). There could be a combination of these mechanisms, such as B and D. 1DI vol 5 voluntarily activated muscle; 1DI mm 5 homologous muscle of the opposite hand.

1994, 1996; Kanouchi *et al.*, 1997). Given these latencies, it is unlikely that the reticulospinal tract is involved in producing mirror movements in these patients, and this is more likely to be due to corticospinal remodelling (Figure 2.2).

2.4.2 Stroke

The use of TMS to measure the entire motor pathway from cortex to muscle is of great interest in the non-invasive measurement of stroke (Bembenek *et al.*, 2012). Since iMEPs are elicited via alternative neurological pathways (reticulospinal/propriospinal), there has been much interest in their potential utility in determining recovery of hand function after corticospinal lesion (Caramia, Iani and Bernardi, 1996; Baker, 2011). This is best exemplified in stroke, where there is significant damage to the corticospinal tract (Fisher, 1992) and iMEPs are upregulated (Schwerin *et al.*, 2008). The minor role that the reticulospinal tract plays in hand control provides a potential route to recovery via strengthening of existing connections rather than regrowing connections.

The reports investigating the role of iMEPs in stroke are contradictory. While some show that patients with positive iMEP responses had a better functional recovery, others show that those with positive iMEP responses had a much worse recovery. Still more have shown how challenging iMEPs can be to produce in this cohort, with Hömberg *et al.*, 1991 producing iMEPs in only 2 out of 51 patients.

Firmly in the camp of iMEPs being a poor prognostic indicator, Turton *et al.*, 1996, 1995 found iMEPs in some stroke patients in EDC and FDI, with iMEPs at lower thresholds. iMEPs of the unaffected side were most often found in patients with a poorer recovery. These iMEPs had similar latencies to the cMEPs but were highly variable, e.g. intact biceps ranged from 17.7-40.5ms. One significant limitation is that they used higher stimulation currents in more affected patients. Since iMEPs are more likely at higher stimulation currents, this could have increased the likelihood of producing iMEP outwith the disease process. In agreement, Netz *et al.*, 1997 used TMS to stimulate the unaffected side of 15 stroke patients. They found iMEPs in those with poor functional recovery and in one patient who clinically demonstrated mirror movements.

By contrast, Caramia *et al.*, 2000 performed TMS at 48hrs and six months after stroke. iMEPs persisted in hand muscles, even in patients with good recovery. Alagona *et al.*, 2001 produced iMEPs in FDI and biceps in healthy controls and stroke patients, showing a slightly better functional outcome in those patients with iMEPs.

Lastly, Trompetto *et al.*, 2000 produced thenar iMEPs in stroke patients. They categorised these patients into three groups: 1) Those without any responses indicating a very poor recovery. 2) Those with larger affected muscles iMEPs than cMEPs which demonstrated good recovery. 3) Those with larger affected muscles cMEPs than unaffected cMEPs which also demonstrated a good recovery.

The clinical picture of hand recovery in the stroke patient is poor fractionated movement with involuntary co-activation of multiple muscles (Lang and Schieber, 2003, 2004; Raghavan *et al.*, 2006). Imbalanced activation is also problematic, with stroke flexors being overactivated to the point of spasm and spasticity, while extensors are frequently weak (Kamper *et al.*, 2003), and this extensor weakness frequently predicts hand function (Fritz *et al.*, 2005).

2.4.3 Neurodevelopmental changes

TMS also offers a tool to produce insights into neurodevelopmental changes during childhood. For instance, Benecke 1991 performed TMS in six patients with hemispherectomy, either early or late in life. All six had iMEPs. Individuals with early hemispherectomy demonstrated short-latency iMEPs, while those with late had much longer iMEPs, suggesting that the process of neurological remodelling adapts with age.

iMEPs have been elicited during early childhood development but disappeared by around age 10 (Müller, Kass-Iliyya and Reitz, 1997; Kim *et al.*, 2019). A systematic review of TMS studies in children with hemiplegic cerebral palsy generally showed a pattern that iMEPs were often present, with latencies similar to the cMEPs (Nardone *et al.*, 2021). This synchronous activation indicates that corticospinal remodelling has occurred, to produce a bilateral motor representation in the unaffected hemisphere, and is consistent with the clinical picture that children with mirror movements have the most ipsilateral corticospinal reorganisation.

However, there were two notable exceptions within the constituent studies. Nezu *et al.*, 1999 found that two of nine patients with significantly longer iMEP latencies had synergistic activation and severe hemiparesis compared to the others. Meanwhile, in a larger cohort of 53 children with hemiplegic cerebral palsy (HCP), those who produced iMEPs from the unaffected hemisphere (who also had prolonged latencies) had worse motor function than those without iMEP responses (Zewdie *et al.*, 2017). If we assume that iMEPs with synchronous latency to cMEP are via a corticospinal pathway, and those with longer latency

are via a reticulospinal/propriospinal pathway, these studies suggest that reticulospinal control hinders recovery.

2.4.4 ALS/MND

Ipsilateral MEPs were first described in ALS patients in a large study investigating their potential application as an indicator of early upper motor neuron disease (Krampfl *et al.*, 2004). This study documented iMEPs in 61% of 37 patients with possible, probable or definite ALS and 47% of 19 patients with suspected ALS. In a subsequent smaller study, 25% of 12 patients with suspected or probable ALS had iMEPs (Wittstock, Wolters and Benecke, 2007). These iMEPs differ from those demonstrated in other studies, as they were elicited at rest, representing significant pathology.

Interestingly, recent studies in patients with ALS investigating the association between mirror movements and structural MRI changes in the corpus callosum (Wittstock *et al.*, 2020; Hübers *et al.*, 2021) or reduced callosal interhemispheric inhibition (Hübers *et al.*, 2021) failed to show any significant correlation. Therefore, these results appear to support the contention that MMs and iMEPs in ALS are not a consequence of pathological interhemispheric interactions. MMs in ALS might be considered a clinical marker of abnormal spinal pathway behaviours (and thus upper motor neurone disease), though clinical MMs were only observed in half of the ALS patients with iMEPs (Krampfl *et al.*, 2004).

2.4.5 Strength

The iMEP to cMEP Amplitude Ratio (ICAR) has been shown to have differing effects on strength with age (Maitland and Baker, 2021, detailed in Chapter 3). Younger individuals demonstrated a negative relationship between standardised strength, while older individuals showed a positive relationship. There was no primary relationship between age and ICAR. Other studies in monkeys have shown that reticulospinal outputs strengthen after corticospinal lesion (Zaaimi *et al.*, 2012), and are related to strength gains (Glover and Baker, 2020).

2.5 Conclusion & Recommendations

iMEPs are a potentially useful tool in determining the upper motor neurone contributions to a wide range of neurological diseases and provide a non-invasive method of comparing the reticulospinal to corticospinal changes in normal human physiology, and in disease

states. It is important that techniques are standardised in order for results to be better standardised between centres (Figure 2.3).

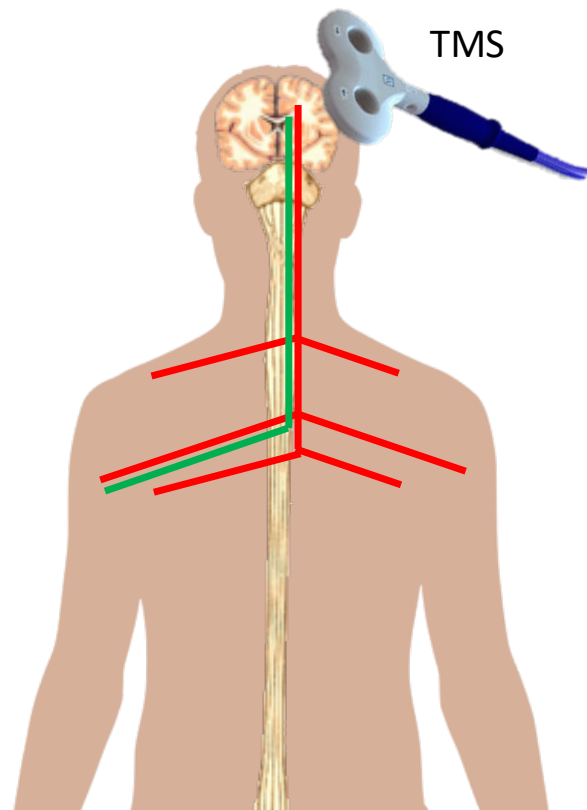


Figure 2.3 Stylised setup diagram indicating Corticospinal tract (green) and reticulospinal tract (red)

I have shown significant variability in the literature regarding ability to elicit iMEPs. While I have discussed specific papers and their limitations, I would summarise that a number of methodological differences may explain this apparent variability. These include rectifying the MEP, which may make it difficult to identify above background activity, inadequate voluntary activation, and inadequate stimulation strength, or stimulating with an inappropriate coil shape.

Based upon the review of the literature performed during this chapter, I would therefore recommend a number of steps to improve the iMEP yield of investigations into the reticulospinal tract. Firstly, it is clear that using a figure-eight or other focal coil is necessary to avoid direct activation of the contra-targeted hemisphere. Next, the level of activation should be measured carefully and stated in the results - while a reasonable level of activation is required (10-30% MVC), it is insufficient to state simply “weak contraction” and

this may result in poor reproducibility of the experiments. In addition, the bilateral nature of the reticulospinal tract seems to require bilateral movements to investigate. These may include homonymous or heteronymous movements, but should not be unilateral. The final significant source of variability lies in the strength of TMS stimulation used, relative to the activation threshold for that muscle. It is unclear what the most successful strategy would be here, but a high level of activation is necessary, and this is likely to be 20-30% above threshold.

2.6 Tables

Table 2.1 Summary of iMEPs in healthy individuals in literature

	Muscles examined	Coil shape	TMS intensity	Voluntary muscle activation	Movement	Number of stimuli averaged	Result	iMEP-cMEP latency difference
Alagona 2001	FDI, Biceps	Figure-eight (7cm)	100%MSO	10-20% MVC & 'Strong' (>50%) contraction	Unilateral & Bilateral	-	No iMEP at 10-20%, strong= 5/8 iMEPs in FDI, 6/8 in biceps	3.5-7ms
Alexander et al., 2007	Trapezius, Serratus Anterior	Figure-eight (9cm)	1.2x resting motor threshold	'weak contraction'	Bilateral	10 (rectified)	iMEPs in trapezius only, in 10/16 subjects	10.5ms
Bawa 2004	Trapezius, Pectoralis, Deltoid, biceps, FCR, ECR, FDI	Double cone (7cm)	10% above active motor threshold	10% MVC	Bilateral	10	iMEPs elicited in all subjects in at least 2 muscles	BiBr: 5-6ms
Basu 1994	Pectoralis, Deltoid, Biceps, FDI	Double cone (11cm) & Figure-8 (5cm)	Double passive threshold for FDI	-	Bilateral	-	iMEPs in 9/15 subjects, with double cone only	Pectoralis, deltoid, biceps: 8.6±1ms after cMEP

Bernard 2011	FDI	Figure-eight (7cm)	110% resting motor threshold	At rest	-	6	iMEPs in 25 of 30 individuals	FDI: 4.14 ± 6.57 ms after cMEP
Carr 1994	FDI, FA Ext, biceps, deltoid, diaphragm, masseter	Double cone (7cm)	10% above active motor threshold	'weak contraction'	Bilateral	5	iMEPs in diaphragm, rectus abdominis, masseter	Diaphragm- 4.2ms Rect. Abd: 2ms Masseter: - 0.1ms
MacKinnon et al., 2004	Pectoralis major, Latissimus dorsi	Figure-eight (9cm)	30-100%MSO	5%MVC	Bilateral	5	iMEPs in one hemisphere in all 7 subjects	5.3 ± 2.9 ms
Maitland 2021	Biceps	Figure-eight (7cm)	0-25% above active motor threshold	Fixed 12kg resistance	Bilateral	20	iMEPs in all aged <50, 81% of aged >50	7.7ms
Netz 1997	Thenar	Figure-eight (7.5cm)	70-90%MSO	10% MVC	Unilateral	10 (rectified)	iMEPs in 2/12 healthy subjects	5 & 6 ms
Tazoe 2014	Biceps	Figure eight (7cm)	100%MSO	30% MVC	Bilateral homonymous/heteronymous	5	N/A- Participants were screened for ability to produce iMEPS	6.8ms

Thompson <i>et al.</i>, 1997	Sterno- cleidomastoid	Figure- eight (5cm)	100%MSO	10%MVC	Bilateral (head flexion)	5	MEPs (any kind) in 8/15 subjects	2 ± 0.6ms
Wasserman 1991	APB, FCR, biceps, deltoid	Figure- eight	100%MSO	10,20,50, 100% MVC	Unilateral	10	iMEPs in 'some individuals'	
Wasserman 1994	FDI, Risorius, Deltoid	Figure- eight	Active threshold	20%MVC	Unilateral	10 (rectified)	iMEPs in at least one site in all individuals	Subj 1: FDI 6.5ms, deltoid 3.5ms Subj 2: FDI 4.5ms
Ziemann 1999	FDI, ADM, OP, wrist extensors & flexors, biceps, triceps	Figure- eight (5cm)	100%MSO	30% MVC	-	20 (rectified)	iMEPs in all subjects, in FDI, ADM, WF/E, biceps	WF: Difference- 5.7 ± 1.1 ms

3. Ipsilateral Motor Evoked Potentials as a measure of the reticulospinal tract in age-related strength changes

3.1 Abstract

Background

The reticulospinal tract (RST) is essential for balance, posture, and strength, all functions which falter with age. We hypothesised that age-related strength reductions might relate to differential changes in corticospinal and reticulospinal connectivity.

Methods

We divided 83 participants (age 20-84) into age groups <50 ($n=29$) and ≥ 50 ($n=54$) years; five of which had probable sarcopenia. Transcranial Magnetic Stimulation (TMS) was applied to the left cortex, inducing motor evoked potentials (MEPs) in the biceps muscles bilaterally. Contralateral (right, cMEPs) and ipsilateral (left, iMEPs) MEPs are carried by mainly corticospinal and reticulospinal pathways respectively; the iMEP/cMEP amplitude ratio (ICAR) therefore measured the relative importance of the two descending tracts. Grip strength was measured with a dynamometer and normalised for age and sex.

Results

We found valid iMEPs in 74 individuals ($n=44$ aged ≥ 50 , $n=29$ <50). Younger adults had a significant negative correlation between normalised grip strength and ICAR ($r=-0.37$, $p=0.045$); surprisingly, in older adults the correlation was also significant, but positive ($r=0.43$, $p=0.0037$).

Discussion

Older individuals who maintain or strengthen their RST are stronger than their peers. We speculate that reduced RST connectivity could predict those at risk of age-related muscle weakness; interventions that reinforce the RST could be a candidate for treatment or prevention of sarcopenia.

3.2 Introduction

3.2.1 Sarcopenia

Sarcopenia ('poverty of flesh') is the progressive degenerative loss of muscle mass and strength associated with ageing. As part of the frailty syndrome, sarcopenia is a major obstacle to the independence, quality of life, and longevity of ageing adults, who are more likely to require hospitalisation and additional care (Shafiee *et al.*, 2017; Cruz-Jentoft *et al.*, 2018). For example, age-related muscle weakness is the leading contributing factor to falls (Rubenstein, 2006), and 1 in 3 people over the age of 65 suffer a fall, with an economic burden to the UK's National Health Service (NHS) of £2.3 billion (NHS England, 2019).

Muscle mass has previously been the primary factor in defining sarcopenia; however with ageing, there is a disproportionate loss of muscle strength compared to mass (Metter *et al.*, 1999). Muscle mass alone is not sensitive in finding individuals with functional limitation due to sarcopenia (Hughes *et al.*, 2001). The European Working Group on Sarcopenia in Older People (EWGSOP) has recently updated the definition of sarcopenia to place primacy on muscle strength and functional parameters rather than muscle bulk (Cruz-Jentoft *et al.*, 2018). This new definition is termed muscle 'quality over quantity', or dynapenia (Clark and Manini, 2008) ('poverty of strength').

A number of recent reviews have commented on whether sarcopenia is primarily a neurological process rather than a muscular one (Clark and Manini, 2008; Clark and Fielding, 2012; Carson, 2018). Briefly, motor system changes with age involve cortical factors such as reduced central activation (Stevens *et al.*, 2003), spinal factors including loss of spinal motor neurons (Henneman, Somjen and Carpenter, 1965; Kawamura *et al.*, 1977; Tomlinson and Irving, 1977), and peripheral factors which include reduced nerve conduction velocity (Metter *et al.*, 1998; Palve and Palve, 2018), remodelling of the motor unit with de/reinnervation (M. Piasecki *et al.*, 2016), and impaired neuromuscular transmission (Willadt, Nash and Slater, 2018).

Clinical features of sarcopenia include reduced gait speed (Abellan Van Kan *et al.*, 2009; Peel, Kuys and Klein, 2013), balance (Mathias, Nayak and Isaacs, 1986) and difficulty rising

from a chair (Jones, Rikli and Beam, 1999; Cesari *et al.*, 2009). Although these activities all require complex motor coordination, they all involve control of proximal and axial muscles.

3.2.2 The reticulospinal tract

Motoneurons are innervated by descending spinal pathways. The pyramidal corticospinal tract is dominant for volitional control of motoneurons (Wiesendanger, 1981), with significant contributions from extrapyramidal pathways including the vestibulospinal and reticulospinal tracts. It is known that corticospinal fibres are lost with ageing (Terao *et al.*, 1994), however loss of fibres in other pathways is not well characterised.

The reticulospinal tract (RST) operates bilaterally (Jankowska *et al.*, 2003; Davidson, Schieber and Buford, 2007), diverging in the spinal cord to innervate large groups of muscles in synergistic patterns (Peterson *et al.*, 1975). This contrasts with the dominant contralateral corticospinal projections which innervate small groups of motoneurone pools (Shinoda, Yokota and Futami, 1981; Buys *et al.*, 1986), allowing fractionation of fine-grade movements (Zaaimi, Dean and Baker, 2018). The RST is involved in postural control (Prentice and Drew, 2001; Schepens and Drew, 2004, 2006) and muscle tone during gait (Takakusaki *et al.*, 2016). It also contributes to motor control of upper limb muscles (Honeycutt, Kharouta and Perreault, 2013; Dean and Baker, 2017). There is a presumed proximal dominance of the RST; however this has not been proven, and RST projections have even been found for the intrinsic hand muscles (Riddle, Edgley and Baker, 2009).

Neural adaptations to strength training have been demonstrated prior to intramuscular changes (Moritani and DeVries, 1979; Sale, 1988). Changes in motor cortical excitability (Kidgell *et al.*, 2017) and cortical inhibitory networks (Nuzzo *et al.*, 2017) occur during strength training, but not in corticospinal connectivity (as assessed by TMS latency in (Kidgell *et al.*, 2010). Consistent with this work in humans, our group recently showed that resistance training in two female nonhuman primates results in intracortical and reticulospinal adaptations, but no change in the corticospinal tract and motoneurone excitability (Glover and Baker, 2020). Based upon this known role of the reticulospinal tract in strength and posture, we wondered whether it might also drive centrally-based changes in sarcopenia.

3.2.3 Ipsilateral Motor Evoked Potentials (iMEPs)

Study of the different descending pathways in humans requires non-invasive ways to assess their function. Transcranial Magnetic Stimulation (TMS) uses brief high-intensity magnetic fields to excite cortical neurones (Barker, Jalinous and Freeston, 1985; Kobayashi

and Pascual-Leone, 2003). When applied over the primary motor cortex (M1), single pulse TMS excites the corticospinal tract and elicits motor evoked potentials (MEPs) in contralateral muscles, which are commonly used to assess corticospinal function (Edgley *et al.*, 1997).

TMS can also elicit iMEPs, particularly when facilitated by strong background contraction (Wassermann *et al.*, 1991; Wassermann, Pascual-Leone and Hallett, 1994), antagonistic (Tazoe and Perez, 2014) or phasic movements (Bawa *et al.*, 2004). iMEPs have higher thresholds for activation and longer latencies than contralateral MEPs (cMEPs), with previous studies of iMEPs using either 10% above active motor threshold (Carr, Harrison and Stephens, 1994; Bawa *et al.*, 2004), or 100% of maximum stimulator output (Wassermann *et al.*, 1991; Tazoe and Perez, 2014). The amplitude and latency of iMEPs are modulated by rotating the head (Ziemann *et al.*, 1999; Tazoe and Perez, 2014), consistent with prior work demonstrating that reticulospinal cells are modulated by neck proprioceptors (Pompeiano *et al.*, 1984; Srivastava *et al.*, 1984).

This latency and facilitation pattern is consistent with transmission via a brainstem relay and the reticulospinal tract, which would add additional synaptic delay. TMS delivered over M1 can activate reticulospinal cells transsynaptically via corticoreticular connections (Fisher, Zaaime and Baker, 2012). The reticulospinal tract originates from multiple nuclei in the pontomedullary reticular formation and projects to the cord bilaterally (Sakai, Davidson and Buford, 2009; Baker, 2011). This extensive divergence explains why ipsilateral muscle responses can be seen even when the stimulus activates only one cortical hemisphere and suggests that iMEPs could be used to assess reticulospinal function (Ziemann *et al.*, 1999).

This was an exploratory study measuring ipsilateral and contralateral motor evoked potentials (iMEPs/cMEPs) as a method of assessing reticulospinal and corticospinal contributions to age-related muscle strength losses in healthy younger and older adults.

3.3 Methods

3.3.1 Subjects

Ethical approval was obtained from the Newcastle University Medical Faculty ethics committee (approval number 14189/2018). We recruited candidates from a local volunteer pool. Exclusion criteria were based upon safety criteria for TMS (Rossi, Hallett and Rossini, 2011), including implanted medical devices and any history of epilepsy or other neurological condition. The clinical investigator (SM) conducted a brief medical interview to assess for any neuromuscular conditions or medications that may impact synaptic transmission. We

explained the purpose and procedure of the experiment, and all subjects signed informed consent to participate.

3.3.2 Anthropometry and sarcopenia stratification

We stratified all participants over the age of 50 using the revised European Working Group on Sarcopenia in Older People (EWGSOP) criteria for sarcopenia (Cruz-Jentoft *et al.*, 2018). The first step of this was to use the SARC-F 5 item questionnaire to screen for self-reported functional limitations of sarcopenia, namely strength, walking, chair rise, stair climbing and falls (Malmstrom *et al.*, 2016).

Hand grip was chosen to measure strength as it is widely used clinical measure, and forms part of sarcopenia diagnostic criteria (Cruz-Jentoft *et al.*, 2018). Participants self-reported their hand dominance. In all individuals, grip strength (F) was measured only in the participant's self-reported dominant hand using a Jamar hydraulic dynamometer (J. A. Preston Corporation, NJ, USA). Following revised EWGSOP criteria (Cruz-Jentoft *et al.*, 2018), we considered all individuals with grip strength below a set level (male <27kg, female <16kg) to have probable sarcopenia.

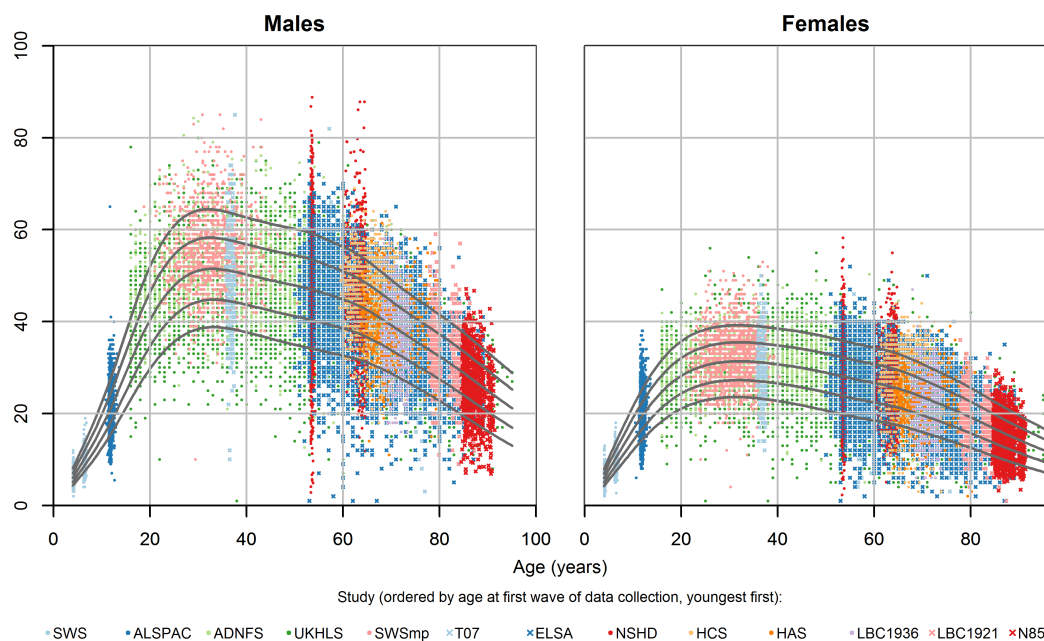


Figure 3.1 Grip strength through the life course. Adapted from Dodds *et al.* 2014.

Grip strength varies widely and non-linearly during the life course, and between genders (Figure 3.1). Grip strength was therefore standardised to age and sex using the 'LMS' method relative to a large UK population dataset (Dodds *et al.*, 2014). Used initially in describing child growth centiles (Cole, 1989), LMS estimates population distributions using

the age and sex-specific skew (L), median (M) and generalised coefficient of variation (S) to produce an individual z-score from measured force F, using the following formula:

$$z = \frac{(F/M)^L - 1}{S \times L}$$

Whole body muscle mass was estimated using anthropometry via a Tanita BC-545n Bioimpedance Analyser (Tanita Europe, Amsterdam, The Netherlands) which utilises the differential impedance of electrical current through the body to estimate the lean muscle mass (LMM) and total weight of the participant. These impedance values have been calibrated on a European population group (Tanita, 2020). Muscle mass is strongly correlated with height, and so was standardised in a similar way to BMI (LMM/height²) as previously described in the literature (Kim, Jang and Lim, 2016).

3.3.3 EMG & TMS Measurements

We recorded electrical signals using Ag/AgCl electrodes (50mm Covidien H34SG) attached bilaterally across the belly of both biceps brachialis. The centre of each electrode was separated by 10cm. This muscle was selected for its involvement in performing the rowing task, and because iMEPs have been reported in healthy subjects using this muscle previously (Turton *et al.*, 1996; Ziemann *et al.*, 1999; Bawa *et al.*, 2004; Tazoe and Perez, 2014).

For TMS, we used a Magstim 200² with a figure-of-eight coil, winding diameter 70mm, placed on the left side of the head in order to produce a right-sided cMEP, and left-sided iMEP. The coil was placed tangential to the scalp and at 45° to the mid-sagittal plane, so that induced current flowed from posterior-lateral to anterior-medial. This placement was irrespective of the subject's handedness.

The subject wore a headband with reflective markers, with similar markers on the TMS coil, with coil position mapping via the Brainsight neural navigation system (Rogue Industries, Montreal, Quebec). The structural shape of the subject's head was mapped using pointers. The 'average MNI head model' was loaded within Brainsight, but this was not used for navigation relative to brain structures; rather, the Brainsight system merely allowed us to maintain the coil over the hot spot, defined relative to the skull. The coil was held in place manually with visual feedback to maintain coil position fixed relative to the head, despite participant movement. We then localised the motor cortical representation of biceps by optimising coil placement with visual feedback from the neural navigation system to produce a maximal amplitude MEP in the contralateral biceps during weak contraction. While there

was some movement of the head during the task, this was extremely small when tracked using Brainsight (<1cm) relative to the very high coil output used (70-100%MSO).

Once we located the hot spot, we determined the active threshold as being the level of TMS output to the nearest 5% of maximum stimulator output that produced a MEP in contralateral biceps during a sustained weak contraction with amplitude greater than 0.3mV in at least 3 of 6 stimuli. This was chosen to prevent coil overheating later in the experiment due to overuse, as previously proposed (Groppa *et al.*, 2012).

3.3.4 Rowing task

Subjects used a seated resistance exercise training machine in a rowing configuration, which provided 12kg of resistance per arm. The rowing machine was configured with two handles and resistance bands to ensure both arms contributed equally and separately to the rowing action, and subjects arm position was observed during the task to ensure consistent bilateral movement. All subjects rowed against the same fixed resistance level. Subjects performed a bilateral rowing movement against this resistance, with movement start cued by an auditory beep. They maintained a vertical torso position and kept hands supinated in order to activate biceps during the contraction.

Head position was maintained at 30° to the left of midline (towards the left biceps). Maximal neck turn maximises iMEP amplitude (Tazoe and Perez, 2014), however this angle was chosen to be safe and feasible while remaining consistent with previous investigations on neck angulation on muscle tone (Aiello *et al.*, 1988). We provided an audible, but non-startling auditory start stimulus at intervals of 5-6s randomly chosen from a uniform distribution, to avoid anticipation (Awiszus, 2003). TMS was applied 300ms after the auditory cue in order to occur during the subjects' movement. A summary of the experimental protocol is shown in Figure 3.2A.

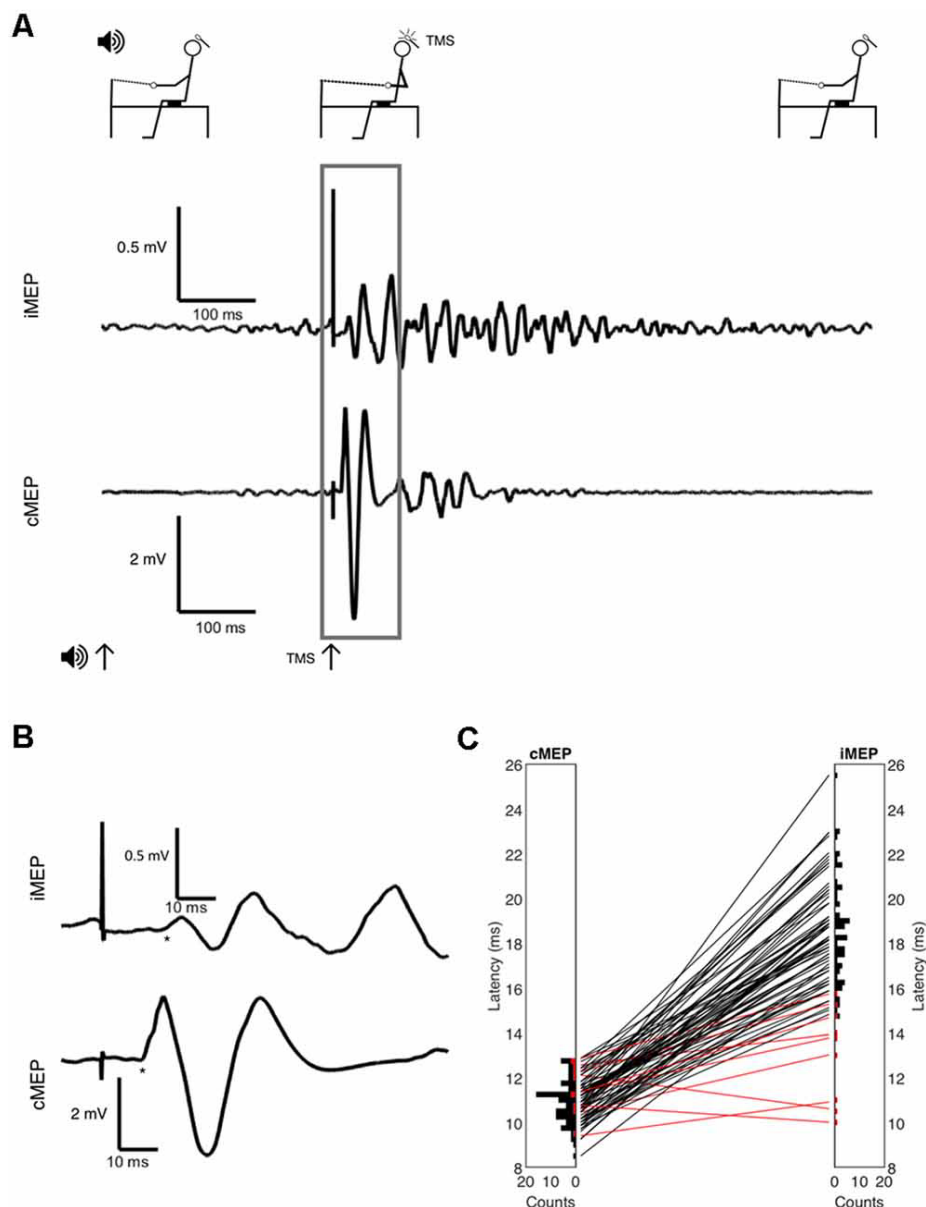


Figure 3.2 Full experimental paradigm showing subject position, onset of auditory cue at $t=0$, onset of TMS at $t=300\text{ms}$, and EMG. Volitional EMG activity builds after auditory cue, with large synchronous MEP after TMS indicated and inset in (B) with selected area and onsets marked with *. (C) Latency histograms and differences between cMEP & iMEP latencies shown. Each line is a subject, with iMEPs deemed invalid due to low latency difference (< 5 ms) in red.

Twenty movements with TMS were performed at each TMS intensity, (0, 5, 10, 15, 20, and 25% of maximum stimulator output above the active motor threshold) in two blocks of ten TMS pulses, for a total of 120 stimuli per subject. To collect background activity, some movements without TMS (audio cue only) were scattered within blocks, meaning up to fourteen movements could be performed per block, including exactly ten movements with added TMS stimuli, and two to four movements without TMS.

The sequence of blocks was arranged randomly but identical between participants. In total, subjects performed 160 rowing movements, and the experiment lasted up to 16 minutes. Participants were observed and questioned for any self-reported fatigue during this with ample opportunity for breaks during the experiment.

EMG activity was amplified using a Digitimer D360 amplifier (Gain 300, bandpass 30 Hz – 2kHz) and sampled at 5KHz using a micro1401 interface (Cambridge Electronic Design (CED), Cambridge, UK) which also controlled the TMS pulse and auditory cue, programmed using Spike2 sequencing software (also CED).

3.3.5 Data and statistical analysis

Data were exported and analysed using Matlab R2019a. The twenty unrectified MEPs within each stimulus intensity were averaged, as were the forty background EMG traces.

To assess validity of iMEPs, a custom program presented averaged MEPs within each TMS intensity and electrode in a random order to one of the authors (SM), who determined onset latency subjectively by the point of divergence from background activity. The rater was blinded to identifying features of participant and laterality and marked onset latency with a cursor.

Matlab was used to measure peak-to-peak amplitudes in the subsequent 10ms of MEP. We then selected the TMS intensity for each participant which elicited the highest valid iMEP amplitude for further analysis. Although cMEPs recruit to higher amplitudes with increased TMS intensity, this is not necessarily true for iMEPs, which may be affected by the ipsilateral cortical silent period (Wassermann *et al.*, 1991; Meyer *et al.*, 1995). Interhemispheric inhibition increases with higher intensities (Ferber *et al.*, 1992), as does iMEP amplitude. Depending on which process increases faster, iMEPs could either grow or diminish with increases in stimulation strength. This means that the highest TMS intensity does not always yield the largest iMEP.

There was no minimum amplitude for an iMEP. Although this has been used previously (Bernard, Taylor and Seidler, 2011), we felt that in older adults the reduced peripheral nerve

conduction velocity (Palve and Palve, 2018) leading to dispersion and lower compound muscle action potential amplitude (Taylor, 1993), would limit the validity of these measures.

After calculating the latency difference between onset of cMEP and iMEP, we then rejected data from subjects where this was less than 5ms as being possibly due to direct activation of the contralateral cerebral hemisphere by current spread (Turton *et al.*, 1995; Ziemann *et al.*, 1999) rather than a true iMEP. While iMEP latencies more than 10ms longer than the cMEP are theoretically compatible with a transcallosal pathway on the basis of latency alone, (Ziemann *et al.*, 1999), this route is unlikely. iMEPs have been detected even in patients with agenesis of the corpus callosum (Ziemann *et al.*, 1999), and transcallosal effects are usually inhibitory, especially at higher intensities (Ferbert *et al.*, 1992; Sohn *et al.*, 2003). Accordingly, no upper bound was set for the latency difference.

The amplitude of iMEPs & cMEPs is affected by many factors, such as excitability of motoneuron pools (Eisen *et al.*, 1991) and peripheral factors that could limit the compound muscle action potential such as muscle density (Yuen and Olney, 1997) and subcutaneous fat (Nordander *et al.*, 2003). To correct measurements for this, we calculated the ipsilateral to contralateral amplitude ratio (ICAR) as previously described (Bawa *et al.*, 2004). Greater ICAR values indicate higher reticulospinal control of muscles, whereas lower ICAR values indicate higher corticospinal control of muscles.

We calculated Pearson correlations between clinical measurements (grip strength, standardised grip strength, height, lean muscle mass) and ICAR. We also compared categorical variables between age groups with Fisher's exact test. Continuous anthropometric measurements were tested for normality using the Anderson-Darling test (Anderson and Darling, 1952).

3.4 Results

3.4.1 Participant characteristics

There were 83 participants; descriptive characteristics are listed in Table 3.1. A bimodal distribution of ages was seen, with means around ages 20 & 70 (Figure 3.3). The experiment was well tolerated, and no participants experienced any adverse symptoms (syncope, seizure and transient hearing changes have previously been reported (Rossi *et al.*, 2009)) or withdrew from the investigation. We elicited valid iMEPs (see Methods for latency criteria) in 73 participants. As expected, raw grip strength was significantly different between age groups ($p=0.01$); however other anthropometric measurements, including

height, weight, gender & handedness were statistically similar (Table 3.1). Normality testing failed to reject the null hypothesis at 5% significance level.

Our participant population was representative, and z-scores of grip strength followed the normal distribution with 55 (66.2%) within the range [-1,+1] and 79 (95.2%) within the range [-2,+2]. The Anderson-Darling test for normality failed to reject the null hypothesis. Five participants met revised EWGSOP criteria for probable sarcopenia, based upon low grip strength.

3.4.2 iMEPs

We were interested to see if the reticulospinal system was implicated in age-related muscle weakness. Ageing affects several parts of the motor system, and it was necessary to delineate these differences first.

cMEP thresholds were significantly ($p=0.026$, t-test) higher in the younger age group (69.5%, 95% CI 64.52-74.45, Cohen's d effect size 0.51) compared to the older age group (63.7%, 95% CI 58.5-66.13). The TMS intensity required to produce maximal iMEP was 80.1% (95% CI 76.9-83.3) across ages, 86.9% (95% CI 82.5-91.2) in those aged <50, and 76.5% (95% CI 72.4-80.6) in those aged ≥ 50 . This was significantly different between age groups (t test $p=0.0016$, Cohen's d effect size 0.71).

We elicited iMEPs from all 29 participants in the younger age group, compared to 44 of 54 older participants. The iMEP success rate was significantly different between age groups ($p=0.013$, Fisher's exact test). We examined this subgroup closer to check whether iMEP non-

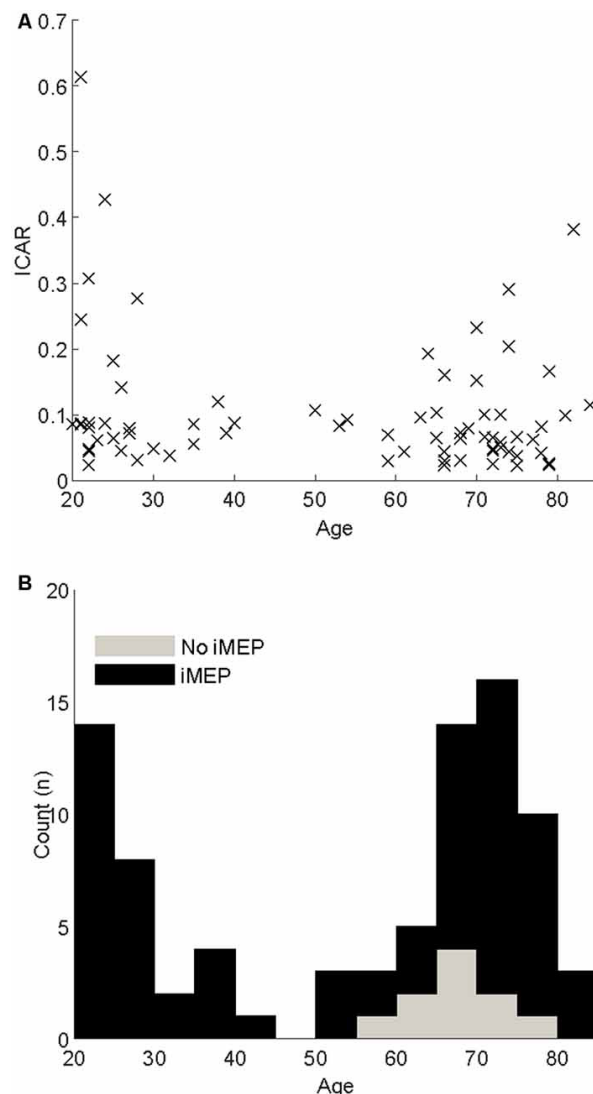


Figure 3.3 (A) Scatter of the Ipsilateral-Contralateral Amplitude Ratio (ICAR) changes with age (B) Stacked histograms indicating the age distribution of participants. Black bars indicate participants where iMEPs were elicited; grey indicates participants without

responders differed from responders, but the two subgroups were of comparable age, gender, handedness and grip strength, with no statistically significant differences (Table 3.1B). While the experiment was not altered for handedness, all data were measured post-hoc to ensure that removal of left-handed individuals did not significantly alter results.

Table 3.1 Participant characteristics. All participants compared in (A), older participants divided by iMEP response in (B). All values compared with Students T-Test, except categorical measures of gender & handedness indicated with F which were compared with Fisher's exact test.

A	Age <50 (n=29)	Age ≥50 (n=54)	p	B		p
				iMEP (n=44)	Age ≥50 No iMEP (n=10)	
Male	11	21		17	4	
Female	18	33	1.00 ^F	27	6	1.00 ^F
Right-handed	27	52	0.61 ^F	42	10	1.00 ^F
Height (SD)	170(9.1)	166.7(13.4)	0.24	167.9(9.7)	161.7(23.8)	0.19
Weight (SD)	67.1(15)	69.1(23.4)	0.68	70(23.4)	65.1(24.2)	0.56
LMM (SD)	47.8(8.4)	49.15(10.5)	0.55	44.4(17.3)	45.2(19.5)	0.90
Grip-kg (SD)	35.2(9.3)	29.6(9.03)	0.01	29.5(8.9)	30(11.3)	0.89
Grip-z (SD)	0.11(1.04)	0.15(1.12)	0.39	0.15(1.11)	-0.17(0.77)	0.39
Valid iMEP	29	44	0.013^F	-	-	-
cMEP threshold (SD)	69.5(13)	63.7(14.1)	0.028	63.6(13.9)	56.5(13.6)	0.14

Example MEPs are shown in Figure 3.2A&B, demonstrating the longer latency and reduced amplitude of iMEPs compared to cMEPs. Mean iMEP amplitude was 0.29 mV (95% CI 0.238-0.349). In ages < 50 this was 0.361 mV (95% CI 0.262-0.459) and 0.248 mV (95% CI 0.181-0.315) in those aged ≥ 50 . This just failed to reach statistical significance (t-test, $p=0.0505$).

iMEP latency followed a much wider distribution (mean 18.6ms, SD 2.3) compared to cMEPs (mean 10.9ms, SD 0.95; *F*-test for equality of variance, $p<0.001$, Figure 3.2C). The mean iMEP latency in ages<50 was 17.8ms (95% CI 16.8-18.7) compared to 19.1ms (95% CI 18.4-19.8) in ages ≥ 50 . This was significantly different (t-test $p = 0.022$, Cohen's *d* effect size 0.61).

3.4.3 Ipsilateral/Contralateral amplitude ratios

ICAR values varied widely between individuals (range 0.02-0.43) but were comparable to previous reports (Wassermann, Pascual-Leone and Hallett, 1994; Bawa *et al.*, 2004). This experiment involved a fixed-weight resistance task, and since MEP behaviour is dependent on the degree of voluntary muscle activation, it was important that any differences observed were not simply a result of differing ability to complete the rowing task. ICAR values across age groups were not significantly correlated with LMM/height², as shown in Figure 3.4 ($r=-0.196$, $p=0.097$), and unrelated to gender ($p=0.833$, t test). ICAR was also uncorrelated with age ($r=-0.175$, $p=0.138$), height ($r=-0.044$, $p=0.713$) or raw uncorrected grip strength ($r=0.011$, $p=0.924$).

After splitting data into age groups, we discovered an intriguing relationship between ICAR and strength measures. ICAR was not correlated with age in younger ($r=-0.21$, $p=0.28$) or older ($p=0.01$, $p=0.95$) age groups. Raw grip strength showed no relationship with ICAR values in younger ($r=-0.203$, $p=0.292$), or older ($r=0.145$, $p=0.348$) age

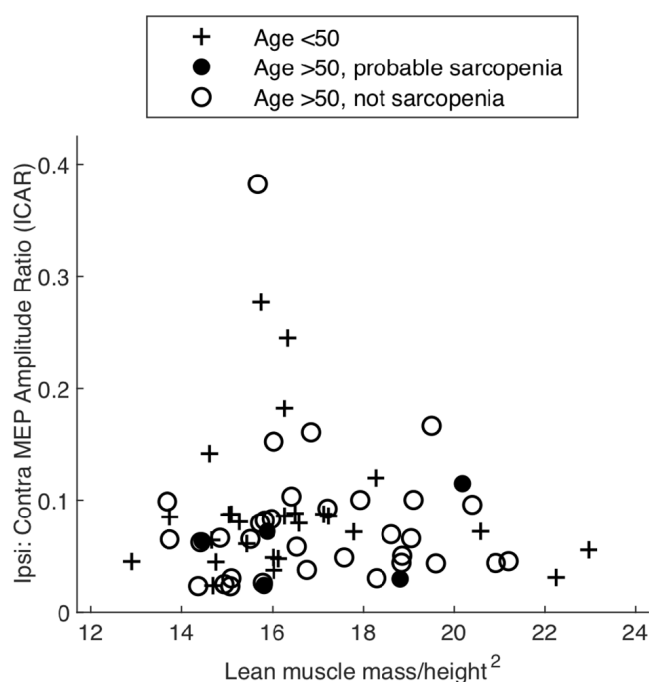


Figure 3.4 Amplitude Ratio (ICAR) compared to a measure of muscularity (Lean muscle/height²) in different age groups & sarcopenia.

groups. However, raw grip strength has a strong non-linear relationship with age and sex (Dodds *et al.*, 2014), which could obscure a more subtle relationship with ICAR. We therefore calculated a standardised z score as described in Methods, which removed the influence of age and sex. This z score measures whether an individual is stronger or weaker than would be expected, given the range of strengths seen across a population of the same age and sex. In the younger cohort, there was a significant negative correlation between standardised grip strength and ICAR ($r=-0.37$, $p=0.045$; Figure 3.5). Surprisingly, in the older cohort this correlation was also significant, but of the opposite (positive) sign ($r=0.43$, $p=0.0037$; Figure 3.5). The two correlation coefficients were significantly different ($p=0.049$) when compared using Fisher's method (Fisher, 1921). Younger subjects who were stronger than expected for their age and sex had smaller ICAR; by contrast, stronger older subjects had greater ICAR.

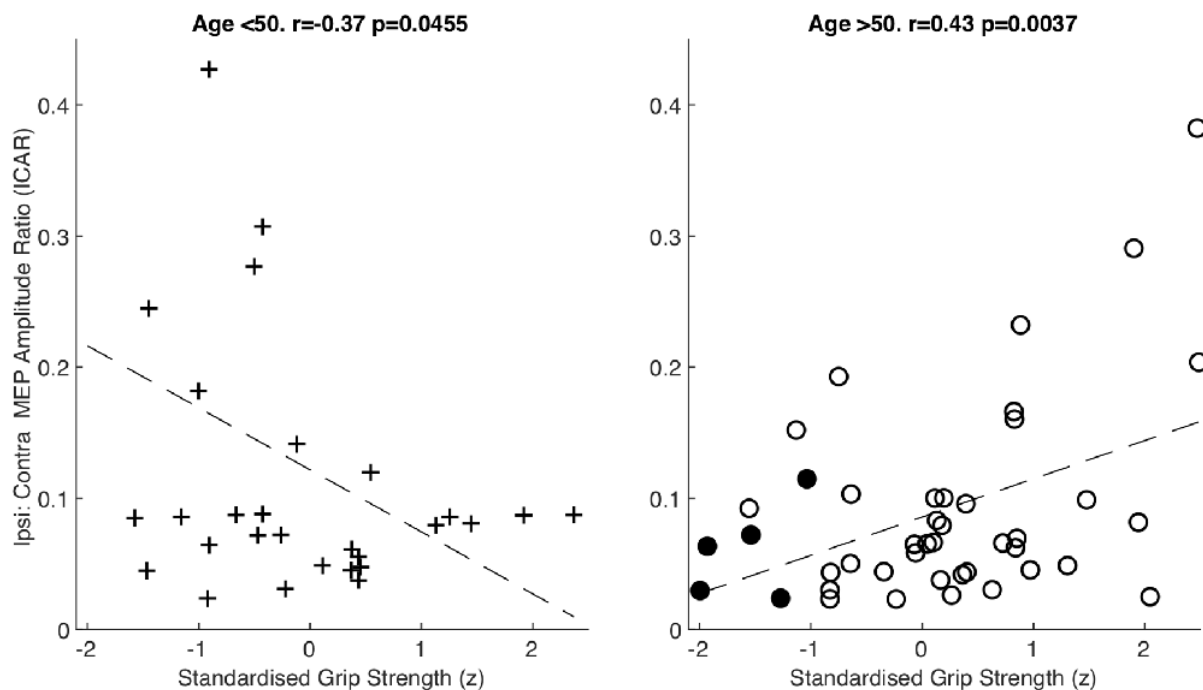


Figure 3.5 Amplitude ratio (ICAR) compared to standardised grip strength in both age groups. Sarcopenic patients are highlighted with filled circles.

3.5 Discussion

In this study, we assessed RST function non-invasively with TMS and a bilateral rowing task to record iMEPs. For the first time in humans, we have demonstrated that strength is related to non-invasive measures of RST function, which differ between younger and older people.

3.5.1 Key findings

In younger adults, those with lower standardised grip strength had higher ICAR values. This was unexpected, given our previous work which showed that strength training enhances the RST (Glover and Baker, 2020); we might therefore have expected the stronger individuals to have larger ICAR, reflecting more prominent RST projections. However, it must be remembered that ICAR is a measure of the ratio of iMEP and cMEP amplitude. In healthy young monkeys, we previously showed that strength training led to an increase in cortical excitability and thus elevated cMEPs (Glover and Baker, 2020). A careful meta-analysis also revealed marginal evidence for increased cMEPs after strength training in humans (Kidgell *et al.*, 2017). Particularly strong young subjects may have both enhanced cMEPs and iMEPs, leading to an unremarkable ICAR which was similar to those of more typical strength.

By recruiting a relatively large number of subjects, we were able to demonstrate significant correlations with functional measures even in the face of considerable inter-subject variability. This includes demonstrating a significantly lower active motor threshold for both cMEPs and iMEPs in older participants, in contrast to previous studies which have shown no relationship (Matsunaga *et al.*, 1998; Wassermann, 2002; Pitcher, Ogston and Miles, 2003). While this could be due to sulcal effacement with age (Parashos and Coffey, 1994) reducing the distance to the TMS focal point, the reduction in brain volume with age (Svennerholm, Boström and Jungbjer, 1997) would be expected to counter this effect, and further investigation is needed to assess this. While we did not record ethnicity during this study, this has not been shown to significantly affect thresholds between Caucasian/Japanese/Han Chinese populations (Suzuki *et al.*, 2021).

As previously reported, iMEPs exhibited a significantly longer latency than the corresponding cMEP in the majority of individuals, supporting mediation by an indirect pathway involving the RST (Ziemann *et al.*, 1999). While iMEP latency was significantly longer in older individuals, this is likely due to reduced peripheral nerve conduction velocities with age (Palve and Palve, 2018).

3.5.2 Potential pathophysiologies

One potential explanation for the high ICAR measures in weaker young subjects is that these individuals were physically weaker due to non-neural factors (e.g. nutrition or genetic factors influencing muscle physiology). As many daily activities require a fixed level of activation, these subjects may have been exposed effectively to a strength training regime merely by performing their activities of daily living. Regularly performing contractions close to maximum effort could have led to strengthening of the RST, as we have previously reported

(Glover and Baker, 2020). If so, this neural adaptation would render these subjects stronger than they would be otherwise, but still weaker than their peers. The situation is perhaps reminiscent of the correlation which we have reported previously in stroke patients, where more severely affected patients show an enhanced RST projection (Choudhury *et al.*, 2019) which likely allows some restoration of function. If so, the negative correlation seen here in young subjects reflects compensation for weakness, rather than part of the underlying cause of weakness itself. A further possibility is that the primary weakness was caused, not only by peripheral factors, but also by mild corticospinal loss. This would also lead to RST strengthening, and further elevate the RST: CST ratio measurement ICAR, in an even closer analogue to our past observations in stroke patients and animals after corticospinal tract lesions (Zaaimi *et al.*, 2012; Choudhury *et al.*, 2019).

3.5.3 Clinical implications

In older adults, a positive correlation between standardised grip strength and ICAR was seen, suggesting that those individuals who successfully maintain or enhance the RST are stronger. This correlation could arise from the effect of lifestyle. If a particular older subject regularly engaged in resistance training, we would expect this to increase muscle strength, and also to enhance RST output. Given the well-documented degeneration in the cortex and CST with ageing, there may be no corresponding changes in cortical excitability, producing the elevated ICAR which we observed. However, it was of interest that the five older subjects with sarcopenia all had low ICAR ratios. This raises the intriguing possibility that the correlation between ICAR and normalised strength may reflect an underlying difference in the biology of age-related RST degeneration across our cohort, with a possible primary role in producing the sarcopenic state. Although this remains only a speculative possibility at the moment, it is a hypothesis worthy of further investigation. If correct, one prediction is that lowered RST output might predict those at risk of age-related muscle weakness and sarcopenia.

3.5.4 Methodological considerations

One limitation which must be acknowledged is that although the motivation for our study was to improve understanding of age-related muscle weakness, we were able to recruit only five sarcopenic patients in our community-based cohort. Still, this did have the advantage of placing changes in sarcopenia in the context of strength variation across the wider population.

It must also be noted that we measured grip strength as our primary measure of sarcopenia due to its widespread use and clinical validity in diagnosis, but iMEPs were elicited on biceps. However, grip strength correlates well with strength through the rest of the body including in the biceps muscle (Hyatt *et al.*, 1990; Cruz-Jentoft *et al.*, 2018). Eliciting iMEPs in the more distal muscles that are related to grip remains extremely challenging (Bawa *et al.*, 2004). The current experimental design therefore seems a reasonable compromise.

We felt that standardising grip strength to age and sex helped to counter for the non-linear variability of grip strength. It was therefore encouraging to see that standardised results demonstrated significant findings, while non-standardised did not.

Correlations between standardised grip strength and ICAR may be led by subjects with ICAR values > 0.2 ; removal of these subjects from the dataset means the correlation was no longer significant in either age group. We reviewed this subgroup of subjects carefully however, and found no reason to believe that there was any discrepancy in their task-performance, anthropometry, nor their behaviour during the experiment. We have therefore included these data. Human strength is highly variable, particularly in older subjects (Dodds *et al.*, 2014), and understanding the range of this variability is important to understand susceptibility to sarcopenia.

Earlier studies showed that the optimal site for iMEPs in biceps is often located anteromedial to that for cMEPs (Tazoe and Perez, 2014). Given the dynamic nature of the rowing task used to test iMEPs, it was impractical here to optimise the iMEP stimulation site, and instead we used the cMEP hot spot. This may mean that the amplitude of iMEPs was underestimated, and likewise may increase iMEP latency and observed iMEP threshold due to increased distance of cortical tissue from the TMS focal point.

The resistance against which subjects rowed was fixed at 12kg force, and it is highly possible that subjects were performing at different proportions of their maximal strength, and therefore different %MVCs. Higher levels of muscle activation have been shown to be more likely to produce iMEPs (Ziemann *et al.*, 1999). The fact that there was no relation between ICAR and raw strength nor LMM argues powerfully that our results are not simply driven by an artefactual effect of differences in contraction level as a percentage of each subject's maximum.

Joint angle and muscle activity level (%MVC) were not measured during this experiment. However, this was a bilaterally symmetric movement, so that there cannot have been differences in muscle activity between the two sides. Both cMEPs and iMEPs were

assessed following stimulation of the same motor cortex (left hemisphere); any changes in cortical excitability related to joint angle would therefore be the same for cMEPs and iMEPs. This might cause both measures to increase or decrease together, but could not alter their ratio as measured by ICAR.

iMEP amplitude is partly dependent upon interhemispheric inhibition (Ferber *et al.*, 1992). It is therefore possible that effects we have demonstrated are not due to reticulospinal tract, but rather interhemispheric inhibition (IHI). To counter this, we have measured the peak iMEP amplitude, across varying TMS intensities, and measured the strongest iMEP response (where IHI is therefore lowest).

3.5.5 Future research

Finally, this work suggests a potential role of the RST for neurorehabilitation of individuals with sarcopenia. Techniques which stimulate the RST, including startling acoustic stimulus (Fernandez-Del-Olmo *et al.*, 2014; Bartels *et al.*, 2020) should be explored to measure the importance of neural adaptations on strength training in a cohort with age-related muscle weakness.

3.5.6 Conclusion

Here we have shown how age-related strength changes are related to the balance of descending motor drive between corticospinal and reticulospinal tract, as measured via non-invasive brain stimulation measure (ICAR).

4. Electrical cross-sectional imaging of human motor units *in vivo*

4.1 Contribution statement

This chapter reflects a paper now published in Clinical Neurophysiology (Maitland *et al.*, 2022). It reflects a wider project with contributions from several other members of staff to manufacture the electrodes and meet safety standards. I was not involved in these steps, however I have been working with this team to develop the electrode, and have contributed to creating the signal processing algorithm described, signal recording, data analysis, and writing a large part of this manuscript.

4.2 Highlights

- Biocompatible, clinically suitable multi-electrode EMG needle
- Hundreds of muscle fibres can be localised from brief (< 5 minute) recordings
- Motor unit territory is shown to overlap *in vivo*

4.3 Abstract

Objectives

In many neuromuscular diseases, weakness results from a disruption in muscle fibres' arrangement within a motor unit. Limitations in current techniques mean that the spatial distribution of fibres in human motor units remains unknown.

Methods

A flexible multi-channel electrode was developed and bonded to a clinical electromyography (EMG) needle. Muscle fibre action potentials were localised using a novel deconvolution method. This was tested using simulated data, and in recordings collected from the tibialis anterior muscle of healthy subjects.

Results

Simulated data indicated good localisation reliability across all sections of the electrode except the end sections. A corrected fibre density was estimated up to 1.4 fibres/mm². Across five recordings from three individuals, between 4 and 14 motor units were detected. Between 1 and 20 muscle fibres were localised per motor unit within the electrode detection area, with up to 220 muscle fibres localised per recording, with overlapping motor unit territories.

Conclusions

We provide the first direct evidence that human motor units spatially overlap, as well as data related to the spatial arrangement of muscle fibres within a motor unit.

Significance

As well as providing insights into normal human motor physiology, this technology could lead to faster and more accurate diagnosis in patients with neuromuscular diseases.

4.4 Introduction

The spatial distribution of muscle fibres within a motor unit is of fundamental interest in both healthy and diseased muscle. To date, the only means of accurately demonstrating the spatial distribution of muscle fibres has been the glycogen depletion technique (Edstrom and Kugelberg, 1968). These complex experiments can only be performed in animals since they require the histological analysis of explanted muscle cross-sections exposed to high-frequency electrical stimulation for several minutes. These experiments demonstrate that individual muscle fibres within a motor unit are widely separated (Bodine *et al.*, 1988; Bodine-Fowler *et al.*, 1990), and that a single motor unit can cover up to 50% of the cross-sectional area of the muscle (Buchthal, Erminio and Rosenfalck, 1959). From this, it has been inferred that the fibres in one motor unit overlap with several other units (Fig 1a). However, since only a single motor unit can be studied per muscle, this has never been shown directly. Furthermore, since only one muscle can be analysed per animal, most studies using the glycogen depletion technique describe 5-10 motor units at best. Consequently, the statistical distribution of muscle fibres within a normal motor unit remains open to debate with random (Edstrom and Kugelberg, 1968), regular (Kugelberg, 1973) and clustered (Buchthal, Guld and Rosenfalck, 1957) models having been proposed. Further neurophysiological investigations of the motor unit include determining the territory of a motor unit with a linear multi-electrode (Buchthal, Erminio and Rosenfalck, 1959), the electrical activity of the whole motor unit via macro EMG (Stålberg and Fawcett, 1982), and the statistical distribution of muscle fibres through the territory of the motor unit via scanning EMG (Stålberg and Dioszeghy, 1991).

Changes in the spatial distribution of muscle fibres within motor units are among the earliest changes in many neuromuscular diseases. For example, in Amyotrophic Lateral Sclerosis (ALS), progressive loss of motor nerve axons removes the nerve supply to those muscle fibres in the dependent motor units (Nijssen, Comley and Hedlund, 2017). Compensatory re-innervation by the surviving axons results in larger motor units containing clusters of closely-packed muscle fibres (Schwartz *et al.*, 1976). Although these changes can be shown using the glycogen depletion technique in animal models, this is only possible in human subjects in a limited capacity via fibre density which measures the number of single fibre action potentials within the limited sampling territory of a single fibre electrode (Sanders *et al.*, 2019) and does not indicate relationship of fibres to one another. Recent developments such as motor unit MRI (Birkbeck *et al.*, 2020) have permitted the size, shape and dimensions of individual human motor units to be determined, but the relatively low

spatial resolution (approximately 1mm² voxel size) makes it impossible to detect the position of individual muscle fibres using this method.

Gross changes in motor unit structure can be inferred from intramuscular electromyography (EMG). Since only a single recording surface at the tip of the needle is used (Whittaker, 2012), the resulting motor unit potential (MUP) represents the temporally and spatially summated activity of every muscle fibre within approximately 2.5 mm of this surface (Dumitru, King and Nandedkar, 1997). Not surprisingly, attempting to infer changes in muscle fibre spatial distribution from this composite 1-dimensional signal requires expert interpretation, and even in the best hands, the technique has only moderate diagnostic accuracy and specificity (Narayanaswami *et al.*, 2016). The small sampling area also requires the needle to be moved to several positions within the muscle, increasing the time taken and the discomfort for the patient.

Early attempts to increase the sampling area with linear multi-electrode arrays with up to 14 recording surfaces (Buchthal, Guld and Rosenfalck, 1957) have not entered routine use due to the large cross-sectional area (up to 4x a conventional EMG needle) and the high manufacturing costs, requiring them to be re-sterilised. Furthermore, limitations in recording apparatus meant that only 1 or 2 channels of data could be recorded simultaneously. Hence, although individual fibres' position along the axis of the electrode could be estimated, the spatial distribution of these fibres within the motor unit cross-section could not be determined (E Stålberg *et al.*, 1976).

Substantial improvements in different technical fields over the last 20 years have now made it feasible to address these limitations. Electrodes have been developed with a high density of recording contacts over their shaft (Rousche *et al.*, 2001; Vetter *et al.*, 2004; Farina *et al.*, 2008; Sohal *et al.*, 2016; Jun *et al.*, 2017; Angotzi *et al.*, 2019; Musk, 2019); these have mainly been used in the central nervous system for recording neural activity, but similar techniques have also been applied to muscle (Muceli *et al.*, 2015). Integrated circuits have been developed incorporating multiple amplifiers and associated digitisation circuitry, allowing multiple channel recording with miniaturised equipment. Finally, computer storage and processing capacity has greatly expanded, making it feasible to deal with high data volumes. Here, we have exploited these advances to develop multi-electrode electromyography arrays with up to 32 contacts capable of simultaneously recording single fibre potentials from multiple motor units. Using this novel system, we can localise up to 220 muscle fibres with ~100 μ m accuracy in human muscle, in effect producing an electrical cross-sectional image of motor unit structure. Such images provide, for the first time, direct

evidence for the overlapping arrangement of motor units, and hold great promise for clinical application.

4.5 Methods

4.5.1 Probe design

We designed flexible multi-electrode arrays (which we named 'MicroEMG') comprising 32 recording surfaces sandwiched between two 10 μ m-thick layers of parylene-C, a biocompatible polymer with sufficient tensile strength to survive insertion through the skin without breakage (Figure 4.1B upper panel) (Sohal *et al.*, 2014). We used a tungsten:titanium (W:Ti) alloy for the electrode surfaces and interconnecting tracks (W:Ti 80:20 ratio) to provide greater flexibility than tungsten alone. Electrode arrays were fabricated on 3-inch diameter silicon wafers using standard semiconductor processing techniques. The recording electrodes were 20 μ m \times 30 μ m stadium shapes to match the recording area of clinical single-fibre EMG needles. The recording electrodes were arranged into 2-parallel rows with 400 μ m spacing and offset by 200 μ m to form a zig-zag pattern (Fig. 1B lower panel). From the first to the last recording electrode, the total length of the zig-zag array was 12.40 mm. These dimensions were chosen such that the array was long enough to record several motor unit cross sections simultaneously from a single insertion, but with sufficient spatial resolution to discriminate potentials recorded from individual muscle fibres (50-100 μ m diameter). Each recording electrode was connected to a bond-pad at the top of the flexible array via W:Ti tracks. The width of each track covered as much of the available area in the array as possible in order to minimise the chance of breakage, thinning progressively from the tip until they were 3 μ m wide with 2.8 μ m spacing as they entered the bond-pad region. To allow these flexible arrays to penetrate muscle, they were bonded to the shaft of a 480 μ m diameter clinical EMG needle (TECA Elite, Natus Neurology, USA) using a 1180-M UV-curable biocompatible adhesive (Dymax MD). The 20 μ m thick arrays occupied approximately 1/3 of the needle's circumference (Figure 4.1B), creating an approximately circular probe with diameter \sim 500 μ m. Bench-top electrical testing showed conduction in 330 out of 352 measured recording sites, a yield of 94% working channels. The average impedance in the functional channels was 502 k Ω \pm 109 k Ω measured at 1 kHz, and no leakage current was detectable between adjacent channels (with a current measurement resolution of 10 nA).

The bondpad region of the probe was clamped against the contacts of a custom-made printed circuit board housing a Intan RHD2132 32-channel low-noise amplifier chip with

integrated analogue-to-digital converter which sampled each channel at 20 kHz with 16-bit precision (Intan Technologies, USA) (Figure 4.1C).

The needle array and subsequent signal processing was designed for a position perpendicular to the muscle fibres, with the plane of the electrode grid arranged in a radial orientation (Figure 4.1D).

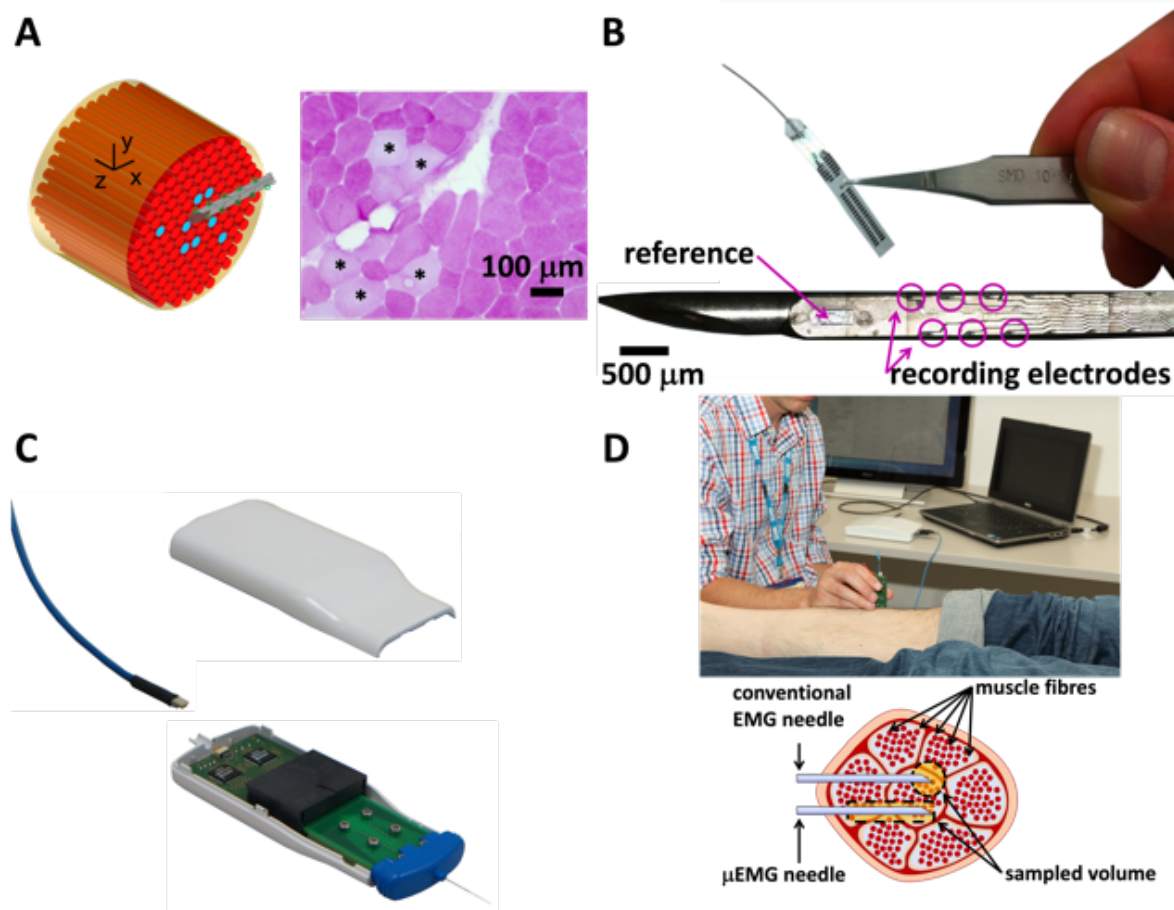


Figure 4.1 (A) Left; Schematic cross-section of a skeletal muscle. Muscle fibres (red cylinders) run approximately parallel to the long axis of the muscle and are grouped into motor units (pink circles). Axis definitions reference for the geometry referred to in all figures and equations. X axis indicates along the direction of the needle, and Y axis is perpendicular to this, radial to the muscle fibre direction. Z axis is perpendicular to the needle and runs along the direction of the muscle fibres. Right; spatial distribution of fibres in a single motor unit revealed by glycogen depletion. Non-depleted fibres stain purple. Depleted fibres (pink areas *) are widely spaced and interdigitate with fibres from several other motor units. (B) Upper panel: 32-channel flexible MicroEMG array comprising two 10 μm thick parylene layers encasing tungsten:titanium conductor prior to bonding. Lower panel: micrograph of MicroEMG array bonded to a conventional EMG needle. A 400μm wide zig-zag array of 32 recording electrodes (purple circles) each of 25 μm diameter extends 12,800 μm along the needle. (C) Sterile MicroEMG probe interfaced with INTAN 32-channel amplifier via a custom-made PCB. (D) Upper panel: system in use to obtain motor unit recordings from the tibialis anterior muscle of a healthy volunteer. Lower panel: conventional EMG (upper) records muscle fibre action potentials within ~1 mm of the needle tip. MicroEMG probe records from up to 32 electrodes spanning a 12.4 × ~2 mm corridor along the needle shaft.

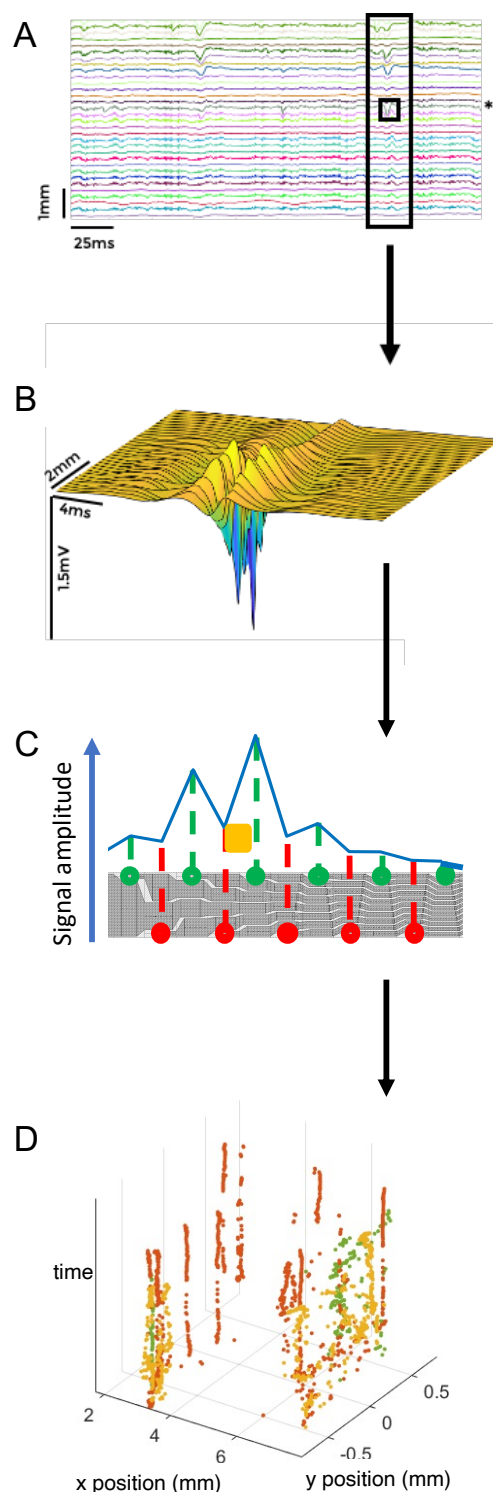
4.5.2 Signal Processing

The signal consists of multiple single fibre discharges, grouped into 1 or more motor unit activations. There are therefore a number of steps in order to meaningfully analyse the signal. After cleaning the signal, the motor unit action potentials must be identified and sorted into template groups. Then for each motor unit discharge, peaks in the signal amplitude must be identified as potential fibre positions. After this, the single fibre discharges must be deconvolved with a tissue function in order to identify the most likely candidate position for the fibre location.

Pre-Processing. Signals underwent band-pass filtering between 500Hz-10KHz. Residual mains noise was removed using an algorithm that removed components synchronous to 50Hz (Riddle and Baker, 2005). Broken channels were identified visually by very low amplitude signals and excluded from further analysis.

Motor unit extraction. Motor unit potential templates (MUPTs) were extracted from complex multi-channel data using a template matching algorithm, which utilised a multiresolution Teager energy operator employing pseudocorrelation (Sedghamiz and Santonocito, 2015; Sedghamiz, 2018). The channel with the highest SNR was selected for MUPT extraction, and the onset time of each potential recorded (Figure 4.2A).

Figure 4.2 Overview of signal analysis pipeline. After acquisition of multi-channel EMG signals (outer window is a multi-channel motor unit potential (MUP), inner window is a single channel MUP) (A) MUPs were extracted from the channel with the highest SNR (marked with *), MUPs were each averaged to produce a multi-electrode MUP (distance indicates x-axis distance) (B). Peaks in signal amplitude around the needle electrode (illustrated to simplify from 3 dimensions to 2 in C) were chosen as the starting point for muscle fibre localisation. Putative fibre location is indicated by the yellow square. Fibres were localised in space on a moving-average window across multiple firings. Fibre positions were tracked through time (Three motor units shown in D) and error values for localisation accuracy were calculated prior to k-means clustering of fibre positions.



Templates were inspected visually, and those which appeared to be noise transients on the basis of morphology or firing frequency were removed from further analysis. For each motor unit, a 10ms window was selected either side of the onsets of each MUPT, and across all the working electrodes of the array (Figure 4.2B) to produce the multi-electrode EMG for each MUPT.

4.5.3 Muscle fibre localisation

In order to reduce noise, ten consecutive motor unit discharges were averaged for analysis, effectively forming a moving average window. The averaged multi-electrode signal was processed with a top-hat transform (Maire *et al.*, 2000) to improve the delineation of transmembrane currents with similar locations and low inter-spike intervals (ISIs) while avoiding noise transients being incorrectly identified as fibre action potentials. Peaks in the rectified multi-electrode signal amplitude (Figure 4.1C) representing the electrodes with minimal radial distance to a fibre were identified using a peak-finding algorithm (Natan, 2013). Peaks were analysed in both time and space. The five EMG channels (an electrode ‘cluster’ as shown in Figure 4.3) surrounding each peak were selected. For each cluster, the 0.5ms of EMG before and after each peak was used in the next step of fibre localisation.

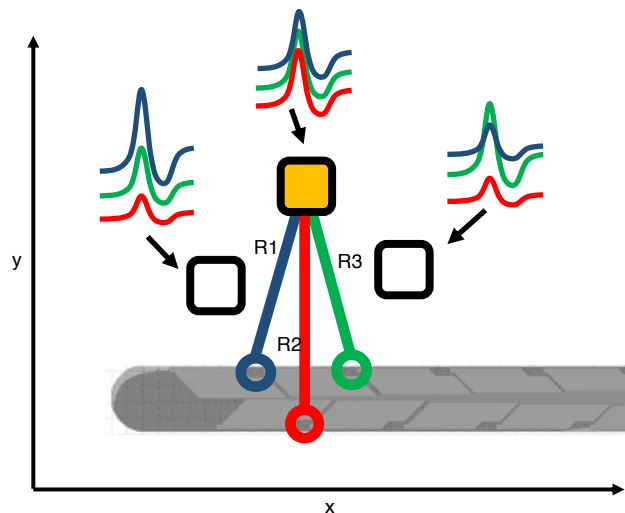


Figure 4.3 Fibre localisation in space, with x and y axes defined relative to the needle electrode. Black hollow squares indicate possible fibre locations, yellow square indicates position with minimum variance in deconvolved electrode potentials. The electrodes and the resulting deconvolved electrode potentials are shown in red, blue and green. A search was performed through possible fibre locations near to the recording electrode cluster. At each location, the Euclidean distance between the putative fibre and nearby recording electrodes was calculated. The potentials recorded at these electrodes were then deconvolved with a tissue function for these distances (R1,2,3) to produce n putative generator waveforms. The variance across these generator waveforms was then calculated, and the location of the fibre defined as the position with minimum variance.

The fibre localisation methodology was based upon the model used by (S. D. Nandedkar and Stålberg, 1983) to simulate single fibre action potentials (SFAP) recordings using a point electrode. This transmembrane current generating function (G_z) used by Nandedkar & Stalberg was derived from a volume conduction model (Rosenfalck, 1969) and was used to estimate the SFAP that would be recorded at a specific location. As the multi-electrode allows for the recording of the SFAPs at multiple sites near the active fibre, the muscle fibre

transmembrane current generating function could be estimated. The method used the convolution of the simulated generator function (G_z) and a weighting function (W).

$$W_{(r,z)} = \frac{1}{4\pi\sigma_r} \left(\frac{I}{\sqrt{Kr^2+z^2}} \right) \quad (1)$$

Where:

z = axial separation

r = radial separation

I = strength of current source

σ_r = radial conductivity

σ_z = axial conductivity

$$K = \sigma_z / \sigma_r$$

We defined the x axis as being parallel to the needle, and y axis as being perpendicular to the needle along the plane of the electrode surfaces. Further review of the geometry involved is described in Figure 4.1A. The weighting function defined by equation (1) describes the potential that would be recorded by a point electrode located at a radial distance r and axial distance z from a cylindrical current source/sink on the surface of the fibre. If the transmembrane current generating function (G_z) can be considered to be a propagating transmembrane current function moving at a constant velocity V along the z axis, this becomes a function in time t with distance d .

$$d = Vt \quad (2)$$

The recorded SFAP $V_{(r,t)}$ at a radial distance r and at some arbitrary location of z , is:

$$V_{(r,z+Vt)} = G_{(z+Vt)} * W_{(r,z)} \quad (3)$$

Where $*$ is the convolution operator, and the transmembrane current passes an electrode at coordinates r, z at $t=0$.

Using a multi-electrode, there are additional electrodes lying on a line of constant z at varying radial distance depending on the electrode separation from the muscle fibre. The SFAP recorded at each of these n sites may be used such that for each electrode, the deconvolution of the weighting function and the recorded SFAP should result in the same transmembrane current function.

$$V_{(r(n),z+vt)} \otimes W_{(r(n),z)} = G_{(z+vt,n)} \quad (4)$$

Where $r(n)$ is the radial distance between the fibre and the n th electrode and \otimes is the deconvolution operator.

The estimation is achieved by searching the solution surface in x and y to minimise the variance of the estimates of G_z . The deconvolution was implemented by the matrix method; in this case, the calculated weighting function for each electrode was constructed as a Toeplitz (diagonal constant) matrix. The matrix contains a sequentially time-shifted vector of the weighting function (Equation 1). This type of matrix has a well-behaved inverse (W^{-1}) such that the estimated G_z for each electrode can be calculated by:

$$V_{(r(n),z+vt)} * W^{-1}_{(r(n),z)} = G_{(z+vt,n)} \quad (5)$$

The radial distance term can be transformed to Cartesian coordinates in x,y . Using a suitable range of x,y coordinates, a solution surface may be defined with an error term:

$$E_{(r(n))} = 1 / (\text{mean}(\text{var}(G_{(z+vt,n)})))$$

An unconstrained non-linear optimisation algorithm (MATLAB function *fminsearch*) was used to find the value of the x,y coordinates which minimised the variance of the convolved multi-electrode potentials for each group of moving averaged motor unit discharges (Figure 4.2). A value of 5 was used for K as suggested by (S. D. Nandedkar and Stålberg, 1983). The variance function was constructed to measure the variance at each time point, and then measure the average of the variances across the window.

4.5.4 Fibre data visualisation

To summarise this localisation across time, the average number of fibres found at each motor unit discharge was calculated (Figure 4.2D). This average fibre count was then used as k to produce a k -means clustering of all the fibre positions. The median position of each cluster was taken to be the normative position of the fibre in calculating fibre density and nearest neighbour distances. The localisation estimate confidence was calculated using the mean consecutive position change. This would mitigate any 'slow drift' of needle position over the 5-minute recording related to operator technique, compared to large 'jumps' in position related to fibres within poor quality fibre potentials. For each motor unit, the distance between each localised fibre and its nearest neighbour was calculated and displayed as a cumulative probability plot. The fibre density was calculated based upon the fibre locations within the area 1mm off the needle's axis (defined as the point along the x axis through the midpoint of the two rows of electrodes with $y=0$). The current clinical definition of fibre density is the mean number of fibre action potentials within the uptake radius of a single fibre

electrode, with position optimised to be as close to a single fibre as possible, across twenty fibres (Stålberg, 1979). Estimates of this uptake radius vary, but range from 236-421 μm (Gath and Stalberg, 1979). We aimed to produce a comparable measurement based on the local fibre arrangements, and so measured the average number of fibres within an arbitrary 400 μm distance of each localised fibre, per motor unit (herein termed the needle fibre density). The motor unit territory was measured as the maximum Euclidean distance between any two fibre pairs. Both measures were again confined to muscle fibres localised to within the area 1mm off the needle's axis.

4.5.5 Modelling

In silico experiments were performed using simulated data to test the likely performance of our electrodes and our fibre-localisation algorithm. We modified a previously published model (Stashuk, 1993), which defines interdigitated motor unit territory, recruitment & firing rates, and realistic attenuation of EMG signal through tissue. Motor units were activated with inter-discharge intervals selected at random from a gamma distribution (Stein, 1965) of 9th order at a rate of around 10Hz. The estimated transmembrane current potential was based upon the product of transmembrane currents, using the linear quadrupole model ((S. D. Nandedkar and Stålberg, 1983)(Andreassen and Rosenfalck, 1981), 1981). We assumed that each fibre was cylindrical and orientated perpendicular to our array, in a medium with cylindrical anisotropy. We adjusted this model's parameters to be physiologically faithful in terms of the change of signal through increasing distances, with most of the signal attenuated at distances exceeding 1mm, as previously described in single fibre experiments (Stalberg and Antoni, 1980). Gaussian and mains noise were then added to the signal to achieve a signal to noise ratio of 5-10 dB.

All results were computed using a consumer laptop (MacBook Pro Intel i5 processor, 2016). The process took between 10 and 25 minutes depending upon the length of the recording and number of motor unit discharges.

Single fibre localisation accuracy. A single fibre was simulated in positions across a 7mm x 1.5mm (10.5mm²) grid in increments of 50 μm surrounding a simulated 32 electrode EMG needle. Error was measured by the Euclidean distance between the predicted and actual location.

Dual fibre resolution. Two fibres were modelled within a 0.8mm range of the needle's axis (defined as the midpoint between the two rows of electrodes), at radial separation of between 50 μm and 1.5mm (50 μm steps) and random orientations. This was repeated with

ISIs of 0.5ms, 1ms, and 2ms. For each linear distance, 100 trials were performed, for a total of 9,000 trials. The estimated number of fibres was recorded for each trial.

Multiple fibre count. Between 5 and 20 fibres were placed with positions selected from the uniform distribution within the central 5mm x 1.4mm (7mm²) search space. Fibre positions were independently selected i.e. there was no constraint on their proximity to one another. This central region was chosen to mitigate the edge effects of recording at the needle's furthest spatial extent. The mean nearest neighbour distance varied from 840µm to 320µm. Fifty trials were performed at each fibre count, with recordings of 10-second duration simulated and the estimated fibre count compared to the modelled number of fibres.

4.5.6 Human recordings

Studies were approved by the Ethics Committee of the Newcastle University Medical Faculty. Five recordings were made from the tibialis anterior muscles in 3 healthy controls, none of whom had any history of neuromuscular disease.

Signals were amplified (gain 200) and sampled to disc at 20 kSamples/s/channel using Intan software, together with the analogue output of a force transducer. Digital data were transmitted over a low voltage differential signal (LVDS) serial peripheral interface (SPI) bus to an interface card and then to a laptop computer. This stored data on a hard disc for later off-line analysis using custom-written MATLAB code (MathWorks, USA). The system was battery powered to ensure mains isolation, and a skin reference was used.

Subjects reclined on a couch with the force output at the ankle joint recorded using a Loadcell Amp PRO force transducer (Elane Electronics, USA). Probes were connected to the amplifier headstage at the bedside, and the probe was inserted into the muscle approximately perpendicular to the skin, with the plane of the electrode grid arranged in a radial orientation (Figure 4.1D). Tibialis anterior was selected since the orientation of its muscle fibres is known, allowing the probe to be oriented such that the fibres ran approximately perpendicular to the plane of the array. Subjects were asked to maintain 10% of the maximum voluntary contraction (MVC) strength under visual feedback for between 1 and 5 minutes. Subjects reported mild discomfort as the probe was inserted, and once in place the probe was held still within the muscle within a single position. Recordings were well-tolerated, and no bruising or bleeding was observed.

4.6 Results

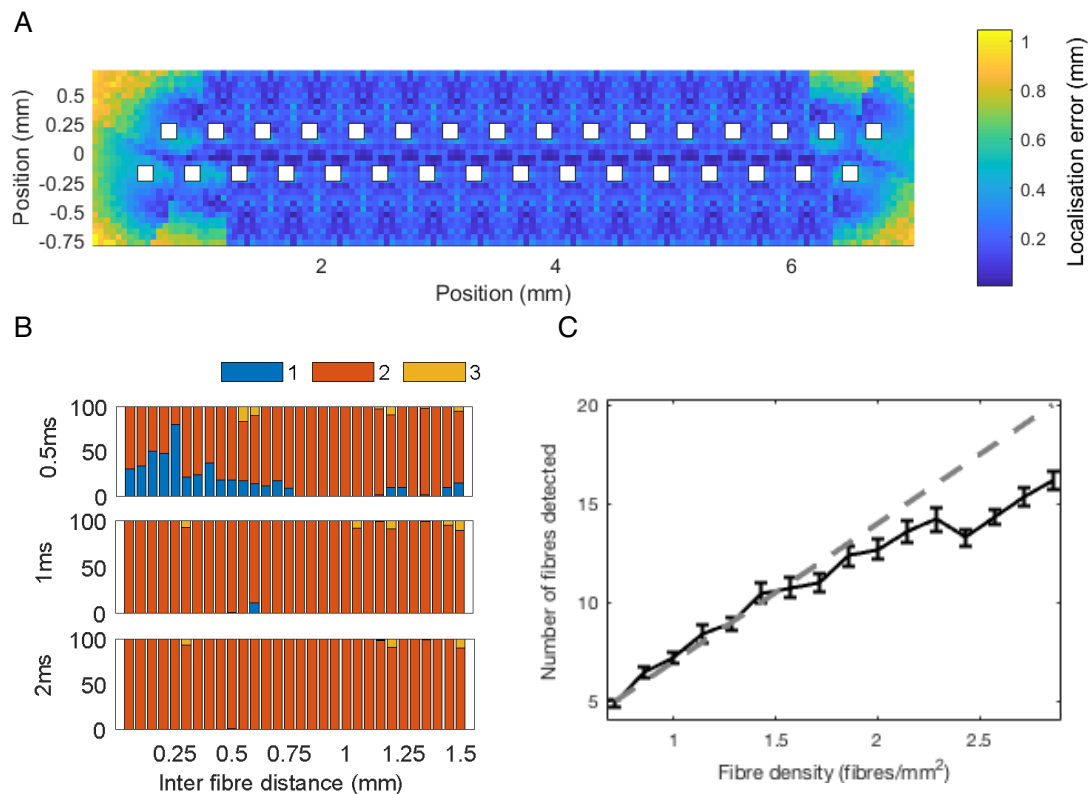


Figure 4.4 Simulated muscle fibre localisation accuracy across the MicroEMG array. A) The localisation error of a single simulated muscle fibre placed across a 10.5mm^2 area, in positions separated by $50\mu\text{m}$. White squares represent the electrode positions in the MicroEMG array. **B)** Fibre number estimate with two fibres and varying inter-fibre distance and inter-spike interval. Fibre number estimate is colour coded (1=blue, 2=red, 3=yellow). At an ISI of 0.5ms, one fibre was often estimated at spatial separations of $<0.5\text{mm}$, whereas at higher ISIs of 1 & 2 ms, 3 fibres were occasionally estimated. **C)** Fibre number estimate of multiple simulated muscle fibres across a central 7mm^2 area. Dashed line indicates the true fibre number, the number of localised fibres and confidence bounds are shown by the solid black line.

4.6.1 Single Fibre Localisation

Across all positions surrounding the electrode array, fibres were localised with a mean error of $176\mu\text{m} \pm 28\mu\text{m}$ (Figure 4.4A). An increased error was seen near the ends of the electrode array, where fewer electrode potentials were within the recording radius of the fibre to allow accurate deconvolution. Fibres within 1mm radius of 4 different recording electrodes were accurately localised to $<100\mu\text{m}$. However, when a fibre was placed more than 0.8mm from the needle's axis, the transmembrane current potential was often indistinguishable from noise, and so no fibre was detected or localised.

4.6.2 Dual Fibre resolution

At ISIs of 2, 1 and 0.5ms, the fibre number estimate was correct in 99.03%, 98.23% and 82.6% of trials respectively over all fibre spatial separations ($50\mu\text{m}$ - 1.5mm). At higher ISIs

of 1 and 2ms, fibre spatial separation did not affect the error rate, while for the lower ISI of 0.5ms, this rate was 91.04% for fibres spatially separated by over 0.5mm. At separations below 0.5mm, the accuracy rate fell to 59.5% (Figure 4.4B).

4.6.3 Multiple fibre localisation

The fibre number was reliably estimated up to 10 simulated fibres (a fibre density of 1.4/mm²). Above this level, the fibre density was underestimated ($R^2=0.91$). For example, at 15 simulated fibres (density 2.1/mm²), a mean of 13.94 fibres (± 0.16) were detected, while at 20 simulated fibres (density 2.8/mm²), a mean of 17.26 fibres (± 0.27) were detected (Figure 4.4C). This reflected the increasing probability that muscle fibres and their respective transmembrane currents were coincident in time and space. The algorithm appeared robust, with limited variability between simulations (the average standard deviation across all trials was 1.06 fibres).

4.6.4 Experimental results

Across five recordings from three individuals, between 4 and 14 motor units were identified per recording. For each recording, the median signal: noise ratio was calculated over all channels using the Spurious Free Dynamic Range (Pojar, 2001; Adimulam and Srinivas, 2017). This median varied from 39.6 to 177 (range 20.3-308.7).

Motor units fired at frequencies between 7.52 and 16.11Hz. We were able to localise up to 20 muscle fibres per motor unit (range 1-20), up to a total of 220 fibres per recording (Figure 4.5C). There was no correlation between the SNR of a recording and the number of fibres localised ($r=0.14$, $p=0.384$).

The median nearest neighbour distances of muscle fibres within a motor unit varied across all of the recordings between 0.54 and 1.21mm. There was also no correlation between the SNR of a recording and the median nearest neighbour distances ($r=-0.09$, $p=0.57$). The mean fibre density per motor unit varied between 0.625 and 1.8 fibres/mm², while the mean clinical needle fibre density measure was 1.22 (SD ± 0.29) across all motor units and all recordings. The motor unit territory size varied between 2.29-9.72mm (median 8.05mm).

Examining the spatial distribution of fibres within motor units, many motor units were seen to be overlapping- no areas were seen with only a muscle fibre population from a single motor unit. (Figure 4.5A). While on some recordings there were 'silent areas' of the electrode array without any muscle fibres, these did not correspond to areas of high impedance nor low SNR.

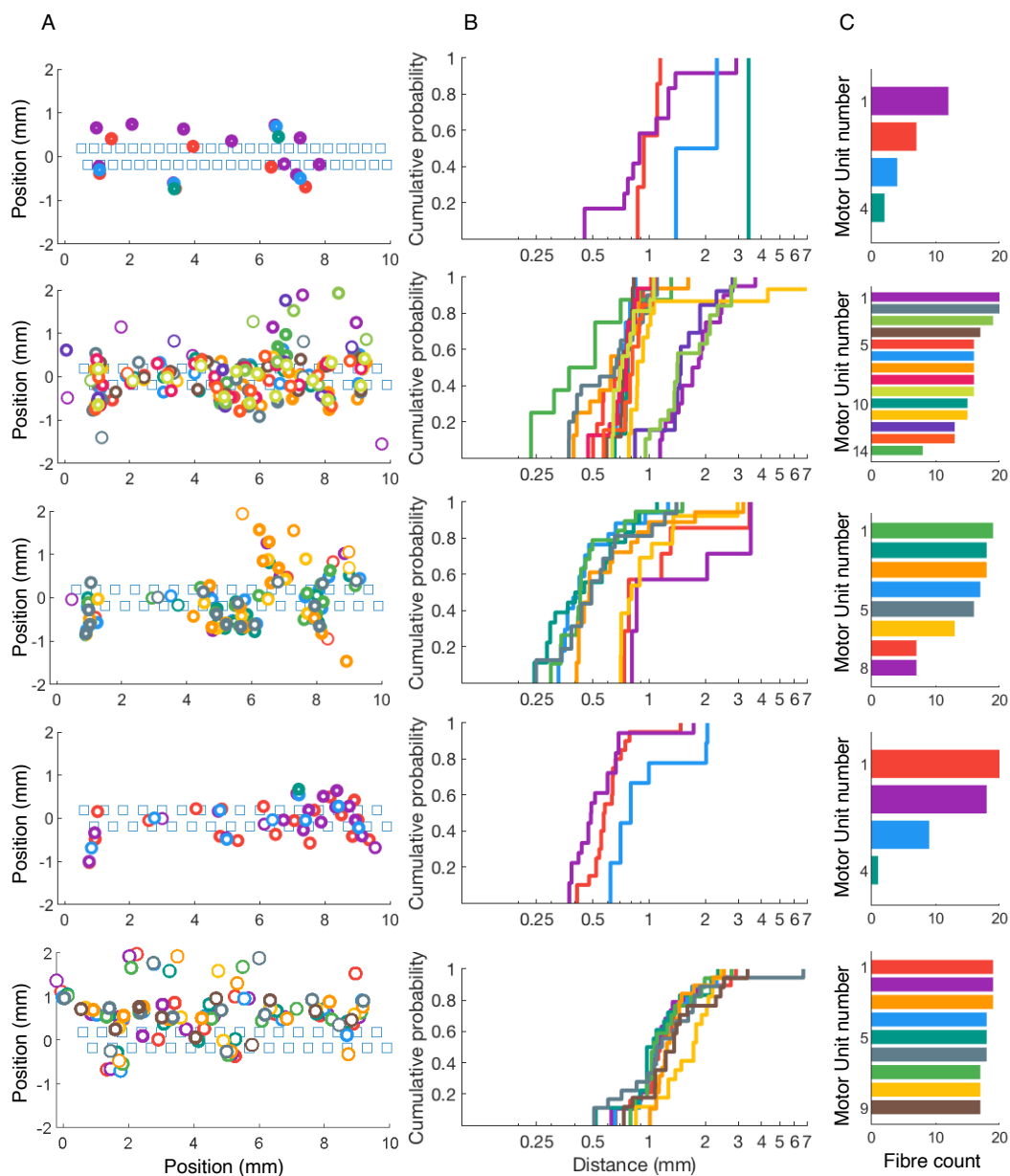


Figure 4.5 Human recordings from the tibialis anterior muscle. Each row represents a different experimental recording. Within one row, each colour represents a different motor unit. **A)** Muscle fibre localisation map, with localisation error represented by the size of the white core at each fibre (larger means more uncertain localisation). Electrode positions are shown as light blue squares. **B)** Cumulative distribution of nearest neighbour distances between fibre pairs, displayed on a log scale (X-axis). **C)** Muscle fibre counts per motor unit.

Fibres were sometimes localised to within the dimensions of the array itself, (e.g. Figure 4.5A, second row). Where only a low number of fibres were localised from a motor unit (Recording 1 & 4), the fibres tended to localise with low radial distance to the needle's axis.

To estimate the statistical distribution of fibres within the muscle, the fibre positions across all recordings were overlaid onto a single map and converted to an absolute position from the midpoint centre of the needle electrode (coordinates 5,0 on Figure 4.5A). The fibres

were seen to be uniformly distributed up to 4cm in the x-axis (parallel to the needle), and 0.75mm in the y axis (perpendicular to the needle) (Figure 4.6). This hypothesis was formally tested using the Kolmogorov-Smirnov test. In both x and y directions, the test failed to reject the null hypothesis, with p-value of x = 0.086, and p-value of y = 0.0714. The fibre spatial characteristics are summarised in Table 5.1.

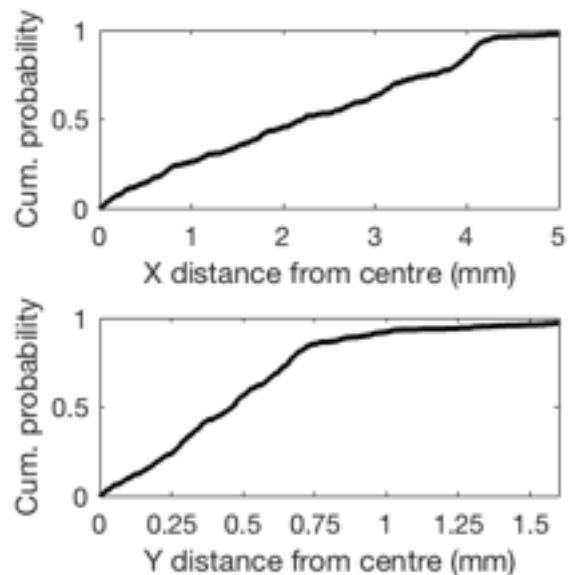


Figure 4.6 Relative fibre position, across all recordings, and all motor units. Distance is relative to the midpoint of the electrode array (5,0 mm on Figure 5A). Fibres were localised with an even distribution within the central 4x0.75mm area. An increased fibre density was seen at the tips of the electrode array (4mm).

Table 4.1 Summary statistics for motor units across five human recordings.

Participant ID	Number of motor units	Motor unit firing rate (95% CI)	Median number of fibres per motor unit (range)	Median nearest neighbour distance (mm) (range)	Mean fibres/mm ² (95% CI)	Median motor unit territory (range)	Mean needle fibre density
1	4	14.16 (13.4-15)	7 (2-11)	1.21 (0.23-0.85)	0.625 (0-1.32)	7.29 (6.28-9.72)	1.33
1	14	7.52 (7.3- 7.74)	7.5 (8-20)	0.8 (0.36- 1.91)	1.57 (1.39-1.75)	8.05 (2.28-8.38)	1.23
1	8	9.11 (8.72-9.49)	17 (7-19)	0.54 (0.38-2.06)	1.44 (1.02-1.85)	7.57 (6.4-8.39)	1.34
2	4	16.11 (15.85-16.37)	14 (1-20)	0.62 (0.61-0.78)	1.2 (0-2.59)	8.32 (8.22-8.62)	1.06
3	9	13.69 (13.29 – 14.09)	18(17-19)	1.16 (1.02-1.81)	1.8 (1.73- 1.87)	7.87 (7.04-8.27)	1.13

4.7 Discussion

We present a novel intramuscular multi-electrode array capable of determining the firing dynamics and location of up to 220 muscle fibres in a human muscle *in vivo* from a single insertion. The arrays are of sufficient length to allow simultaneous cross-sectional imaging of multiple motor units from both deep and superficial regions of the muscle.

Until now, the only means of directly determining muscle fibre spatial distribution in single motor units has been the glycogen depletion method. Although variations of these experiments have been performed in humans (Garnett *et al.*, 1979), it remains the case that fibre spatial distribution in single human motor units cannot be estimated using this technique. Conventional electromyography can provide information on human motor unit structure, and by using a variety of needle electrodes with spatial scales ranging from individual muscle fibres, i.e. single fibre EMG (Ekstedt and Stålberg, 1971) to entire motor units, e.g. macro EMG (Stalberg and Stålberg, 1980) or scanning EMG (Dieszeghy and Diószeghy, 2002), it is possible to gain information on the density of fibres within motor units and their spatial extent. However, these techniques are time-consuming and require multiple insertions into the muscle to provide sufficient sampling. More importantly, since only a single recording surface is used, the resulting voltage vs time signal represents the spatially and temporally summated activity of every muscle fibre within the pick-up area of each electrode. It is therefore *a priori* impossible to deconvolve this complex 1-dimensional Motor Unit Potential into the constituent 2-dimensional pattern of muscle fibre potentials.

The method we have demonstrated here represents a very different approach to the source localisation problem compared to other applications in neuroscience. For example, source localisation of EEG data relies upon an accurate anatomical model of the skull and brain tissue relative to the electrodes in order to inversely reconstruct the direction and strength of current dipoles (Michel and Brunet, 2019). This is due to the directional and 2-dimensional nature of the SFEMG signal approximating a vector. Other methods including multilateration were found to have a higher level of error, and this led to a “mirroring” problem where the possible fibre location could be on either side of the electrode array.

In producing this methodology, we have made a number of assumptions. When considering that a single fibre travels in the z axis, we assumed that the electrode was orientated absolutely perpendicular in both x & y planes (Figure 1 provides reference to axes). While angulation of the needle in the Y axis would not affect this process, a rotation of the needle such that it might be angled $<90^\circ$ with respect to the X-axis would distort the

convolution function, such that this would not converge correctly. While we have not modelled this, we propose that any rotation would result in a fibre location which is closer to the needle than in reality due to this effect.

4.7.1 Modelling studies

Because the spatial distribution of muscle fibres in human motor units is not known, we had no gold standard against which to compare the results of our human experiments. We therefore modelled our fibre-localisation algorithm's performance using single, paired, or multiple muscle fibres at a variety of biologically relevant spatial separations and inter-spike intervals. Our simulations suggested that fibres would be accurately localised within a corridor extending approximately 0.8mm on either side of our arrays, at temporal separations above 0.5ms and radial spatial separations above 0.5mm. Below these separations, our algorithm could fail to separate fibres, tending to under-estimate the true fibre density. Fibre localisation was least accurate at the tips of the electrode, where muscle fibre potentials were recorded by fewer electrodes.

4.7.2 Human recordings

Using our arrays, a large number of motor units and their constituent muscle fibres could be studied from relatively brief recordings. Accurate localisation of up to 220 fibres could be obtained *in vivo* from a 60-second recording without the need for needle movement. Critically, by localising fibres from multiple motor units simultaneously, the relationship between fibres in neighbouring units could be determined. We found that fibres from multiple motor units overlapped in any given region of the array. Although an overlapping pattern has long been inferred from glycogen depletion and EMG studies, ours is the first direct evidence of this arrangement in either an animal model or a human. Previous studies of human motor units have estimated between 10-15 motor units within a given the pick-up area of a concentric EMG electrode (Edstrom and Kugelberg, 1968), and our data of 4-14 motor units per recording is consistent with this.

One important limitation in these early experiments relates to the relatively high noise level encountered during recordings. This had a number of impacts. Firstly, the narrower filter range may have distorted the shape of the recorded electrode potentials used for localisation. This is because muscle tissue acts to attenuate higher-frequency components of a signal, and therefore the high-pass filter may reduce the contributions of the potential at greater z-distances from the electrode, along the length of the fibre, affecting the weighting function described in Equation 1. Secondly, several noise transients were isolated via the MUPT extraction process, and these necessitated manual removal. In the future we would

seek to improve the noise environment for future iterations. Finally, the necessity of averaging over a set number of discharges meant that some more active motor units would be more reliably averaged than others, and this also limits the temporal resolution of this methodology.

Depending upon the reliability of the MUP template matching used, it is also possible that MUPTs may have been either split or merged. If split, the MUPT would be expected to produce additional motor units with constituent fibres located at similar positions around the needle electrode. If merging occurs, MUPTs would affect localisation due to multi-electrode potentials from multiple MUPs being merged. We feel this is unlikely for several reasons. Firstly, the very short duration of single-fibre action potentials means that coincidence of single-fibre potentials from different motor units is rare. Secondly, we have shown in our results that fibres belonging to different motor units frequently occupy differing positions within the sample area, with limited overlap (Figure 4.5). Despite this, improvements in the MUP template matching algorithm will also be sought for the future.

The fibre localisation results are consistent with our modelling work, localising multiple fibres throughout the centre of the recording area. Beyond 0.8mm of the electrode array, far fewer muscle fibres were localised, consistent with the attenuation of single-fibre signal through tissue we have seen in our modelling. Fibres found beyond 0.8mm likely represent muscle fibres with increased fibre diameter, with correspondingly increased amplitude transmembrane currents which were better distinguished from noise.

It is possible to calculate nearest neighbour distance distributions from single fibre positions, as described in glycogen depletion studies of cat soleus and tibialis anterior (Bodine-Fowler *et al.*, 1990). Perhaps not surprisingly our results suggest larger median nearest neighbour distances in humans than in cats (0.54-1.21mm compared to ~0.1mm). However, compared to whole muscle sampling of other methods (Bodine-Fowler *et al.*, 1990), MicroEMG uses a narrow and relatively short sampling corridor size. The edge effects of this sampling region may mean that the true nearest neighbour to a fibre lies outside the detection boundary, thus overestimating the nearest neighbour distance (Floresroux and Stein, 1996).

The ability to localise fibres in 2-dimensions relative to the recording array allows a true fibre density for each motor unit to be calculated. This has previously been estimated as 2.6 fibres/mm² in motor units of biceps brachii, based on post-mortem studies in neonates where an average of 163 fibres per motor unit were found (Christensen, 1959), and a motor unit territory of 9mm diameter (Buchthal, Erminio and Rosenfalck, 1959; Hilton-Brown and Stålberg, 1983a). Our data show lower fibre densities of between 0.625-1.8 fibres/mm². This

lower range may be due to failure to detect all of the fibre potentials near to the electrode, or the inability of our algorithm to separate temporally and spatially adjacent fibres. Conversely, using data from neonatal muscle in which individual fibres have a lower diameter may over-estimate fibre density in adult muscles. It may be that the true value lies somewhere between these extremes.

Comparing the values of mean needle fibre density, across all recordings, we produced a value of 1.22 ± 0.29 fibres. This compares favourably to the literature, where normative data indicate a fibre density of 1.36 ± 0.11 (Hilton-Brown, Nandekar and Stålberg, 1985), although we showed much more variability. The motor unit territory dimensions were also within the range reported for previous multielectrode studies (Buchthal, Guld and Rosenfalck, 1957; Buchthal, Erminio and Rosenfalck, 1959; E. Stålberg *et al.*, 1976; Schwartz *et al.*, 1976), although most of these were performed in the biceps brachii muscle. These motor unit dimensions are highly likely to be underestimates, since the fibres of the outer extent of the motor unit may lie beyond the detection range of the electrode on one or both sides, and the electrode position was not optimised to transect the entire motor unit.

It is reasonable to question the location of fibres that appear to be 'within' the dimensions of the needle. We suspect that in these cases the majority of the muscle fibre does occupy this position on either side of the array, with a short segment being deformed away from this position by the array itself. We therefore consider that these positions are a reasonable representation of the iso-electric angle over the whole length of the muscle fibre.

On detailed review of our fibre localisation algorithm, we found an important limitation. We noted apparent clustering of fibres near to the ends of the electrode array. Our modelling showed that localisation error is increased in these areas, likely due to the reduced number of electrode potentials which can be used for signal deconvolution in the search space.

In fact, fibres that are located beyond the length of the needle produce significant electrode potentials on only the closest electrodes. Normally, our algorithm always uses 5 electrode potentials to localise the fibre in space. Where fewer electrode potentials are available, the optimal search position remains biased towards the middle electrode of the 5 electrode potentials. Referring to Figure 4.4A, fibres located between $x=0-0.75\text{mm}$ will all result in estimated positions surrounding $x=0.75\text{mm}$. This has the net effect of clustering fibres with true position $x < 0.75\text{mm}$ at position $x=0.75\text{mm}$, and a similar effect will occur at the opposite end of the needle ($x > 6\text{mm}$).

Our fibre localisation algorithm often failed to distinguish fibres with low separations in both space and inter-spike-interval (Fig. 4C). Hence, it is possible that adjacent fibres within

the same motor unit would be interpreted as a single fibre, leading to overestimation of nearest neighbour distance and an underestimate of the fibre density.

In healthy tissue, data from glycogen depletion experiments indicate that the number of adjacencies is either the same as would be expected from random innervation (Brandstater and Lambert 1973) or fewer adjacencies than random (Willison *et al.*, 1980), with 12% of fibres occurring in groups (Brandstater and Lambert, 1973; Bodine *et al.*, 1988). However, in reinnervated muscle, adjacencies occur more often (Schwartz *et al.*, 1976), which is potentially problematic for our technique which aims to improve diagnosis of neuromuscular diseases such as amyotrophic lateral sclerosis. To mitigate this in the future, we aim to study the transmembrane currents produced by the fibre localisation algorithm. Where fibres are grouped and temporally coincident, we would expect to see significantly larger transmembrane currents owing to the adjacency of multiple fibres activating simultaneously.

There are further limitations with our technique; the images produced represent a ~2 mm diameter core through multiple motor units rather than demonstrating an entire motor unit cross-section. Additionally, the modelling of fibre localisation is based upon a tissue convolution function that is homogenous and anisotropic. Heterogeneity in the tissue media may lead to localisation errors, and so this technique may be less accurate in sarcopenic or cachectic muscle where more connective tissue or fatty infiltrate can be present.

Despite these limitations, the ability to rapidly gather information on fibre density and spatial organisation *in vivo* during voluntary muscle contraction provides a powerful alternative to the glycogen depletion technique for the study of human motor physiology and pathology.

For the purposes of this study, we have optimised our algorithm for correctly identifying muscle fibre positioning surrounding the needle electrode. However, since our technique might enable reconstruction of the muscle fibre transmembrane current potential shape and current amplitude, this raises the exciting possibility that other muscle fibre properties may be estimated.

Our system moves electromyography from the interpretation of a highly abstract 1-dimensional motor unit potential to the creation of a 2-dimensional image, promising a step-change in both diagnostic accuracy and ease of use. Our findings in healthy human muscle also provide the first baseline data against which disease-induced changes in muscle fibre spatial distribution can be compared.

The future of the MicroEMG device requires integration with clinical EMG equipment. Current clinical setups already have the ability to sample from large multi-electrode arrays,

and further work is underway to prove the suitability of MicroEMG to the clinical environment.

5. Ultrasound-Guided Motor Unit Scanning EMG (UltraMUSE)

5.1 Highlights

- An ultrasound scanner was used to guide a concentric EMG needle through the centre of a human motor unit.
- A manual motor unit transect was performed, with concurrent imaging to determine the needle tip position.
- This technique is straightforward and yields similar information to more complex and time-consuming methods such as scanning EMG.

5.2 Abstract

Objectives

We sought to target an EMG needle through the centre of a single motor unit in order to estimate motor unit dimensions and internal structure. We developed a modification of the scanning EMG protocol to enable visualisation and targeting of the motor unit using ultrasound imaging.

Methods

Single motor unit twitches in tibialis anterior muscle were elicited via stimulation of the fibular nerve, visualised with ultrasound and targeted with an intramuscular EMG electrode. The electrode was moved by hand in small steps through the motor unit territory. Ultrasound video output was synchronised to EMG capture, and the needle position was tracked at each step.

Results

Eight recordings from six participants were collected. The technique was quick and easy to perform (mean time 6.1 minutes) with reasonable spatial resolution (mean step size 1.85mm), yielding motor unit territory sizes (defined as the transect length) between 1.53-14.65mm (mean 7.15 mm).

Conclusions

Ultrasound-guided motor unit scanning EMG is a quick and accurate method of obtaining a targeted motor unit transect. Further work is needed to improve the spatial resolution of the technique.

Significance

This combination of two readily-available clinical tools provides insights into the dimensions and internal structure of the motor unit as a marker for neuromuscular conditions.

5.3 Introduction

Conventional needle electromyography records the motor unit potential (MUP), the spatially summated electrical activity from muscle fibres within the vicinity of the needle tip. With appropriate filter settings, information on local fibre density can be obtained, but the dimensions of the motor unit and its internal structure cannot be determined. Several techniques have been developed that seek to address this lack of spatial information; including multi-electrodes (Buchthal, Guld and Rosenfalck, 1957; E. Stålberg *et al.*, 1976; Maitland *et al.*, 2021), paired needle insertions (McMillan and Hannam, 1991), and more recently, motor unit MRI (Birkbeck *et al.*, 2020). Perhaps the best known of these is scanning EMG (Stalberg and Antoni, 1980). In this technique, a single-fibre EMG (SFEMG) electrode is inserted into the muscle to act as a trigger for single motor unit activity during voluntary contraction. A second, concentric needle electrode is then inserted 1-3cm from the SFEMG electrode to record the single motor unit potential. The needle is then advanced deeper into the motor unit until the MUP is no longer recorded, before being withdrawn back through the motor unit in fixed increments, typically 50 μ m or 100 μ m. In this way a continuous representation of electrical activity within a corridor of the motor unit is created.

Scanning EMG has been used to measure motor unit territory in muscular dystrophy (Hilton-Brown and Stålberg, 1983a), and motor unit territory and temporal dispersion in neurogenic and myogenic disease (Stålberg and Dioszeghy, 1991; Gootzen, Vingerhoets and Stegeman, 1992). Most papers using scanning EMG have demonstrated no changes in motor unit territory size in either myogenic (Hilton-Brown and Stålberg, 1983a, 1983b) or neurogenic (Gootzen, Vingerhoets and Stegeman, 1992) disease, with one exception which showed a significant increase in the tibialis anterior muscle in patients with amyotrophic lateral sclerosis (Stålberg and Dioszeghy, 1991). In contrast, notable internal structural changes within the motor unit have been shown in both disease groups, including fragmentation, silent areas, and increased polyphasic segments (Dieszeghy and Diószeghy, 2002).

Scanning EMG has a number of limitations, which perhaps explain why it has never entered routine clinical use. First, it requires the insertion of two needles into the muscle and specialised equipment (computer-controlled stepper motor), increasing the time taken whilst limiting its availability. Second, it does not consider skin elasticity or the stiction of the muscle surrounding the needle. This means that although the stepper motor may produce a defined and highly accurate step size in relation to the skin surface, there is no guarantee that the needle tip will have moved by the equivalent amount in relation to the motor unit.

Tissue stiction may be altered in neuromuscular diseases, as a result of intramuscular fat infiltration, fibrosis or increased fibre density, potentially increasing this error.

The most fundamental limitation of both scanning EMG and multi-electrode techniques is that the needle is inserted 'blind', and the trajectory of the needle through the motor unit remains unknown. Assuming a circular motor unit cross-section, the path of the needle is a chord to that circle. If performed blindly, a linear path of a needle through the unit may be anywhere between two tangents to the circle (Figure 5.1). As a result, a random chord length may be anywhere between zero and the true diameter of the unit:

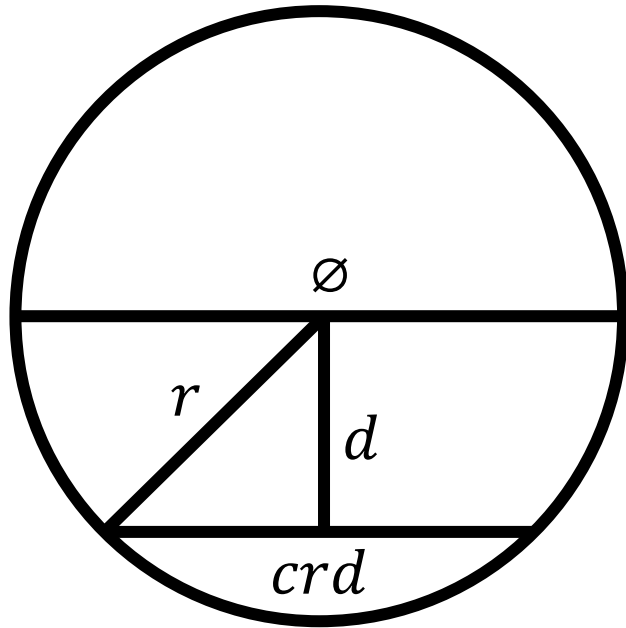


Figure 5.1 Effect of needle path on estimated motor unit dimensions. The true maximal motor unit dimension (diameter, \emptyset), as measured by a perfect bisect of the motor unit with the EMG needle, is underestimated by every other chord through the motor unit (crd) for which $d > 0$.

$$2\sqrt{r^2 - d^2} \quad (1)$$

Where: r is the radius of the circle

d is the distance of the chord away from the centre of the circle (range $\pm r$)

\emptyset is the diameter of the circle = $2r$

Since the distribution of chord lengths is one-tailed with respect to the maximum diameter of the motor unit, the median chord length can be assumed to be at the midpoint between the diameter and a tangent at r which is at $d = \frac{r}{2}$.

$$2\sqrt{r^2 - \left(\frac{r}{2}\right)^2} = 1.73r = 0.866\emptyset \quad (2)$$

Therefore the median random EMG scan through a circular motor unit will underestimate the maximal diameter by a factor of ~ 0.87 .

This is further complicated by the shape of the motor unit territory which, based upon histological data in animals, may be oval (Bodine *et al.*, 1988) or crescent-shaped (Edstrom and Kugelberg, 1968). More recent data using motor unit MRI in humans has revealed even more complex motor unit outlines, including spider shaped and split (Birkbeck *et al.*, 2020). These more complex motor unit outlines are likely to be under-estimated to an even greater degree than the idealised circular outline, since there will be many more potential shorter transect paths.

We sought to overcome these problems by using concurrent muscle imaging to target a single concentric EMG needle through the centre of a motor unit, and to directly measure the step sizes as the needle was withdrawn. We chose ultrasound as it is non-invasive, almost ubiquitously available, and is widely used to visualise EMG needles to target specific muscles such as the upper leg and diaphragm (Boon *et al.*, 2008; Gentile *et al.*, 2020). Crucially, it also has the spatial and temporal resolution to resolve single motor unit activity (Bokuda *et al.*, 2020).

5.4 Methods

Ethical approval was obtained from Newcastle University Faculty of Medical Sciences Research Ethics Committee (reference: 2130/12840). Participants were recruited from a local volunteer pool & faculty staff members. Exclusion criteria were: history of a bleeding disorder, use of anticoagulants, implanted pacemaker or cardiac defibrillator, and those with neurological or neuromuscular conditions.

5.4.1 Experimental setup

Peripheral nerve stimulation was via a DS5 constant current bipolar stimulator (Digitimer, UK). Stimulation was a square pulse of width 0.3-3ms at current ranges 0-10mA, delivered at 2Hz. Pulse width and current were adjusted to selectively activate a single motor unit twitch. EMG activity was sampled at 10Khz, and amplified (gain 500 or 1000) using a D440 EMG amplifier (Digitimer, UK) with high-pass filter 3Hz, low pass 10Khz, and Humbug inline mains noise eliminator (Quest Scientific, Canada), and sampled using a Micro1401 data acquisition unit (Cambridge Electronic Design, UK), which also triggered the bipolar stimulator (Figure 5.2).

Ultrasound guidance was achieved using a Philips EPiQ with eL18-4 linear transducer, frequency 2-20Mhz. The video signal from the ultrasound machine was captured using a video capture device sampling at 60Hz (Elgato HD60, USA), and the clock signal from the

1401 was connected to the auxiliary sound input of the video capture device to synchronise ultrasound images with EMG and nerve stimulation.

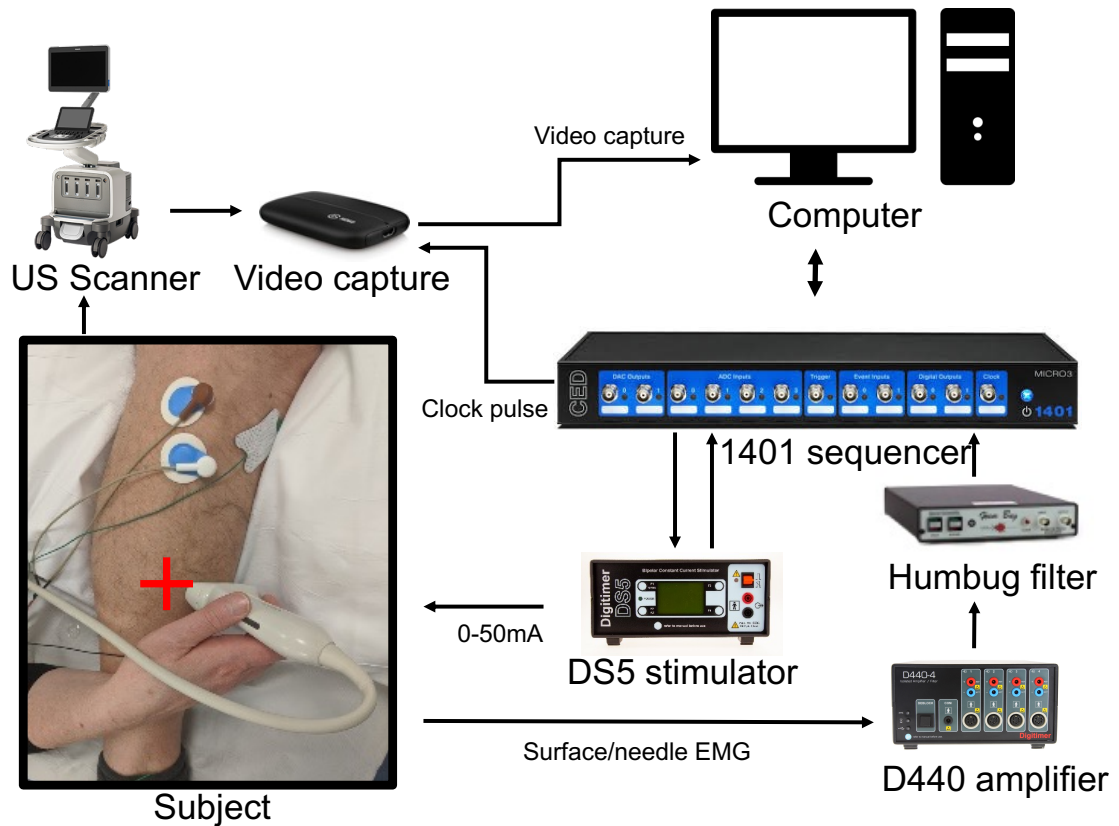


Figure 5.2 Experimental setup diagram. CED 1401 sequencer controlled stimulation and sampled EMG. DS5 stimulator provided peripheral nerve stimulation of fibular nerve. EMG was sampled by D440 amplifier, filtered, and mains noise removed with Humbug. Video output from ultrasound scanner was synchronised with EMG sampling via the 1401 clock signal, input as audio to the video capture device. Inset shows stimulating electrodes over the fibular nerve at the fibular head and ultrasound probe placed over the tibialis anterior muscle. Needle was inserted at indicated red cross, in plane with ultrasound probe.

5.4.2 Procedure

Subjects lay reclined and fully relaxed on an examination couch. The skin surface was cleaned using alcohol wipes, and skin preparation was used to improve conductivity at stimulating electrode sites (NeuroPrep). Surface electrodes (50mm Covidien H34SG) were placed at the fibular head in order to stimulate the fibular nerve (Rigoard, 2020). The ultrasound probe was placed on the anterolateral surface of the lower leg, directly above the tibialis anterior muscle, with the probe oriented perpendicular to the muscle. Electrical stimulation was gradually increased to elicit a visible single motor unit twitch. Our criteria for single motor unit activity on ultrasound were based upon those used to determine single motor unit electrical activity:

1. Motion must be synchronous to electrical stimulation.

2. Motion must occur within a spatially discrete and consistent region of the image, without overlapping into other regions of activity.
3. Motion must appear and disappeared in an all or nothing manner depending on stimulation intensity and show alternation when close to threshold.

For point 1, it was occasionally necessary during targeting to adjust the stimulation frequency to distinguish vascular pulsation from motor unit twitches. The stimulation frequency was then returned to 2Hz for the duration of the experiment.

The single motor unit twitch was targeted using a 14 gauge concentric EMG needle under ultrasound guidance. In order for the muscle and needle to be visualised simultaneously, the needle was inserted at an angle of between 30-45°, in-plane with the probe. The needle was deliberately targeted towards the centre of the region of movement (Figure 5.3, Supplementary File 1 for video of needle targeting & withdrawal).

The needle was advanced through the centre of the motor unit and out the other side of it, beyond the region of visible twitch. The needle was then withdrawn in increments as small as the operator could make and held in each position for 20 stimuli. Needle movements were marked on the recording using synchronous keyboard input.

Post-hoc, all data were analysed using MATLAB 2019a. In order to correct for movement of the ultrasound probe or distortion of the muscle tissue, the needle tip coordinates (x,y) in each step in needle position were labelled on-screen by a human operator (SM), as well as the x,y coordinates of the edges of $k=3$ fascial planes, which acted as landmarks. Between steps the x,y change of each landmark position was measured, and the mean change was used to compensate the needle tip coordinates for this change. This form of Procrustes analysis (Gower, 1975), negating the rotational aspect which was not a concern for

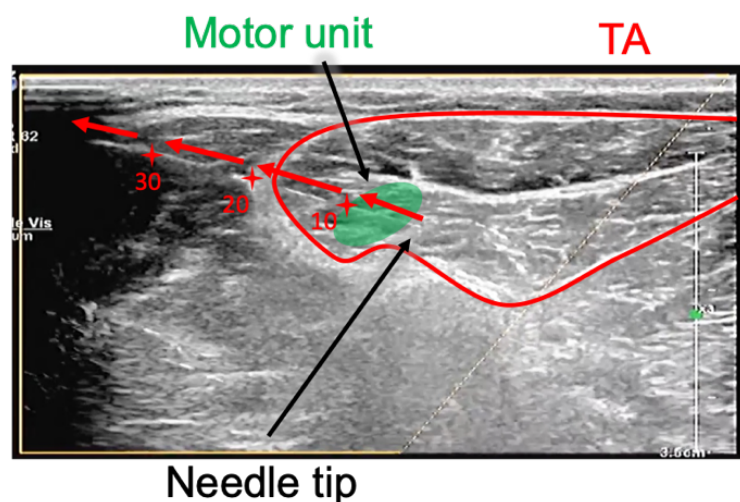


Figure 5.3 Needle in situ (white linear structure from top left to labelled needle tip) in a motor unit within tibialis anterior (TA). The needle has been targeted through the centre of the motor unit and advanced through it until the MUP is no longer detectable, before being withdrawn along the same trajectory by hand. Red arrows indicate withdrawal direction, with numbers indicating (approximate) needle position in mm. For video demonstrating the movement of the needle through the muscle, see Supplementary file 1.

ultrasound imaging data, allows us to correct the needle position for probe drift or tissue distortion:

$$\Delta Landmark_i = \frac{\sum Landmark_i - Landmark_{i+1}}{k}$$

Where $k = 3$ (the number of landmarks used)

$$Corrected\ needle\ position_i = needle\ position_i - \Delta Landmark_i$$

The EMG traces were analysed offline to measure the spatial extent of each motor unit. This was defined as the positions of the outermost traces which demonstrated synchronous MUP activity greater than $50\mu V$, as in scanning EMG (Stålberg and Eriksson, 1987). Motor unit parameters including amplitude, duration and jiggle were marked manually on unrectified, unaveraged traces in each position, with the amplitude defined as the maximum peak-peak amplitude at any position within the motor unit, and the duration defined as the longest duration of any position within the motor unit.

5.4.3 Modelling motor unit dimensions

We were interested in the potential impact of varying motor unit territory shapes on average transect lengths compared to a theoretical circular motor unit territory, and the effect of targeting the centre of the motor unit (MU) territory on these estimates.

We built simulations to exhaustively estimate the chord length of different two-dimensional motor unit shapes, as found in Birkbeck *et al.*, 2020. We drew approximately 500x500 pixel shapes (circle, wide ellipse, narrow ellipse, pennate) and measured their chord lengths through every possible chord in 1-pixel increments, in every orientation, rotating the shape about its origin in 1-degree steps. Where the chord passed through two borders (e.g. the limbs of the pennate shape), the gap between was discounted; the length was considered the sum of the chord lengths of limb 1 + limb 2. We compared the median lengths of those chords that traversed the centre of the shape (simulating needle targeting) versus those that did not (simulating 'blind' needle insertion).

5.5 Results

5.5.1 Modelling

As expected, the median of random chord lengths always underestimated the true motor unit diameter (Table 5.1). Our modelling confirmed the theoretical underestimate of 86% median diameter for a circular motor unit territory. We also confirmed that any deviation from a circular outline increased this error, with the median diameter of ‘narrower’ shapes underestimating the true maximal diameter much more than ‘wider’ shapes (narrow ellipse 28%, pennate 56%, wide ellipse 60%). Modelling targeting the needle through the centre of the MU reduced this error for every shape tested, for instance 74% for a wide ellipse targeted vs 60% blind, and reduced the variance of the transect lengths in every shape.

Table 5.1 Simulated motor unit diameters measured exhaustively in every orientation. Results are standardised measures to the maximal diameter (i.e. 100%). Untargeted refers to transects through every position in the motor unit, Targeted refers only to transects

Shape	Example	Untargeted	Targeted
		Median underestimate (SD)	Median underestimate (SD)
Circle		86% (22%)	100% (3%)
Wide Ellipse		60% (21%)	74% (12%)
Narrow Ellipse		28% (17%)	33% (14%)
Pennate		56% (20%)	62% (18%)

5.5.2 Practical aspects

Eight recordings were collected from six individuals aged 29 – 49 (Table 5.2). The mean time from needle placement to withdrawal was 6.1 minutes. There was a clear learning effect, with the first recording taking 12 minutes and the last only 3 minutes. Only minor discomfort was described by participants, mostly during initial needle insertion. Only minor, self-resolving bleeding was experienced, consistent with a routine clinical EMG recording. We discovered during preliminary experiments that conduction between the ultrasound gel and the needle shaft could occur, resulting in a direct current offset that saturated the amplifier. This was resolved by covering the ultrasound probe and gel with a surgical probe cover.

Stimulation currents to achieve single motor unit activation ranged from 2.6-7.9mA. The mean step size of the needle between positions across all recordings was 1.85 mm (SD 1.07). For individual recordings, the mean step size ranged from 1.03 to 2.91mm. Between three and eight positions (median = 4.5) were recorded from within each motor unit.

5.5.3 Motor unit parameters

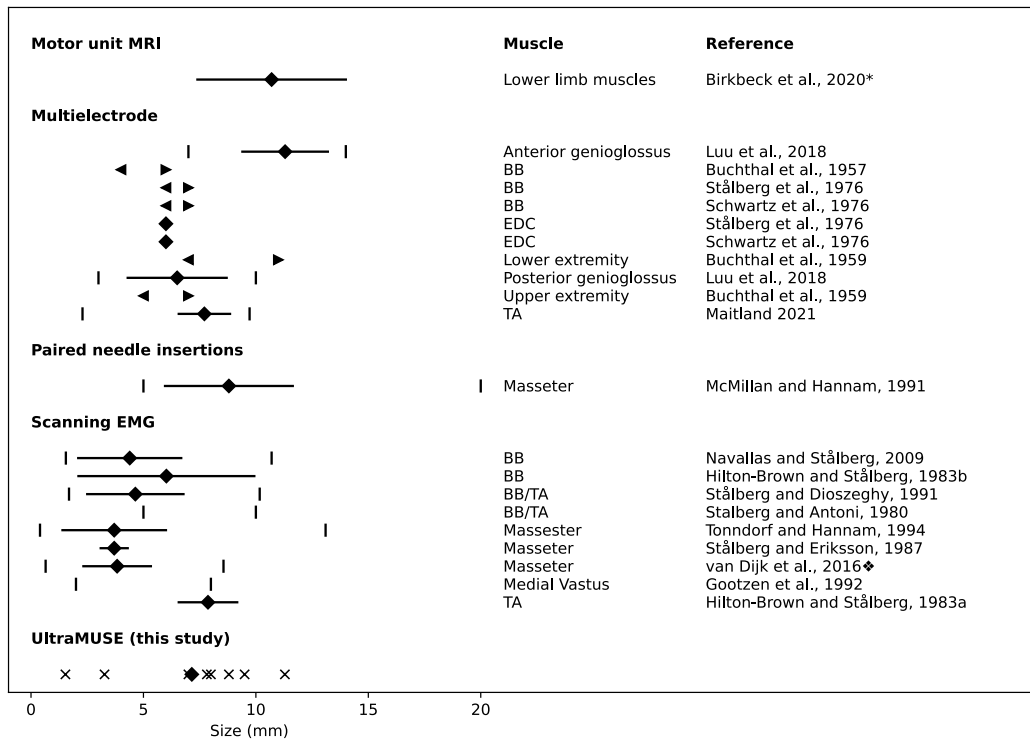


Figure 5.4 Motor unit territory dimensions collected from the literature. ♦ = mean, with ◀▶ where a mean range was specified. Lines demonstrate the SD, and whiskers are the range. BB=Biceps brachii, EDC = Extensor digitorum communis, TA = Tibialis anterior. References legend: *Maximum Feret diameter, ★ Additional analysis of existing published data ♦Personal communication in addition to published data.

Quantitative analysis of MUPs is described in Table 5.2 and summarised in Figure 5.4. The appearance of the MUP changed as the needle traversed the motor unit, with a diffuse inverted ‘cannula potential’ at deeper positions giving way to a classic triphasic motor unit potential at more superficial positions. Alternation was demonstrated, with either a consistent MUP outline or a flat trace seen at each needle position (Figure 5.5A). The motor unit territory sizes varied widely, ranging from 1.53 to 14.65mm (mean = 7.15). The maximal motor unit amplitudes of each transect ranged from 101-520 μ V (mean= 219 μ V) and were always located towards the centre of the motor unit, i.e. never at the furthest extent. MUP durations varied from 2.8-10.2ms. No recordings demonstrated silent regions (areas within the motor unit territory with amplitude < 50 μ V).

The latency measurement was consistent within a given transect, but varied widely between recordings from 4.3 to 37ms. Four recordings demonstrated consistent MUP onsets with jiggle below the sampling frequency (<0.1 ms), while in four recordings, there was visible jiggle of the MUP onset, ranging from 0.4-0.7ms (Recording ID 3, Figure 5.5B).

Figure 5.5 Example EMG scans from healthy human TA muscle. For each scan, the Y-origin indicates the position of the needle from the deepest starting position; higher Y value indicates a shallower position. Stimulus artefact can be seen at time = 0. Each trace (n=20) is shown at each position. A) Diffuse cannula potential at deeper positions giving way to triphasic MUP, inset to highlight alternation & MUP shape (recording ID=8). B) Evolving activity within the motor unit (recording ID=7). Both the deep (y=7mm) and superficial (y=18mm) boundaries are included, permitting MU territory to be estimated. C) Example of both alternation and MUP latency jiggle (recording ID=4). D) Enlarged view of a single motor unit transect, with traces at each position averaged. (recording ID=2).

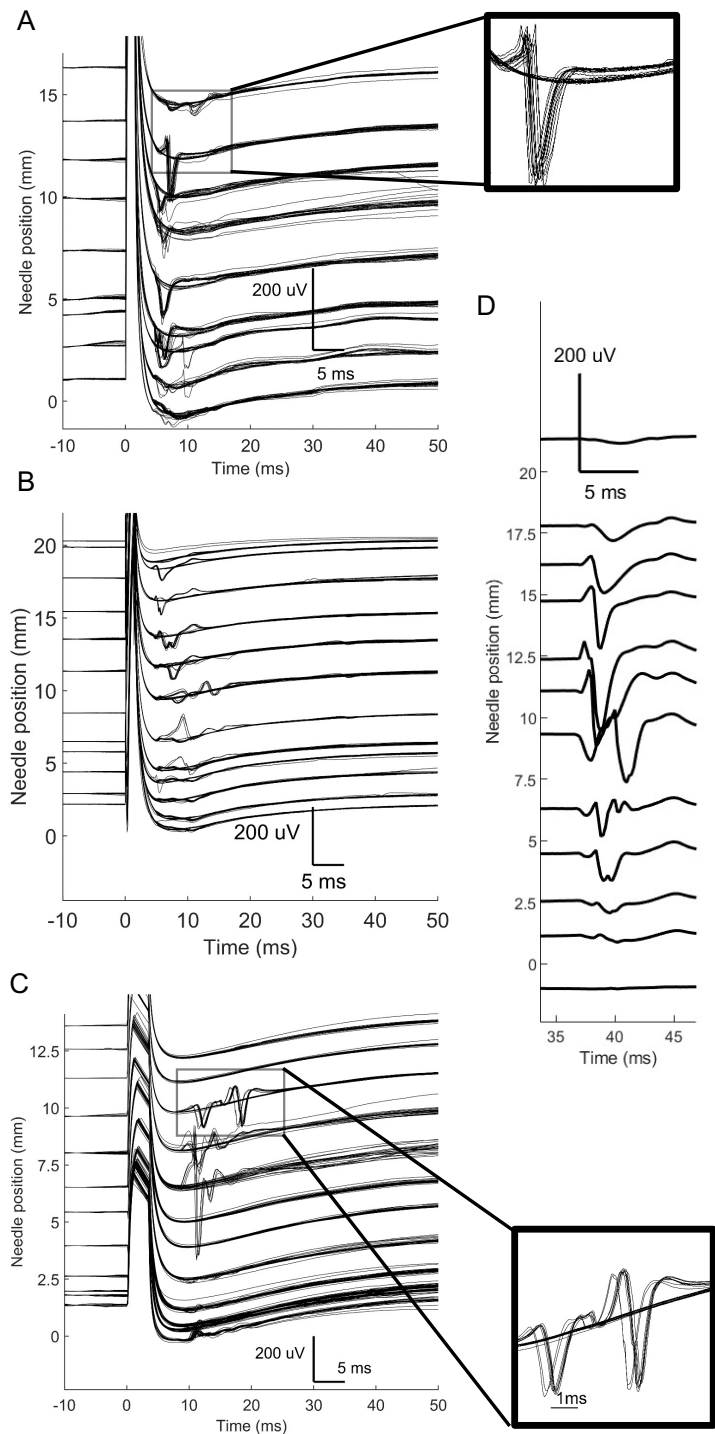


Table 5.2 Measured parameters of single motor unit scans. * Earliest onset of any position with valid MUP (amplitude >50 μ V). **Longest duration of any valid MUP.

ID	Stimulation current (mA)	Experiment Duration (minutes)	Transect length (mm)	Transect length (steps)	Onset latency (ms)*	MUP Duration (ms)**	Max MUP amplitude (μ V)	Maximum jiggle (ms)
1	3.64	12:07	7.82	5	37	5.6	134	-
2	3.87	07:54	11.29	8	37	5.8	200	-
3	7.95	06:38	1.53	4	6.8	5.27	190	-
4	6.58	05:04	8.8	6	9.6	10.2	250	0.5
5	6.99	04:05	3.27	3	8.9	9.4	520	0.7
6	3.4	06:34	8	3	4.3	7.9	237	0.4
7	5.5	02:59	7	5	5.3	7.9	101	-
8	2.60	03:33	9.5	4	4.8	2.8	119	0.7
Mean	5.07	06:06	7.15	4.75	14.2	6.86	219	-

5.6 Discussion

Previous studies have reported a wide range of normal human motor unit dimensions, with mean territories ranging from 3.7-11.3mm. These estimates come from a variety of techniques, including multi-electrode studies, paired needle insertion and scanning EMG, and include data from several muscles (Figure 5.4). Comparing our results to data obtained using scanning EMG from tibialis anterior, we see that our mean territory of 7.15mm is well within the range obtained using this method. This is despite us using electrical stimulation to activate motor units in contrast to voluntary activation in scanning EMG.

By directly visualising the MU we could ensure that the needle passed through both the deepest and most superficial boundary of the motor unit i.e. it included the entire motor unit transect. This is not necessarily the case in scanning EMG, and it is notable that some published images of MU transects show MUP activity extending to the edge of the scan (e.g. Corera *et al.*, 2017). These estimates of MU dimension, therefore, represent a partial transect length rather than the true length.

Direct visualisation also allows the centre of the MU to be targeted. Our modelling confirms the theoretical median underestimate of 0.86 for a blindly sampled circular motor unit, and that the degree to which the maximum diameter is underestimated is even larger for more complex motor unit outlines. In practice, we found that the positioning of the ultrasound probe and the need to achieve good needle visualisation necessitated a relatively fixed trajectory of 30-45° to the skin surface, which meant that we could not always traverse the MU along its longest axis. Nevertheless, our modelling indicates that targeting the centre of the MU reduces the negative measurement bias irrespective of MU orientation.

One undoubted limitation of our technique is the relatively large step size compared to scanning EMG. Whereas in the latter a step-size of 50 μ m is routinely used, in our hands manual withdrawal of the needle produced a step size of around 1.85 millimetres. Similarly, whilst a scanning EMG corridor of 2cm will therefore contain 400 MUP traces, we only obtained between 3 and 8 per motor unit transect. It is worth pointing out that in scanning EMG, a median spatial filtering of 3, 5, or 7 adjacent traces is typically applied (Stalberg and Antoni, 1980) in order to remove contamination from concurrently firings MUPs, with a corresponding increase in the effective step size. Nevertheless, it remains the case that the spatial resolution of our technique is far lower than traditional scanning EMG. A potential manifestation of this is that whilst scanning EMG can reveal silent areas within the MU transect, we failed to detect any. Whilst this may be because we were studying healthy muscle in which silent areas are rarely seen, it is equally possible that they were skipped

over during our manual transects as silent areas have a mean length of only 0.16mm in healthy muscle (Stålberg and Dioszeghy, 1991). The small number of recording positions also limits the technique in adequately describing the complexity of the motor unit in terms of fractions and temporal dispersion.

We did not control for temperature during this experiment. Lower temperature has previously been shown to reduce conduction velocity (Dioszeghy and Stålberg, 1992), as well as increasing MUAP duration and reducing MUAP amplitude (Mallette *et al.*, 2018). We would therefore not recommend comparing these parameters from our recordings without controlling for temperature.

Our experience during the experiment was that there was clear stiction of the needle to the surrounding muscle tissue. This resulted in a non-linear 'limited elasticity' deformation of the surrounding tissue, pulling the surrounding muscle along with the needle for smaller movements, above which the muscle suddenly yielded and moved in relation to the needle. This phenomenon has been described in surgical robotic models with tissue phantoms (Asadian, Patel and Kermani, 2014), and presumably also occurs during scanning EMG. It may be the case that the step size that we observed is limited more by tissue stiction than by the smallest movement that a human operator (or indeed a stepper motor) can produce. Our direct imaging of the needle tip did at least allow us to compensate for this effect; hence, although our technique permits only sparse sampling of the MU transect, the precise location of those samples is known. Whether this, plus the ability to target the centre of the MU, compensates for the reduced spatial resolution in detecting clinically relevant changes in motor unit structure remains to be seen, and further studies in patients with neuromuscular disease are planned.

The use of electrical stimulation allowed us to selectively activate single motor units and avoid the need for a second SFEMG needle to act as a trigger. In some recordings step-wise jiggle in the MUP latency was observed. We suspect that this was a result of alternation in the site of action potential initiation in the fibular nerve at the low stimulation intensities that were used. Similarly, in some recordings the MUP latency was too high to have resulted from direct action potential propagation along the nerve. In these cases, we suspect that the MU was activated via an H-reflex. We feel the results remain valid in these instances since the targeted MU still fulfilled all of our criteria for being a single MU. The stimulation artefact is present on all traces. Since the latency of stimulation response was extremely low in most recordings, attempted removal of the stimulation artefact also affected the MUP, removal was not attempted.

Our aim was to develop a quick and accurate means of estimating MU dimensions and structure using readily-available clinical equipment. We achieved this in some respects, in that with minimal training we were able to obtain single MU transects in a few minutes. There was a clear learning effect, and in later experiments, we could reliably obtain recordings within 3 minutes. Our technique has the advantage over scanning EMG of targeting the centre of the MU, thereby producing a more accurate estimate of the MU dimensions, albeit at the expense of significantly reduced information as to its internal structure. In its current iteration our experimental setup remains rather complex and cumbersome, particularly the external synchronisation of the EMG recordings with the ultrasound video output. However, with the increased availability of EMG machines with integrated ultrasound capability, there is no fundamental reason why a single system incorporating all of these features could not be developed.

5.7 Supplementary File 1- needle insertion withdrawal.mp4. Video of ultrasound guided needle targeting, demonstrating the single motor unit twitch (centre of screen), insertion of needle through centre of motor unit, and stepwise withdrawal.

Available from <https://github.com/stuartbman/UltraMUSEvideos>

6. General discussion

6.1 Overview

In this thesis I have aimed to explore new methods of examining the health of the motor unit and how these can be applied to sarcopenia.

Sarcopenia is a multi-factorial disease, involving nutritional (Paddon-Jones and Rasmussen, 2009), oxidative stress (Howard *et al.*, 2007), and exercise factors (Raguso *et al.*, 2006), however even considering all of these factors does not explain all of the spectrum of disease in sarcopenia. As an example, even examining the strength of octogenarian Olympic athletes, there were still a large number with a significant reduction in strength, despite their presumed strong physical characteristics, good health and genetics to be able to compete at an Olympic level (Power *et al.*, 2016).

Understanding the neurological contributions to sarcopenia is vital in order to better characterise this disease, and current methods of examining the peripheral motor system are often inadequate.

6.2 Summary

In Chapter 2 I reviewed iMEPs and how they have been used in the literature to assess upper motor neurone disease and the balance of control between the reticulospinal/propriospinal tract and the dominant corticospinal tract. This interesting modification of the TMS methodology enables non-invasive measurement of the reticulospinal tract, and has demonstrated abnormal function in a number of neurological presentations, including mirror movements, stroke, and ALS.

Chapter 3 applied the principles of iMEPs into healthy controls of younger and older adults to measure the effect of the reticulospinal tract on strength. While the participants were largely fit and healthy, I still found a comparable number of patients with sarcopenia to what would be expected in the community. I showed an interesting relationship between the iMEP/cMEP amplitude ratio (ICAR). ICAR was negatively correlated with age & sex adjusted grip strength in the younger adults, but positively correlated in older adults. This is an interesting result from a number of standpoints. Firstly, we showed that there is not a primary correlation between ICAR and age, indicating that the reticulospinal tract does not adapt with age. This means that the origin of sarcopenia may be borne in youth, but not

revealed until a later point, possibly due to loss of corticospinal fibres (Tomlinson and Irving, 1977).

Moving to the peripheral nervous system, I next considered what neuromuscular changes might look like in age-related muscle weakness. Considering sarcopenia as at least partly a neurogenic condition, we would expect to find evidence of denervation/reinnervation, however this is not clear. This might partly be because current routine clinical methods of assessing the internal motor unit structure are slow and laborious, and have poor inter-rater variability, which makes comparison between health and disease challenging. To counter for this, we have developed Micro-EMG, a single needle multielectrode which samples from 32 channels simultaneously. This device can transect one or more motor units and, by processing the resulting multi-electrode single fibre potentials, localise muscle fibres in the space neighbouring the needle. In Chapter 4, I tested this methodology using simulated EMG data, and healthy controls. This technique reliably localised hundreds of muscle fibres across twenty or more motor units.

In the book “zero to one”, Peter Thiel describes how the future can be advanced through innovations. Compared to incremental “one to n” improvements which can improve the status quo, zero-to-one innovations revolutionise and disrupt their sector. These include improving something by an order of magnitude; the example given includes SpaceX cutting the cost of a space launch by a factor of 10, permitting new scientific and space missions which never would have previously been possible. The Micro-EMG device offers a way to reliably record from several orders of magnitude more muscle fibres, without any specialist training. With this scale of improvement, it is entirely possible that the field of neurophysiology may be changed in response to this zero-to-one innovation.

Lastly, in Chapter 5, I consider other more clinical measures of determining motor unit characteristics. To do this, we transect a single motor unit using an intramuscular EMG needle electrode, guided by ultrasound. I demonstrated the potential improvements of a guided transect to the physiologist compared to unguided transects, and how these can potentially improve the inter-rater reliability of existing measures such as scanning EMG. I performed this investigation in a number of healthy controls and demonstrated good agreement with existing motor unit dimensions. These results indicate that this is a useful modification to existing methodology, which uses well-known clinical equipment in use in many hospitals today.

6.3 Measuring performance

I aimed to better characterise the neurophysiological changes occurring during sarcopenia, both from an upper and lower motor neurone perspective. While central changes during sarcopenia have been widely described, these were beyond the scope of this investigation, and I aimed only to focus on the spinal and peripheral motor system. For the upper motor neurone investigations, I have demonstrated significant changes in iMEPs in age-related muscle weakness. Given that iMEP/cMEP ratio does not change with age, but affects strength significantly, this could potentially indicate a biomarker for sarcopenia, and a raft of other neurological diseases. This technique has been widely described in the literature, however there is significant variation in how this has been performed. I would recommend standardisation according to the parameters I have described in Chapter 1, namely related to voluntary muscle activation, focal figure-eight coil use, and standardised above-threshold stimulator activation. In this context, it will be easier to characterise what normal healthy iMEP response is, and how this changes in disease.

For peripheral motor system changes, I have produced two potentially useful methodologies. When considering neurogenic disease, clinical measures may be either non-invasive (surface EMG, ultrasound) or invasive (biopsy, intramuscular EMG). While surface EMG has been used for providing estimates of motor unit numbers, this requires specialist testing requirements, and co-operation by the patient to either entirely relax the muscle involved, or to voluntarily contract (i.e. MUNIX), as well as often needing highly standardised testing environments including skin temperature or stabilising of limbs. If performed incorrectly, the resulting value can be wildly inaccurate, significantly affecting the inter-rater reliability of the experiment. Ultrasound may be used to detect fasciculation, a key marker of motor unit disease, however this finding indicates that motor unit death is likely already occurring, putting it outside the role of predictive biomarker, and is poorly quantifiable beyond no/little/florid fasciculation. Turning to invasive measures, muscle biopsy is largely unacceptable to patients who find the procedure painful, and results require histopathological interpretation and yet do not provide an indication of motor unit number or size. Intramuscular EMG requires significant specialist training to consultant level, is still highly variable between operators, and is highly time-consuming, requiring a detailed and careful investigation. By using standardised multi-electrode EMG it is possible to obtain similar histological measures of motor unit size, muscle fibre density, without specialist training to adequately position and adjust the intramuscular needle electrode, and so I feel that Micro-EMG is a significant option for examining the motor unit in health and disease. While Micro-EMG requires specialist equipment at this time, a potential bridging solution for

more immediate clinical benefit lies in UltraMUSE, which uses existing clinical technology (Ultrasound) to provide similar (albeit at significantly less spatial resolution) insights into the internal motor unit structure and size.

One major limitation during this investigation was COVID. Landing during my second year this curtailed all in-person experiments, and even after re-opening limited the involvement of any older participants. This significantly affected my plans which would have included using the Micro-EMG device in patients with neuromuscular disease and sarcopenia. Despite this, I have been able to prove several new methodologies for investigation and apply them to healthy subjects.

6.4 Next steps

In order to support and best utilise the conclusions of this thesis, I would recommend a number of investigations considering the complimentary methodologies described.

Firstly, it is clear that UltraMUSE and Micro-EMG are highly complimentary. By combining these approaches, a single motor unit can be transected perfectly by a multi-electrode, and then the internal motor unit structure sampled. This would combine the spatial resolution of Micro-EMG with the benefits of targeting the very centre of a motor unit as described mathematically in Chapter 4. Indeed, further work is underway to target a motor unit obtained on MRI with co-registered MRI/Ultrasound, using the Micro-EMG needle.

While the data on iMEPs was suitably interesting for sarcopenia, it raises a number of clinical questions. The first and most important of these is the relationship of iMEPs to recovery. It's therefore prudent to next plan an interventional study in young and elderly, measuring the effects of strength training on iMEPs. Given that strength improvements far exceed hypertrophy of muscle (Ahtiainen *et al.*, 2003; Pearcey *et al.*, 2021), the duration of such a study need not be overly-long, but should utilise the standardised methodology as described in Chapter 1 in order to better compare results.

For Micro-EMG, further studies in patients and healthy controls are inevitable, and it will be interesting to see how the changes described could potentially be a useful biomarker. Biomarker development in neurological disease has been extremely challenging, and this has hampered the development of new therapies for neurological disease, instead relying on proxy measures which may be removed from the disease in question.

The UltraMUSE experiment requires much simplification in order for it to be used as a clinical tool. For clinical purposes, it may not be necessary for such tightly synchronised EMG activity to ultrasound capture, and this may be abandoned in favour of a simpler investigation with only needle tracking and distance measurement; both features which are available on existing ultrasound equipment. The neurophysiologist could then aim to insert the needle under weak voluntary contraction, mark the location of onset of EMG activity, and then mark the offset after transecting the motor unit region in order to produce a measure of motor unit dimension.

7. References

- Abellan Van Kan, G. *et al.* (2009) 'Gait speed at usual pace as a predictor of adverse outcomes in community-dwelling older people an International Academy on Nutrition and Aging (IANA) task force', *Journal of Nutrition, Health and Aging*, 13(10), pp. 881–889. doi:10.1007/s12603-009-0246-z.
- Adimulam, M.K. and Srinivas, M.B. (2017) 'Modeling of EXG (ECG, EMG and EEG) non-idealities using MATLAB', in *Proceedings - 2016 9th International Congress on Image and Signal Processing, BioMedical Engineering and Informatics, CISP-BMEI 2016*. Institute of Electrical and Electronics Engineers Inc., pp. 1584–1589. doi:10.1109/CISP-BMEI.2016.7852968.
- Ahtiainen, J.P. *et al.* (2003) 'Muscle hypertrophy, hormonal adaptations and strength development during strength training in strength-trained and untrained men', *European Journal of Applied Physiology*, 89(6), pp. 555–563. doi:10.1007/s00421-003-0833-3.
- Aiello, I. *et al.* (1988) 'Tonic neck reflexes on upper limb flexor tone in man.', *Experimental neurology*, 101(1), pp. 41–49. doi:10.1016/0014-4886(88)90063-5.
- Aizawa, H. *et al.* (1990) 'An output zone of the monkey primary motor cortex specialized for bilateral hand movement', *Experimental Brain Research*, 82(1), pp. 219–221. doi:10.1007/BF00230856.
- Alagona, G. *et al.* (2001) 'Ipsilateral motor responses to focal transcranial magnetic stimulation in healthy subjects and acute-stroke patients', *Stroke*, 32(6), pp. 1304–1309. doi:10.1161/01.STR.32.6.1304.
- Alexander, C. *et al.* (2007) 'Differential control of the scapulothoracic muscles in humans', *The Journal of Physiology*, 580(3), pp. 777–786. doi:10.1113/jphysiol.2006.126276.
- Alfen, N.V. *et al.* (2011) 'Detection of fibrillations using muscle ultrasound: Diagnostic accuracy and identification of pitfalls', *Muscle & Nerve*, 43(2), pp. 178–182. doi:10.1002/mus.21863.
- Anderson, T.W. and Darling, D.A. (1952) 'Asymptotic Theory of Certain "Goodness of Fit" Criteria Based on Stochastic Processes', *Ann. Math. Statist.*, 23(2), pp. 193–212. doi:10.1214/aoms/1177729437.
- Andreassen, S. and Rosenfalck, A. (1981) 'Relationship of intracellular and extracellular action potentials of skeletal muscle fibers.', *Critical reviews in bioengineering*, 6(4), pp. 267–306.
- Angotzi, G.N. *et al.* (2019) 'SiNAPS: An implantable active pixel sensor CMOS-probe for simultaneous large-scale neural recordings', *Biosensors and Bioelectronics*, 126, pp. 355–364. doi:10.1016/j.bios.2018.10.032.
- Arnold, W.D. and Clark, B.C. (2017) 'Is sarcopenia driven by motor neuron/unit loss? An unresolved question', *Muscle & Nerve*, 55(6), pp. 930–930. doi:10.1002/mus.25649.

- Asadian, A., Patel, R.V. and Kermani, M.R. (2014) 'Dynamics of translational friction in needle-tissue interaction during needle insertion', *Annals of Biomedical Engineering*, 42(1), pp. 73–85. doi:10.1007/s10439-013-0892-5.
- Awiszus, F. (2003) 'Chapter 2 TMS and threshold hunting', in Paulus, W. et al. (eds) *Transcranial Magnetic Stimulation and Transcranial Direct Current Stimulation*. Elsevier, pp. 13–23. doi:https://doi.org/10.1016/S1567-424X(09)70205-3.
- Baker, S.N. (2011) 'The primate reticulospinal tract, hand function and functional recovery', *The Journal of Physiology*, 589(23), pp. 5603–5612. doi:10.1113/jphysiol.2011.215160.
- Baker, S.N. and Lemon, R.N. (1995) 'Non-linear summation of responses in averages of rectified EMG', *Journal of Neuroscience Methods*, 59(2), pp. 175–181. doi:10.1016/0165-0270(94)00180-O.
- Baker, S.N. and Lemon, R.N. (1998) 'Computer Simulation of Post-Spike Facilitation in Spike-Triggered Averages of Rectified EMG', *Journal of Neurophysiology*, 80(3), pp. 1391–1406. doi:10.1152/jn.1998.80.3.1391.
- Barker, A.T., Jalinous, R. and Freeston, I.L. (1985) 'Non-invasive magnetic stimulation of human motor cortex', *The Lancet*. Elsevier, pp. 1106–1107. doi:10.1016/S0140-6736(85)92413-4.
- Bartels, B.M. et al. (2020) 'Experts, but not novices, exhibit StartReact indicating experts use the reticulospinal system more than novices', *Journal of Motor Behavior*, pp. 1–7. doi:10.1080/00222895.2020.1732860.
- Basu, A. and Turton, B. (1994) 'Activation of ipsilateral upper-limb muscles by transcranial magnetic stimulation in man', *CAMBRIDGE UNIV PRESS 40 ...*, p. 144.
- Bawa, P. et al. (2004) 'Bilateral responses of upper limb muscles to transcranial magnetic stimulation in human subjects', *Experimental Brain Research*, 158(3), pp. 385–390. doi:10.1007/s00221-004-2031-x.
- Beudart, C. et al. (2016) 'Sarcopenia in daily practice: assessment and management', *BMC geriatrics*, 16(1), p. 170. doi:10.1186/s12877-016-0349-4.
- Bembenek, J.P. et al. (2012) 'The prognostic value of motor-evoked potentials in motor recovery and functional outcome after stroke – a systematic review of the literature', *Functional neurology*, 27(2), pp. 79–84.
- Benecke, R., Meyer, B.-U. and Freund, H.-J. (1991) 'Reorganisation of descending motor pathways in patients after hemispherectomy and severe hemispheric lesions demonstrated by magnetic brain stimulation', *Experimental Brain Research*, 83(2), pp. 419–426. doi:10.1007/BF00231167.
- Bernard, J.A., Taylor, S.F. and Seidler, R.D. (2011) 'Handedness, dexterity, and motor cortical representations', *Journal of Neurophysiology*, 105(1), pp. 88–99. doi:10.1152/jn.00512.2010.
- Bianchi, S. (2008) 'Ultrasound of the peripheral nerves', *Joint Bone Spine*, 75(6), pp. 643–649. doi:10.1016/j.jbspin.2008.07.002.

- Birkbeck, M.G. *et al.* (2020) 'Non-invasive imaging of single human motor units', *Clinical neurophysiology: official journal of the International Federation of Clinical Neurophysiology*, 131(6), pp. 1399–1406. doi:10.1016/j.clinph.2020.02.004.
- Bodine, S.C. *et al.* (1988) 'Spatial distribution of motor unit fibers in the cat soleus and tibialis anterior muscles: local interactions', *The Journal of Neuroscience*, 8(6), pp. 2142–2152. doi:10.1523/jneurosci.08-06-02142.1988.
- Bodine-Fowler, S. *et al.* (1990) 'Spatial distribution of muscle fibers within the territory of a motor unit', *Muscle & Nerve*, 13(12), pp. 1133–1145. doi:10.1002/mus.880131208.
- Bokuda, K. *et al.* (2020) 'Relationship between EMG-detected and ultrasound-detected fasciculations in amyotrophic lateral sclerosis: A prospective cohort study', *Clinical Neurophysiology*, 131(1), pp. 259–264. doi:10.1016/j.clinph.2019.08.017.
- Boon, A.J. *et al.* (2008) 'Ultrasound-guided needle EMG of the diaphragm: Technique description and case report', *Muscle & Nerve*, 38(6), pp. 1623–1626. doi:10.1002/mus.21187.
- Boon, A.J., Smith, J. and Harper, C.M. (2012) 'Ultrasound Applications in Electrodiagnosis', *PM&R*, 4(1), pp. 37–49. doi:10.1016/j.pmrj.2011.07.004.
- Brandstater, M. and Lambert, E. (1973) 'Motor unit anatomy', in Desmedt, J. (ed.) *New Developments in EMG and Clinical Neurophysiology*. Basel: Karger, pp. 14–22.
- Britton, T.C., Meyer, B.U. and Benecke, R. (1991) 'Central motor pathways in patients with mirror movements.', *Journal of Neurology, Neurosurgery & Psychiatry*, 54(6), p. 505 LP – 510. doi:10.1136/jnnp.54.6.505.
- Buchthal, F., Erminio, F. and Rosenfalck, P. (1959) 'Motor Unit Territory in Different Human Muscles', *Acta Physiologica Scandinavica*, 45(1), pp. 72–87. doi:10.1111/j.1748-1716.1959.tb01678.x.
- Buchthal, F., Guld, C. and Rosenfalck, P. (1957) 'Multielectrode Study of the Territory of a Motor Unit', *Acta Physiologica Scandinavica*, 39(1), pp. 83–104. doi:10.1111/j.1748-1716.1957.tb01411.x.
- Buys, E.J. *et al.* (1986) 'Selective facilitation of different hand muscles by single corticospinal neurones in the conscious monkey.', *The Journal of Physiology*, 381(1), pp. 529–549. doi:10.1113/jphysiol.1986.sp016342.
- Caccia, M.R. *et al.* (1973) 'Cutaneous reflexes in small muscles of the hand', *Journal of Neurology, Neurosurgery & Psychiatry*, 36(6), pp. 960–977. doi:10.1136/jnnp.36.6.960.
- Campbell, M.J., McComas, A.J. and Petito, F. (1973) 'Physiological changes in ageing muscles.', *Journal of neurology, neurosurgery, and psychiatry*, 36(2), pp. 174–82. doi:10.1136/JNnp.36.2.174.
- Capaday, C. *et al.* (1991) 'Evidence for a contribution of the motor cortex to the long-latency stretch reflex of the human thumb.', *The Journal of Physiology*, 440(1), pp. 243–255. doi:https://doi.org/10.1113/jphysiol.1991.sp018706.

- Caramia, M.D. *et al.* (2000) 'Ipsilateral activation of the unaffected motor cortex in patients with hemiparetic stroke', *Clinical Neurophysiology*, 111(11), pp. 1990–1996. doi:[https://doi.org/10.1016/S1388-2457\(00\)00430-2](https://doi.org/10.1016/S1388-2457(00)00430-2).
- Caramia, M.D., Iani, C. and Bernardi, G. (1996) 'Cerebral plasticity after stroke as revealed by ipsilateral responses to magnetic stimulation', *Neuroreport*, 7(11), pp. 1756–1760. doi:10.1097/00001756-199607290-00012.
- Carr, L.J., Harrison, L.M. and Stephens, J.A. (1994) 'Evidence for bilateral innervation of certain homologous motoneurone pools in man.', *The Journal of Physiology*, 475(2), pp. 217–227. doi:10.1113/jphysiol.1994.sp020063.
- Carson, R.G. (2018) 'Get a grip: individual variations in grip strength are a marker of brain health', *Neurobiology of Aging*. Elsevier Inc., pp. 189–222. doi:10.1016/j.neurobiolaging.2018.07.023.
- Cesari, M. *et al.* (2009) 'Added value of physical performance measures in predicting adverse health-related events: Results from the health, aging and body composition study', *Journal of the American Geriatrics Society*, 57(2), pp. 251–259. doi:10.1111/j.1532-5415.2008.02126.x.
- Choudhury, S. *et al.* (2019) 'The Relationship Between Enhanced Reticulospinal Outflow and Upper Limb Function in Chronic Stroke Patients', *Neurorehabilitation and Neural Repair*, 33(5), pp. 375–383. doi:10.1177/1545968319836233.
- Christensen, E. (1959) 'Topography of terminal motor innervation in striated muscles from stillborn infants.', *American journal of physical medicine*, 38(2), pp. 65–78.
- Christova, M.I. *et al.* (2006) 'Motor cortex excitability during unilateral muscle activity', *Journal of Electromyography and Kinesiology*, 16(5), pp. 477–484. doi:10.1016/j.jelekin.2005.09.002.
- Chung, T. *et al.* (2018) 'Increased Single-Fiber Jitter Level Is Associated With Reduction in Motor Function With Aging', *American Journal of Physical Medicine & Rehabilitation*, 97(8), pp. 551–556. doi:10.1097/PHM.0000000000000915.
- Cincotta, M. *et al.* (1994) 'Abnormal projection of corticospinal tracts in a patient with congenital mirror movements', *Neurophysiologie Clinique/Clinical Neurophysiology*, 24(6), pp. 427–434. doi:[https://doi.org/10.1016/S0987-7053\(05\)80075-9](https://doi.org/10.1016/S0987-7053(05)80075-9).
- Cincotta, M. *et al.* (1996) 'Hand motor cortex activation in a patient with congenital mirror movements: a study of the silent period following focal transcranial magnetic stimulation', *Electroencephalography and Clinical Neurophysiology/Electromyography and Motor Control*, 101(3), pp. 240–246. doi:10.1016/0924-980X(96)95621-0.
- Cincotta, M. *et al.* (2006) 'Mechanisms underlying mirror movements in Parkinson's disease: a transcranial magnetic stimulation study', *Movement Disorders: Official Journal of the Movement Disorder Society*, 21(7), pp. 1019–1025. doi:10.1002/mds.20850.
- Clark, B.C. and Manini, T.M. (2008) 'Sarcopenia != Dynapenia', *The Journals of Gerontology Series A: Biological Sciences and Medical Sciences*, 63(8), pp. 829–834. doi:10.1093/gerona/63.8.829.

- Clark, D.J. and Fielding, R.A. (2012) 'Neuromuscular contributions to age-related weakness.', *The journals of gerontology. Series A, Biological sciences and medical sciences*, 67(1), pp. 41–7. doi:10.1093/gerona/glr041.
- Cohen, D. and Cuffin, B.N. (1991) 'Developing a More Focal Magnetic Stimulator. Part I', *Journal of Clinical Neurophysiology*, 8(1), pp. 102–111. doi:10.1097/00004691-199101000-00013.
- Cohen, L.G. *et al.* (1991) 'Congenital mirror movements: abnormal organization of motor pathways in two patients', *Brain*, 114(1), pp. 381–403. doi:10.1093/brain/114.1.381.
- Cole, T.J. (1989) 'Using the LMS method to measure skewness in the NCHS and dutch national height standards', *Annals of Human Biology*, 16(5), pp. 407–419. doi:10.1080/03014468900000532.
- Corera, Í. *et al.* (2017) 'Motor unit profile: A new way to describe the scanning-EMG potential', *Biomedical Signal Processing and Control*, 34, pp. 64–73. doi:10.1016/j.bspc.2016.12.020.
- Cracco, R.Q. *et al.* (1989) 'Comparison of human transcallosal responses evoked by magnetic coil and electrical stimulation', *Electroencephalography and Clinical Neurophysiology/Evoked Potentials Section*, 74(6), pp. 417–424. doi:10.1016/0168-5597(89)90030-0.
- Cruz-Jentoft, A.J. *et al.* (2018) 'Sarcopenia: revised European consensus on definition and diagnosis', *Age and Ageing* [Preprint]. doi:10.1093/ageing/afy169.
- Danek, A., Heye, B. and Schroedter, R. (1992) 'Cortically evoked motor responses in patients with Xp22.3-linked Kallmann's syndrome and in female gene carriers', *Annals of Neurology*, 31(3), pp. 299–304. doi:https://doi.org/10.1002/ana.410310312.
- Davidson, A.G., Schieber, M.H. and Buford, J.A. (2007) 'Bilateral spike-triggered average effects in arm and shoulder muscles from the monkey pontomedullary reticular formation', *Journal of Neuroscience*, 27(30), pp. 8053–8058. doi:10.1523/JNEUROSCI.0040-07.2007.
- Dean, L.R. and Baker, S.N. (2017) 'Fractionation of muscle activity in rapid responses to startling cues', *Journal of Neurophysiology*, 117(4), pp. 1713–1719. doi:10.1152/jn.01009.2015.
- Dieszeghy, P. and Diószeghy, P. (2002) 'Scanning electromyography', *Muscle & Nerve*, 25(S11), pp. S66–S71. doi:10.1002/mus.10150.
- Dioszeghy, P. and Stålberg, E. (1992) 'Changes in motor and sensory nerve conduction parameters with temperature in normal and diseased nerve', *Electroencephalography and Clinical Neurophysiology/Evoked Potentials Section*, 85(4), pp. 229–235. doi:10.1016/0168-5597(92)90110-W.
- Dodds, R.M. *et al.* (2014) 'Grip Strength across the Life Course: Normative Data from Twelve British Studies', *PLoS ONE*. Edited by J. Vina, 9(12), p. e113637. doi:10.1371/journal.pone.0113637.
- Dorfman, L.J. and Bosley, T.M. (1979) 'Age-related changes in peripheral and central nerve conduction in man', *Neurology*, 29(1), pp. 38–44. doi:10.1212/wnl.29.1.38.

- Drey, M. *et al.* (2013) 'The Motor Unit Number Index (MUNIX) in sarcopenic patients', *Experimental Gerontology*, 48(4), pp. 381–384. doi:10.1016/j.exger.2013.01.011.
- Drey, M. *et al.* (2014) 'Motoneuron Loss Is Associated With Sarcopenia', *Journal of the American Medical Directors Association*, 15(6), pp. 435–439. doi:10.1016/j.jamda.2014.02.002.
- Dumitru, D., King, J.C. and Nandedkar, S.D. (1997) 'Motor unit action potentials recorded with concentric electrodes: physiologic implications', *Electroencephalography and Clinical Neurophysiology/Electromyography and Motor Control*, 105(5), pp. 333–339. doi:10.1016/s0924-980x(97)00025-8.
- Edgley, S.A. *et al.* (1997) 'Comparison of activation of corticospinal neurons and spinal motor neurons by magnetic and electrical transcranial stimulation in the lumbosacral cord of the anaesthetized monkey.', *Brain*, 120(5), pp. 839–853. doi:10.1093/brain/120.5.839.
- Edstrom, L. and Kugelberg, E. (1968) 'Histochemical composition, distribution of fibres and fatiguability of single motor units. Anterior tibial muscle of the rat.', *Journal of Neurology, Neurosurgery & Psychiatry*, 31(5), pp. 424–433. doi:10.1136/jnnp.31.5.424.
- Edström, L. and Larsson, L. (1987) 'Effects of age on contractile and enzyme-histochemical properties of fast- and slow-twitch single motor units in the rat.', *The Journal of Physiology*, 392(1), pp. 129–145. doi:10.1113/jphysiol.1987.sp016773.
- Eisen, A. *et al.* (1991) 'Age-dependent decline in motor evoked potential (MEP) amplitude: with a comment on changes in Parkinson's disease', *Electroencephalography and Clinical Neurophysiology/Evoked Potentials Section*, 81(3), pp. 209–215. doi:https://doi.org/10.1016/0168-5597(91)90074-8.
- Eisen, A., Entezari-Taher, M. and Stewart, H. (1996) 'Cortical projections to spinal motoneurons: Changes with aging and amyotrophic lateral sclerosis', *Neurology*, 46(5), pp. 1396–1396. doi:10.1212/WNL.46.5.1396.
- Ekstedt, J. and Stålberg, E. (1971) 'Single fibre EMG (method and normal results).', *Electroencephalography and clinical neurophysiology*, 30(3), pp. 258–259.
- Erim, Z. *et al.* (1999) 'Effects of Aging on Motor-Unit Control Properties', *Journal of Neurophysiology*, 82(5), pp. 2081–2091. doi:10.1152/jn.1999.82.5.2081.
- Farina, D. *et al.* (2008) 'Multichannel thin-film electrode for intramuscular electromyographic recordings.', *Journal of applied physiology (Bethesda, Md. : 1985)*, 104(3), pp. 821–827. doi:10.1152/japplphysiol.00788.2007.
- Farmer, S.F., Ingram, D.A. and Stephens, J.A. (1990) 'Mirror movements studied in a patient with Klippel-Feil syndrome.', *The Journal of Physiology*, 428(1), pp. 467–484. doi:10.1113/jphysiol.1990.sp018222.
- Ferbert, A. *et al.* (1992) 'Interhemispheric inhibition of the human motor cortex.', *The Journal of Physiology*, 453(1), pp. 525–546. doi:10.1113/jphysiol.1992.sp019243.
- Fernandez-Del-Olmo, M. *et al.* (2014) 'Startle Auditory Stimuli Enhance the Performance of Fast Dynamic Contractions', *PLoS ONE*. Edited by M.S. Malmierca, 9(1), p. e87805. doi:10.1371/journal.pone.0087805.

- Fisher, C.M. (1992) 'Concerning the mechanism of recovery in stroke hemiplegia', *The Canadian Journal of Neurological Sciences. Le Journal Canadien Des Sciences Neurologiques*, 19(1), pp. 57–63.
- Fisher, K.M., Zaaimi, B. and Baker, S.N. (2012) 'Reticular formation responses to magnetic brain stimulation of primary motor cortex', *The Journal of Physiology*, 590(16), pp. 4045–4060. doi:10.1113/jphysiol.2011.226209.
- Fisher, R.A. (1921) 'On the " Probable Error" of a Coefficient of Correlation Deduced from a Small Sample.'
- Floresroux, E.M. and Stein, M.L. (1996) 'A new method of edge correction for estimating the nearest neighbor distribution', *Journal of Statistical Planning and Inference*, 50(3), pp. 353–371. doi:10.1016/0378-3758(95)00063-1.
- Fritz, S.L. *et al.* (2005) 'Active Finger Extension Predicts Outcomes After Constraint-Induced Movement Therapy for Individuals With Hemiparesis After Stroke', *Stroke*, 36(6), pp. 1172–1177. doi:10.1161/01.STR.0000165922.96430.d0.
- Garnett, R.A. *et al.* (1979) 'Motor unit organization of human medial gastrocnemius.', *The Journal of Physiology*, 287(1), pp. 33–43. doi:10.1113/jphysiol.1979.sp012643.
- Gath, I. and Stalberg, E. (1979) 'Measurements of the Uptake Area of Small-Size Electromyographic Electrodes', *IEEE Transactions on Biomedical Engineering*, BME-26(6), pp. 374–376. doi:10.1109/TBME.1979.326505.
- Gentile, L. *et al.* (2020) 'Ultrasound guidance increases diagnostic yield of needle EMG in plegic muscle', *Clinical Neurophysiology*, 131(2), pp. 446–450. doi:10.1016/j.clinph.2019.10.012.
- Gilchrist, J.M. (1992) 'Single fiber EMG reference values: A collaborative effort', *Muscle & Nerve*, 15(2), pp. 151–161. doi:10.1002/mus.880150205.
- Gilmore, K.J. *et al.* (2017) 'Motor unit number estimation and neuromuscular fidelity in 3 stages of sarcopenia', *Muscle & Nerve*, 55(5), pp. 676–684. doi:10.1002/mus.25394.
- Glover, I.S. and Baker, S.N. (2020) 'Cortical, Corticospinal, and Reticulospinal Contributions to Strength Training', *The Journal of neuroscience: the official journal of the Society for Neuroscience*, 40(30), pp. 5820–5832. doi:10.1523/JNEUROSCI.1923-19.2020.
- Goldring, S. and Ratcheson, R. (1972) 'Human Motor Cortex: Sensory Input Data from Single Neuron Recordings', *Science*, 175(4029), pp. 1493–1495. doi:10.1126/science.175.4029.1493.
- Gooch, C.L. *et al.* (2014) 'Motor unit number estimation: A technology and literature review', *Muscle & Nerve*, 50(6), pp. 884–893. doi:10.1002/mus.24442.
- Gootzen, T.H.J.M., Vingerhoets, D.J.M. and Stegeman, D.F. (1992) 'A study of motor unit structure by means of scanning EMG', *Muscle & Nerve: Official Journal of the American Association of Electrodiagnostic Medicine*, 15(3), pp. 349–357.
- Gower, J.C. (1975) 'Generalized procrustes analysis', *Psychometrika*, 40(1), pp. 33–51. doi:10.1007/BF02291478.

- Groppa, S. *et al.* (2012) 'A practical guide to diagnostic transcranial magnetic stimulation: report of an IFCN committee', *Clinical neurophysiology: official journal of the International Federation of Clinical Neurophysiology*, 2012/02/19 edn, 123(5), pp. 858–882. doi:10.1016/j.clinph.2012.01.010.
- Günther, R. *et al.* (2019) 'Motor Unit Number Index (MUNIX) of hand muscles is a disease biomarker for adult spinal muscular atrophy', *Clinical Neurophysiology*, 130(2), pp. 315–319. doi:10.1016/j.clinph.2018.11.009.
- Häkkinen, V. *et al.* (1995) 'Which structures are sensitive to painful transcranial electric stimulation?', *Electromyography and Clinical Neurophysiology*, 35(6), pp. 377–383.
- Henneman, E., Somjen, G. and Carpenter, D.O. (1965) 'Functional significance of cell size in spinal motoneurons', *Journal of neurophysiology*, 28, pp. 560–80. doi:10.1152/jn.1965.28.3.560.
- Hilton-Brown, P., Nandekar, S.D. and Stålberg, E.V. (1985) 'Simulation of fibre density in single-fibre electromyography and its relationship to macro-EMG', *Medical and Biological Engineering and Computing*, 23(6), pp. 541–546. doi:10.1007/BF02455308.
- Hilton-Brown, P. and Stålberg, E. (1983a) 'Motor unit size in muscular dystrophy, a macro EMG and scanning EMG study.', *Journal of Neurology, Neurosurgery & Psychiatry*, 46(11), pp. 996–1005.
- Hilton-Brown, P. and Stålberg, E. (1983b) 'The motor unit in muscular dystrophy, a single fibre EMG and scanning EMG study.', *Journal of Neurology, Neurosurgery & Psychiatry*, 46(11), p. 981 LP – 995. doi:10.1136/jnnp.46.11.981.
- Hömberg, V., Stephan, K.M. and Netz, J. (1991) 'Transcranial stimulation of motor cortex in upper motor neurone syndrome: its relation to the motor deficit', *Electroencephalography and Clinical Neurophysiology/Evoked Potentials Section*, 81(5), pp. 377–388. doi:https://doi.org/10.1016/0168-5597(91)90027-U.
- Honeycutt, C.F., Kharouta, M. and Perreault, E.J. (2013) 'Evidence for reticulospinal contributions to coordinated finger movements in humans', *Journal of Neurophysiology*, 110(7), pp. 1476–1483. doi:10.1152/jn.00866.2012.
- Howard, C. *et al.* (2007) 'Oxidative protein damage is associated with poor grip strength among older women living in the community', *Journal of applied physiology (Bethesda, Md. : 1985)*, 103(1), pp. 17–20. doi:10.1152/jappphysiol.00133.2007.
- Hübers, A. *et al.* (2021) 'Functional and structural impairment of transcallosal motor fibres in ALS: a study using transcranial magnetic stimulation, diffusion tensor imaging, and diffusion weighted spectroscopy', *Brain Imaging and Behavior*, 15(2), pp. 748–757. doi:10.1007/s11682-020-00282-x.
- Hughes, V.A. *et al.* (2001) 'Longitudinal Muscle Strength Changes in Older Adults: Influence of Muscle Mass, Physical Activity, and Health', *The Journals of Gerontology Series A: Biological Sciences and Medical Sciences*, 56(5), pp. B209–B217. doi:10.1093/gerona/56.5.B209.
- Hyatt, R.H. *et al.* (1990) 'Association of Muscle Strength with Functional Status of Elderly People', *Age and Ageing*, 19(5), pp. 330–336. doi:10.1093/ageing/19.5.330.

- Jacobsen, A.B. *et al.* (2017) 'Reproducibility, and sensitivity to motor unit loss in amyotrophic lateral sclerosis, of a novel MUNE method: MScanFit MUNE', *Clinical Neurophysiology*, 128(7), pp. 1380–1388. doi:10.1016/J.CLINPH.2017.03.045.
- Jankowska, E. *et al.* (2003) 'Neuronal basis of crossed actions from the reticular formation on feline hindlimb motoneurons', *Journal of Neuroscience*, 23(5), pp. 1867–1878. doi:10.1523/jneurosci.23-05-01867.2003.
- Jones, C.J., Rikli, R.E. and Beam, W.C. (1999) 'A 30-s chair-stand test as a measure of lower body strength in community-residing older adults', *Research Quarterly for Exercise and Sport*, 70(2), pp. 113–119. doi:10.1080/02701367.1999.10608028.
- Jun, J.J. *et al.* (2017) 'Fully integrated silicon probes for high-density recording of neural activity', *Nature*, 551(7679), pp. 232–236. doi:10.1038/nature24636.
- Kamper, D. g. *et al.* (2003) 'Relative contributions of neural mechanisms versus muscle mechanics in promoting finger extension deficits following stroke', *Muscle & Nerve*, 28(3), pp. 309–318. doi:10.1002/mus.10443.
- Kanouchi, T. *et al.* (1997) 'Role of the ipsilateral motor cortex in mirror movements.', *Journal of Neurology, Neurosurgery & Psychiatry*, 62(6), p. 629 LP – 632. doi:10.1136/jnnp.62.6.629.
- Kawamura, Y. *et al.* (1977) 'Lumbar Motoneurons of Man II: The Number and Diameter Distribution of Large- and Intermediate-Diameter Cytons in "Motoneuron Columns" of Spinal Cord of Man', *Journal of Neuropathology & Experimental Neurology*, 36(5), pp. 861–870. doi:10.1097/00005072-197709000-00010.
- Keizer, K. and Kuypers, H.G.J.M. (1989) 'Distribution of corticospinal neurons with collaterals to the lower brain stem reticular formation in monkey (*Macaca fascicularis*)', *Experimental Brain Research*, 74(2), pp. 311–318. doi:10.1007/BF00248864.
- Khedr, E.M. and Trakhan, M.N. (2001) 'Localization of diaphragm motor cortical representation and determination of corticodiaphragmatic latencies by using magnetic stimulation in normal adult human subjects', *European Journal of Applied Physiology*, 85(6), pp. 560–566. doi:10.1007/s004210100504.
- Kidgell, D.J. *et al.* (2010) 'Neurophysiological Responses After Short-Term Strength Training of the Biceps Brachii Muscle', *The Journal of Strength & Conditioning Research*, 24(11).
- Kidgell, D.J. *et al.* (2017) 'Corticospinal responses following strength training: a systematic review and meta-analysis', *European Journal of Neuroscience*, 46(11), pp. 2648–2661. doi:10.1111/ejn.13710.
- Kim, E.-D. *et al.* (2019) 'Ten-Year Follow-Up of Transcranial Magnetic Stimulation Study in a Patient With Congenital Mirror Movements: A Case Report', *Annals of Rehabilitation Medicine*, 43(4), pp. 524–529. doi:10.5535/arm.2019.43.4.524.
- Kim, K.M., Jang, H.C. and Lim, S. (2016) 'Differences among skeletal muscle mass indices derived from height-, weight-, and body mass index-adjusted models in assessing sarcopenia', *The Korean Journal of Internal Medicine*, 31(4), pp. 643–650. doi:10.3904/kjim.2016.015.

- Kimura, Jun. (2013) *Electrodiagnosis in diseases of nerve and muscle : principles and practice*.
- Klass, M., Baudry, S. and Duchateau, J. (2008) 'Age-related decline in rate of torque development is accompanied by lower maximal motor unit discharge frequency during fast contractions', *Journal of Applied Physiology*, 104(3), pp. 739–746. doi:10.1152/jappphysiol.00550.2007.
- Kobayashi, M. and Pascual-Leone, A. (2003) 'Transcranial magnetic stimulation in neurology', *The Lancet Neurology*, 2(3), pp. 145–156. doi:https://doi.org/10.1016/S1474-4422(03)00321-1.
- Konishi, T. *et al.* (1981) 'Myasthenia gravis: relation between jitter in single-fiber EMG and antibody to acetylcholine receptor.', *Neurology*, 31(4), pp. 386–92.
- Kouzi, I. *et al.* (2014) 'Motor unit number estimation and quantitative needle electromyography in stroke patients', *Journal of Electromyography and Kinesiology*, 24(6), pp. 910–916. doi:10.1016/j.jelekin.2014.09.006.
- Krampfl, K. *et al.* (2004) 'Mirror movements and ipsilateral motor evoked potentials in ALS', *Amyotrophic Lateral Sclerosis and Other Motor Neuron Disorders*, 5(3), pp. 154–163. doi:10.1080/14660820410019657.
- Kugelberg, E. (1973) 'Histochemical composition, contraction speed and fatiguability of rat soleus motor units', *Journal of the Neurological Sciences*, 20(2), pp. 177–198. doi:10.1016/0022-510x(73)90029-4.
- Kuppuswamy, A. *et al.* (2008) 'Cortical control of erector spinae muscles during arm abduction in humans', *Gait and Posture*, 27(3), pp. 478–484. doi:10.1016/j.gaitpost.2007.06.001.
- Kuypers, H. (1981) 'Handbook of physiology, Sec I, The nervous system, Vol II, Motor control. Part I'.
- Kwon, Y.N. and Yoon, S.S. (2017) 'Sarcopenia: Neurological Point of View.', *Journal of bone metabolism*, 24(2), pp. 83–89. doi:10.11005/jbm.2017.24.2.83.
- Lang, C.E. and Schieber, M.H. (2003) 'Differential Impairment of Individuated Finger Movements in Humans After Damage to the Motor Cortex or the Corticospinal Tract', *Journal of Neurophysiology*, 90(2), pp. 1160–1170. doi:10.1152/jn.00130.2003.
- Lang, C.E. and Schieber, M.H. (2004) 'Reduced Muscle Selectivity During Individuated Finger Movements in Humans After Damage to the Motor Cortex or Corticospinal Tract', *Journal of Neurophysiology*, 91(4), pp. 1722–1733. doi:10.1152/jn.00805.2003.
- Lawrence, D.G. and Kuypers, H.G.J.M. (1968) 'The functional organization of the motor system in the monkey1: ii. The effects of lesions of the descending brain-stem pathway', *Brain*, 91(1), pp. 15–36. doi:10.1093/brain/91.1.15.
- Ling, S.M. *et al.* (2009) 'Age-Associated Changes in Motor Unit Physiology: Observations From the Baltimore Longitudinal Study of Aging', *Archives of Physical Medicine and Rehabilitation*, 90(7), pp. 1237–1240. doi:10.1016/J.APMR.2008.09.565.

- MacKinnon, C.D., Quartarone, A. and Rothwell, J.C. (2004) 'Inter-hemispheric asymmetry of ipsilateral corticofugal projections to proximal muscles in humans', *Experimental Brain Research*, 157(2), pp. 225–233. doi:10.1007/s00221-004-1836-y.
- Maire, E. *et al.* (2000) 'Development of an ultralow-light-level luminescence image analysis system for dynamic measurements of transcriptional activity in living and migrating cells.', *Analytical biochemistry*, 280(1), pp. 118–127. doi:10.1006/abio.2000.4503.
- Maitland, S. *et al.* (2021) 'Electrical cross-sectional imaging of human motor units in vivo', *Clinical Neurophysiology (In press)* [Preprint], (In press). Available at: In press.
- Maitland, S. *et al.* (2022) 'Electrical cross-sectional imaging of human motor units in vivo', *Clinical Neurophysiology* [Preprint]. doi:10.1016/j.clinph.2021.12.022.
- Maitland, S. and Baker, S.N. (2021) 'Ipsilateral Motor Evoked Potentials as a Measure of the Reticulospinal Tract in Age-Related Strength Changes', *Frontiers in Aging Neuroscience*, 13. Available at: <https://www.frontiersin.org/article/10.3389/fnagi.2021.612352>.
- Mallette, M.M. *et al.* (2018) 'The effects of local forearm muscle cooling on motor unit properties', *European Journal of Applied Physiology*, 118(2), pp. 401–410. doi:10.1007/s00421-017-3782-y.
- Malmstrom, T.K. *et al.* (2016) 'SARC-F: a symptom score to predict persons with sarcopenia at risk for poor functional outcomes', *Journal of Cachexia, Sarcopenia and Muscle*, 7(1), pp. 28–36. doi:10.1002/jcsm.12048.
- Mathias, S., Nayak, U.S.L. and Isaacs, B. (1986) 'Balance in elderly patients: The "get-up and go" test', *Archives of Physical Medicine and Rehabilitation*, 67(6), pp. 387–389.
- Matsunaga, K. *et al.* (1998) 'Age-dependent changes in physiological threshold asymmetries for the motor evoked potential and silent period following transcranial magnetic stimulation', *Electroencephalography and Clinical Neurophysiology/Electromyography and Motor Control*, 109(6), pp. 502–507. doi:[https://doi.org/10.1016/S1388-2457\(98\)00020-0](https://doi.org/10.1016/S1388-2457(98)00020-0).
- Mayer, R.F. (1963) 'Nerve conduction studies in man', *Neurology*, 13, pp. 1021–30.
- Mayston, M. (1997) 'Mirror movements in X-linked Kallmann's syndrome. I. A neurophysiological study', *Brain*, 120(7), pp. 1199–1216. doi:10.1093/brain/120.7.1199.
- McCambridge, A.B., Stinear, J.W. and Byblow, W.D. (2016) 'Are ipsilateral motor evoked potentials subject to intracortical inhibition?', *Journal of Neurophysiology*, 115(3), pp. 1735–1739. doi:10.1152/jn.01139.2015.
- McComas, A.J. *et al.* (1971) 'Electrophysiological estimation of the number of motor units within a human muscle.', *Journal of neurology, neurosurgery, and psychiatry*, 34(2), pp. 121–31.
- McMillan, A.S. and Hannam, A.G. (1991) 'Motor-unit territory in the human masseter muscle', *Archives of Oral Biology*, 36(6), pp. 435–441. doi:10.1016/0003-9969(91)90134-G.
- Merton, P.A. and Morton, H.B. (1980) 'Stimulation of the cerebral cortex in the intact human subject', *Nature*, 285(5762), p. 227. doi:10.1038/285227a0.

- Metter, E.J. *et al.* (1998) 'The relationship of peripheral motor nerve conduction velocity to age-associated loss of grip strength', *Aging Clinical and Experimental Research*, 10(6), pp. 471–478. doi:10.1007/BF03340161.
- Metter, E.J. *et al.* (1999) 'Muscle Quality and Age: Cross-Sectional and Longitudinal Comparisons', *The Journals of Gerontology Series A: Biological Sciences and Medical Sciences*, 54(5), pp. B207–B218. doi:10.1093/gerona/54.5.B207.
- Meyer, B.U. *et al.* (1990) 'Technical approaches to hemisphere-selective transcranial magnetic brain stimulation.', *Electromyography and clinical neurophysiology*, 30(5), pp. 311–318.
- Meyer, B.U. *et al.* (1995) 'Inhibitory and excitatory interhemispheric transfers between motor cortical areas in normal humans and patients with abnormalities of the corpus callosum', *Brain*, 118(2), pp. 429–440. doi:10.1093/brain/118.2.429.
- Michel, C.M. and Brunet, D. (2019) 'EEG Source Imaging: A Practical Review of the Analysis Steps', *Frontiers in Neurology*, 10. Available at: <https://www.frontiersin.org/article/10.3389/fneur.2019.00325> (Accessed: 1 February 2022).
- Milner-Brown, H.S., Stein, R.B. and Yemm, R. (1973) 'The orderly recruitment of human motor units during voluntary isometric contractions', *The Journal of Physiology*, 230(2), pp. 359–370. doi:10.1113/jphysiol.1973.sp010192.
- Moritani, T. and DeVries, H.A. (1979) 'Neural factors versus hypertrophy in the time course of muscle strength gain', *American Journal of Physical Medicine*, 58(3), pp. 115–130.
- Morley, J.E. (2018) 'Treatment of sarcopenia: the road to the future', *Journal of Cachexia, Sarcopenia and Muscle*, 9(7), pp. 1196–1199. doi:10.1002/jcsm.12386.
- Moukas, M. *et al.* (2002) 'Muscular mass assessed by ultrasonography after administration of low-dose corticosteroids and muscle relaxants in critically ill hemiplegic patients', *Clinical Nutrition*, 21(4), pp. 297–302. doi:10.1054/clnu.2001.0532.
- Mrówczyński, W. *et al.* (2015) 'Physiological consequences of doublet discharges on motoneuronal firing and motor unit force.', *Frontiers in cellular neuroscience*, 9, p. 81. doi:10.3389/fncel.2015.00081.
- Muceli, S. *et al.* (2015) 'Accurate and representative decoding of the neural drive to muscles in humans with multi-channel intramuscular thin-film electrodes', *Journal of Physiology*, 593(17), pp. 3789–3804. doi:10.1113/JP270902.
- Muellbacher, W., Artner, C. and Mamoli, B. (1999) 'The role of the intact hemisphere in recovery of midline muscles after recent monohemispheric stroke', *Journal of Neurology*, 246(4), pp. 250–256. doi:10.1007/s004150050343.
- Müller, K., Kass-Iliyya, F. and Reitz, M. (1997) 'Ontogeny of ipsilateral corticospinal projections: A developmental study with transcranial magnetic stimulation', *Annals of Neurology*, 42(5), pp. 705–711. doi:10.1002/ana.410420506.
- Musk, E. (2019) 'An integrated brain-machine interface platform with thousands of channels', *Journal of Medical Internet Research*, 21(10), p. e16194. doi:10.2196/16194.

- Nakamichi, K.-I. and Tachibana, S. (2000) 'Enlarged median nerve in idiopathic carpal tunnel syndrome', *Muscle & Nerve*, 23(11), pp. 1713–1718. doi:10.1002/1097-4598(200011)23:11<1713::AID-MUS7>3.0.CO;2-G.
- Nandedkar, S. and Stålberg, E. (1983) 'Simulation of macro EMG motor unit potentials', *Electroencephalography and Clinical Neurophysiology*, 56(1), pp. 52–62. doi:10.1016/0013-4694(83)90006-8.
- Nandedkar, S.D. and Stålberg, E. (1983) 'Simulation of single muscle fibre action potentials.', *Medical & biological engineering & computing*, 21(2), pp. 158–65.
- Narayanaswami, P. *et al.* (2016) 'Critically re-evaluating a common technique: Accuracy, reliability, and confirmation bias of EMG.', *Neurology*, 86(3), pp. 218–223. doi:10.1212/WNL.0000000000002292.
- Nardone, R. *et al.* (2021) 'Brain functional reorganization in children with hemiplegic cerebral palsy: Assessment with TMS and therapeutic perspectives', *Neurophysiologie Clinique* [Preprint]. doi:10.1016/j.neucli.2021.09.002.
- Narici, M. V. and Maffulli, N. (2010) 'Sarcopenia: characteristics, mechanisms and functional significance', *British Medical Bulletin*, 95(1), pp. 139–159. doi:10.1093/bmb/ldq008.
- Natan (2013) *Fast 2D peak finder*, MATLAB Central File Exchange. Available at: <https://www.mathworks.com/matlabcentral/fileexchange/37388-fast-2d-peak-finder>).
- Nathan, P.W. (1994) 'Effects on movement of surgical incisions into the human spinal cord', *Brain*, 117(2), pp. 337–346. doi:10.1093/brain/117.2.337.
- Nathan, P.W., Smith, M. and Deacon, P. (1996) 'Vestibulospinal, reticulospinal and descending propriospinal nerve fibres in man', *Brain*, 119(6), pp. 1809–1833. doi:10.1093/brain/119.6.1809.
- Nathan, P.W. and Smith, M.C. (1955) 'Long descending tracts in man: i. Review of present knowledge', *Brain*, 78(2), pp. 248–303. doi:10.1093/brain/78.2.248.
- Netz, J., Lammers, T. and Hömberg, V. (1997) 'Reorganization of motor output in the non-affected hemisphere after stroke', *Brain*, 120(9), pp. 1579–1586. doi:10.1093/brain/120.9.1579.
- Nezu, A. *et al.* (1999) 'Functional recovery in hemiplegic cerebral palsy: ipsilateral electromyographic responses to focal transcranial magnetic stimulation', *Brain and Development*, 21(3), pp. 162–165. doi:10.1016/S0387-7604(98)00094-1.
- NHS England (2019) *NHS England » Frailty resources*. Available at: <https://www.england.nhs.uk/ourwork/clinical-policy/older-people/frailty/frailty-resources/> (Accessed: 29 April 2019).
- Nijssen, J., Comley, L.H. and Hedlund, E. (2017) 'Motor neuron vulnerability and resistance in amyotrophic lateral sclerosis', *Acta Neuropathologica*, 133(6), pp. 863–885. doi:10.1007/s00401-017-1708-8.
- Nordander, C. *et al.* (2003) 'Influence of the subcutaneous fat layer, as measured by ultrasound, skinfold calipers and BMI, on the EMG amplitude', *European Journal of Applied Physiology*, 89(6), pp. 514–519. doi:10.1007/s00421-003-0819-1.

- Nuzzo, J.L. *et al.* (2017) 'Effects of Four Weeks of Strength Training on the Corticomotoneuronal Pathway', *Medicine and Science in Sports and Exercise*, 49(11), pp. 2286–2296. doi:10.1249/MSS.0000000000001367.
- Paddon-Jones, D. and Rasmussen, B.B. (2009) 'Dietary protein recommendations and the prevention of sarcopenia', *Current opinion in clinical nutrition and metabolic care*, 12(1), pp. 86–90. doi:10.1097/MCO.0b013e32831cef8b.
- Padua, L. *et al.* (2007) 'Contribution of ultrasound in a neurophysiological lab in diagnosing nerve impairment: A one-year systematic assessment', *Clinical Neurophysiology*, 118(6), pp. 1410–1416. doi:10.1016/j.clinph.2007.03.011.
- Palve, S.S. and Palve, S.B. (2018) 'Impact of Aging on Nerve Conduction Velocities and Late Responses in Healthy Individuals.', *Journal of neurosciences in rural practice*, 9(1), pp. 112–116. doi:10.4103/jnrp.jnrp_323_17.
- Parashos, I.A. and Coffey, C.E. (1994) 'Anatomy of the ageing brain', *Principles and practice of geriatric psychiatry*, pp. 36–50.
- Pearcey, G.E.P. *et al.* (2021) 'Chronic resistance training: is it time to rethink the time course of neural contributions to strength gain?', *European Journal of Applied Physiology*, 121(9), pp. 2413–2422. doi:10.1007/s00421-021-04730-4.
- Peel, N.M., Kuys, S.S. and Klein, K. (2013) 'Gait speed as a measure in geriatric assessment in clinical settings: A systematic review', *Journals of Gerontology - Series A Biological Sciences and Medical Sciences*. Oxford Academic, pp. 39–46. doi:10.1093/gerona/gls174.
- Peterson, B.W. *et al.* (1975) 'Patterns of projection and branching of reticulospinal neurons', *Experimental Brain Research*, 23(4), pp. 333–351. doi:10.1007/BF00238019.
- Piasecki, M. *et al.* (2016) 'Age-dependent motor unit remodelling in human limb muscles', *Biogerontology*, 17(3), pp. 485–496. doi:10.1007/s10522-015-9627-3.
- Piasecki, M. *et al.* (2016) 'Age-related neuromuscular changes affecting human vastus lateralis', *The Journal of Physiology*, 594(16), pp. 4525–4536. doi:10.1113/JP271087.
- Piasecki, M. *et al.* (2018) 'Failure to expand the motor unit size to compensate for declining motor unit numbers distinguishes sarcopenic from non-sarcopenic older men', *The Journal of Physiology*, 596(9), pp. 1627–1637. doi:10.1113/JP275520@10.1111/(ISSN)1469-7793.ECMAY18.
- Pierrot-Deseilligny, E. (1996) 'Transmission of the cortical command for human voluntary movement through cervical propriospinal premotoneurons', *Progress in Neurobiology*, 48(4), pp. 489–517. doi:10.1016/0301-0082(96)00002-0.
- Pillen, S. *et al.* (2009) 'Muscles alive: Ultrasound detects fibrillations', *Clinical Neurophysiology*, 120(5), pp. 932–936. doi:https://doi.org/10.1016/j.clinph.2009.01.016.
- Pitcher, J.B., Ogston, K.M. and Miles, T.S. (2003) 'Age and sex differences in human motor cortex input–output characteristics', *The Journal of Physiology*, 546(2), pp. 605–613. doi:https://doi.org/10.1113/jphysiol.2002.029454.

- Podsiadlo, D. and Richardson, S. (1991) 'The timed "Up & Go": a test of basic functional mobility for frail elderly persons', *Journal of the American Geriatrics Society*, 39(2), pp. 142–148. doi:10.1111/j.1532-5415.1991.tb01616.x.
- Pompeiano, O. *et al.* (1984) 'Convergence and interaction of neck and macular vestibular inputs on reticulospinal neurons', *Neuroscience*, 12(1), pp. 111–128. doi:10.1016/0306-4522(84)90142-8.
- Power, G.A. *et al.* (2016) 'Motor unit number and transmission stability in octogenarian world class athletes: Can age-related deficits be outrun?', *Journal of applied physiology* (Bethesda, Md. : 1985), 121(4), pp. 1013–1020. doi:10.1152/jappphysiol.00149.2016.
- Pozar, D.M. (2001) 'Microwave and RF Design of Wireless Systems', in: Wiley, p. 103,104.
- Prentice, S.D. and Drew, T. (2001) 'Contributions of the Reticulospinal System to the Postural Adjustments Occurring During Voluntary Gait Modifications', *Journal of Neurophysiology*, 85(2), pp. 679–698. doi:10.1152/jn.2001.85.2.679.
- Raghavan, P. *et al.* (2006) 'Patterns of Impairment in Digit Independence After Subcortical Stroke', *Journal of Neurophysiology*, 95(1), pp. 369–378. doi:10.1152/jn.00873.2005.
- Raguso, C.A. *et al.* (2006) 'A 3-year longitudinal study on body composition changes in the elderly: role of physical exercise', *Clinical Nutrition (Edinburgh, Scotland)*, 25(4), pp. 573–580. doi:10.1016/j.clnu.2005.10.013.
- Reimers, K. *et al.* (1993) 'Skeletal muscle sonography: a correlative study of echogenicity and morphology', *Journal of Ultrasound in Medicine*, 12(2), pp. 73–77. doi:10.7863/jum.1993.12.2.73.
- Riddle, C.N. and Baker, S.N. (2005) 'Manipulation of peripheral neural feedback loops alters human corticomuscular coherence', *The Journal of physiology*. 2005/05/26 edn, 566(Pt 2), pp. 625–639. doi:10.1113/jphysiol.2005.089607.
- Riddle, C.N., Edgley, S.A. and Baker, S.N. (2009) 'Direct and indirect connections with upper limb motoneurons from the primate reticulospinal tract', *Journal of Neuroscience*, 29(15), pp. 4993–4999. doi:10.1523/JNEUROSCI.3720-08.2009.
- Rigoard, P. (2020) 'The Fibular Nerve', in Rigoard, P. (ed.) *Atlas of Anatomy of the peripheral nerves: The Nerves of the Limbs – Expert Edition*. Cham: Springer International Publishing, pp. 406–435. doi:10.1007/978-3-030-49179-6_17.
- Roeleveld, K. *et al.* (1997) 'Motor unit size estimation: confrontation of surface EMG with macro EMG', *Electroencephalography and Clinical Neurophysiology*, 105(3), pp. 181–188. doi:10.1016/s0924-980x(97)96670-4.
- Rosenfalck, P. (1969) 'Intra- and extracellular potential fields of active nerve and muscle fibres. A physico-mathematical analysis of different models.', *Acta physiologica Scandinavica. Supplementum*, 321, pp. 1–168.
- Rossi, S. *et al.* (2009) 'Safety, ethical considerations, and application guidelines for the use of transcranial magnetic stimulation in clinical practice and research.', *Clinical neurophysiology: official journal of the International Federation of Clinical Neurophysiology*, 120(12), pp. 2008–39. doi:10.1016/j.clinph.2009.08.016.

- Rossi, S., Hallett, M. and Rossini, P.M. (2011) 'Screening questionnaire before TMS: An update', *Clinical Neurophysiology*, 122, p. 1686. doi:10.1016/j.clinph.2010.12.037.
- Rouiller, E.M. *et al.* (1994) 'Transcallosal connections of the distal forelimb representations of the primary and supplementary motor cortical areas in macaque monkeys', *Experimental Brain Research*, 102(2), pp. 227–243. doi:10.1007/BF00227511.
- Rousche, P.J. *et al.* (2001) 'Flexible polyimide-based intracortical electrode arrays with bioactive capability', *IEEE Transactions on Biomedical Engineering*, 48(3), pp. 361–370. doi:10.1109/10.914800.
- Rubenstein, L.Z. (2006) 'Falls in older people: epidemiology, risk factors and strategies for prevention', *Age and Ageing*, 35(suppl_2), pp. ii37–ii41. doi:10.1093/ageing/af1084.
- Sakai, K. *et al.* (1997) 'Preferential activation of different I waves by transcranial magnetic stimulation with a figure-of-eight-shaped coil', *Experimental Brain Research*, 113(1), pp. 24–32. doi:10.1007/BF02454139.
- Sakai, S.T., Davidson, A.G. and Buford, J.A. (2009) 'Reticulospinal neurons in the pontomedullary reticular formation of the monkey (*Macaca fascicularis*)', *Neuroscience*, 163(4), pp. 1158–1170. doi:10.1016/j.neuroscience.2009.07.036.
- Sale, D.G. (1988) 'Neural adaptation to resistance training', *Medicine and Science in Sports and Exercise*, 20(5), pp. S135–S145. doi:10.1249/00005768-198810001-00009.
- Sale, M. V. and Semmler, J.G. (2005) 'Age-related differences in corticospinal control during functional isometric contractions in left and right hands', *Journal of Applied Physiology*, 99(4), pp. 1483–1493. doi:10.1152/jappphysiol.00371.2005.
- Sanders, D.B. *et al.* (2019) 'Guidelines for single fiber EMG', *Clinical Neurophysiology*. Elsevier Ireland Ltd, pp. 1417–1439. doi:10.1016/j.clinph.2019.04.005.
- Schepens, B. and Drew, T. (2004) 'Independent and convergent signals from the pontomedullary reticular formation contribute to the control of posture and movement during reaching in the cat', *Journal of Neurophysiology*, 92(4), pp. 2217–2238. doi:10.1152/jn.01189.2003.
- Schepens, B. and Drew, T. (2006) 'Descending signals from the pontomedullary reticular formation are bilateral, asymmetric, and gated during reaching movements in the cat', *Journal of Neurophysiology*, 96(5), pp. 2229–2252. doi:10.1152/jn.00342.2006.
- Schutta, H.S., Abu-Amero, K.K. and Bosley, T.M. (2010) 'Exceptions to the Valsalva doctrine', *Neurology*, 74(4), pp. 329–335. doi:10.1212/WNL.0b013e3181cbcd84.
- Schwartz, M.S. *et al.* (1976) 'The reinnervated motor unit in man: A single fibre EMG multielectrode investigation', *Journal of the Neurological Sciences*, 27(3), pp. 303–312. doi:https://doi.org/10.1016/0022-510X(76)90003-4.
- Schwerin, S. *et al.* (2008) 'Ipsilateral versus contralateral cortical motor projections to a shoulder adductor in chronic hemiparetic stroke: Implications for the expression of arm synergies', *Experimental Brain Research*, 185(3), pp. 509–519. doi:10.1007/s00221-007-1169-8.

- Sedghamiz, H. (2018) 'BioSigKit: A Matlab Toolbox and Interface for Analysis of BioSignals', *Journal of Open Source Software*, 3(30), p. 671. doi:10.21105/joss.00671.
- Sedghamiz, H. and Santonocito, D. (2015) 'Unsupervised detection and classification of motor unit action potentials in intramuscular electromyography signals', in *2015 E-Health and Bioengineering Conference (EHB)*. IEEE, pp. 1–6. doi:10.1109/EHB.2015.7391510.
- Seidler, R.D. *et al.* (2010) 'Motor control and aging: links to age-related brain structural, functional, and biochemical effects.', *Neuroscience and biobehavioral reviews*, 34(5), pp. 721–33. doi:10.1016/j.neubiorev.2009.10.005.
- Shafiee, G. *et al.* (2017) 'Prevalence of sarcopenia in the world: a systematic review and meta- analysis of general population studies', *Journal of Diabetes & Metabolic Disorders*, 16(1), p. 21. doi:10.1186/s40200-017-0302-x.
- Shefner, J.M. *et al.* (2004) 'The use of statistical MUNE in a multicenter clinical trial', *Muscle & Nerve*, 30(4), pp. 463–469. doi:10.1002/mus.20120.
- Shinoda, Y., Yokota, J.I. and Futami, T. (1981) 'Divergent projection of individual corticospinal axons to motoneurons of multiple muscles in the monkey', *Neuroscience Letters*, 23(1), pp. 7–12. doi:10.1016/0304-3940(81)90182-8.
- Škarabot, J. *et al.* (2016) 'Corticospinal and transcallosal modulation of unilateral and bilateral contractions of lower limbs', *European Journal of Applied Physiology*, 116(11–12), pp. 2197–2214. doi:10.1007/s00421-016-3475-y.
- Sohal, H.S. *et al.* (2014) 'The sinusoidal probe: a new approach to improve electrode longevity', *Frontiers in Neuroengineering*, 7. doi:10.3389/fneng.2014.00010.
- Sohal, H.S. *et al.* (2016) 'Design and Microfabrication Considerations for Reliable Flexible Intracortical Implants', *Frontiers in Mechanical Engineering*, 2, p. 27. doi:10.3389/fmech.2016.00005.
- Sohn, Y.H. *et al.* (2003) 'Excitability of the ipsilateral motor cortex during phasic voluntary hand movement.', *Experimental brain research*, 148(2), pp. 176–185. doi:10.1007/s00221-002-1292-5.
- Soteropoulos, D.S., Edgley, S.A. and Baker, S.N. (2011) 'Lack of Evidence for Direct Corticospinal Contributions to Control of the Ipsilateral Forelimb in Monkey', *Journal of Neuroscience*, 31(31), pp. 11208–11219. doi:10.1523/JNEUROSCI.0257-11.2011.
- Spagnolo, F. *et al.* (2013) 'Interhemispheric Balance in Parkinson's Disease: A Transcranial Magnetic Stimulation Study', *Brain Stimulation*, 6(6), pp. 892–897. doi:10.1016/j.brs.2013.05.004.
- Srivastava, U.C. *et al.* (1984) 'Responses of medullary reticulospinal neurons to sinusoidal rotation of neck in the decerebrate cat', *Neuroscience*, 11(2), pp. 473–486. doi:10.1016/0306-4522(84)90038-1.
- Stålberg, E. *et al.* (1976) 'The normal motor unit in man', *Journal of the Neurological Sciences*, 27(3), pp. 291–301. doi:10.1016/0022-510x(76)90002-2.

- Stålberg, E. *et al.* (1976) 'The normal motor unit in man: A single fibre EMG multielectrode investigation', *Journal of the Neurological Sciences*, 27(3), pp. 291–301. doi:10.1016/0022-510X(76)90002-2.
- Stålberg, E. (1979) 'Single fibre electromyography', *Trends in Neurosciences*, 2, pp. 185–188. doi:10.1016/0166-2236(79)90075-4.
- Stalberg, E. (1980) 'Macro EMG, a new recording technique.', *Journal of Neurology, Neurosurgery & Psychiatry*, 43(6), pp. 475–482. doi:10.1136/jnnp.43.6.475.
- Stålberg, E. *et al.* (2016) 'Reference values for jitter recorded by concentric needle electrodes in healthy controls: A multicenter study', *Muscle & Nerve*, 53(3), pp. 351–362. doi:10.1002/mus.24750.
- Stalberg, E. and Antoni, L. (1980) 'Electrophysiological cross section of the motor unit', *Journal of Neurology Neurosurgery and Psychiatry*, 43(6), pp. 469–474. doi:10.1136/jnnp.43.6.469.
- Stålberg, E. and Dioszeghy, P. (1991) 'Scanning EMG in normal muscle and in neuromuscular disorders', *Electroencephalography and Clinical Neurophysiology/Evoked Potentials Section*, 81(6), pp. 403–416. doi:https://doi.org/10.1016/0168-5597(91)90048-3.
- Stålberg, E. and Eriksson, P.-O. (1987) 'A scanning electromyographic study of the topography of human masseter single motor units', *Archives of Oral Biology*, 32(11), pp. 793–797. doi:https://doi.org/10.1016/0003-9969(87)90005-7.
- Stålberg, E. and Fawcett, P.R. (1982) 'Macro EMG in healthy subjects of different ages.', *Journal of Neurology, Neurosurgery & Psychiatry*, 45(10), pp. 870–878.
- Stalberg, E. and Stålberg, E. (1980) 'Macro EMG, a new recording technique.', *Journal of Neurology, Neurosurgery & Psychiatry*, 43(6), pp. 475–482. doi:10.1136/jnnp.43.6.475.
- Stålberg, E. and Trontelj, J. (1979) *Single fibre electromyography*. doi:10.1002/mus.880030218.
- Stålberg, E. V. and Sonoo, M. (1994) 'Assessment of variability in the shape of the motor unit action potential, the "jiggle," at consecutive discharges', *Muscle & Nerve*, 17(10), pp. 1135–1144. doi:10.1002/mus.880171003.
- Stashuk, D.W. (1993) 'Simulation of electromyographic signals', *Journal of Electromyography and Kinesiology*, 3(3), pp. 157–173. doi:10.1016/S1050-6411(05)80003-3.
- Stein, R.B. (1965) 'A Theoretical Analysis of Neuronal Variability', *Biophysical Journal*, 5(2), pp. 173–194. doi:10.1016/S0006-3495(65)86709-1.
- Stevens, J.E. *et al.* (2003) 'Are voluntary muscle activation deficits in older adults meaningful?', *Muscle & Nerve*, 27(1), pp. 99–101. doi:10.1002/mus.10279.
- Suzuki, Y.-I. *et al.* (2021) 'Effect of racial background on motor cortical function as measured by threshold tracking transcranial magnetic stimulation', *Journal of Neurophysiology*, 126(3), pp. 840–844. doi:10.1152/jn.00083.2021.

Svennerholm, L., Boström, K. and Jungbjer, B. (1997) 'Changes in weight and compositions of major membrane components of human brain during the span of adult human life of Swedes', *Acta neuropathologica*, 94(4), pp. 345–352.

Takakusaki, K. *et al.* (2016) 'Brainstem control of locomotion and muscle tone with special reference to the role of the mesopontine tegmentum and medullary reticulospinal systems', *Journal of Neural Transmission*. Springer-Verlag Wien, pp. 695–729. doi:10.1007/s00702-015-1475-4.

Tanita (2020) *Product Manuals*. Available at: <https://tanita.eu/help-guides/products-manuals/>.

Tassinari, C.A. *et al.* (2003) 'Transcranial magnetic stimulation and epilepsy', *Clinical Neurophysiology*, 114(5), pp. 777–798. doi:10.1016/S1388-2457(03)00004-X.

Taylor, P.K. (1993) 'CMAP dispersion, amplitude decay, and area decay in a normal population', *Muscle & Nerve*, 16(11), pp. 1181–1187. doi:10.1002/mus.880161107.

Tazoe, T. and Perez, M.A. (2014) 'Selective activation of ipsilateral motor pathways in intact humans', *Journal of Neuroscience*, 34(42), pp. 13924–13934. doi:10.1523/JNEUROSCI.1648-14.2014.

Terao, S. *et al.* (1994) 'Age-related changes of the myelinated fibers in the human corticospinal tract: a quantitative analysis', *Acta Neuropathologica*, 88(2), pp. 137–142. doi:10.1007/BF00294506.

Thickbroom, G.W. *et al.* (2002) 'Motor outcome after subcortical stroke: MEPs correlate with hand strength but not dexterity', *Clinical Neurophysiology*, 113(12), pp. 2025–2029. doi:10.1016/S1388-2457(02)00318-8.

Thompson, M.L., Thickbroom, G.W. and Mastaglia, F.L. (1997) 'Corticomotor representation of the sternocleidomastoid muscle.', *Brain*, 120(2), pp. 245–255. doi:10.1093/brain/120.2.245.

Tomlinson, B.E. and Irving, D. (1977) 'The numbers of limb motor neurons in the human lumbosacral cord throughout life', *Journal of the Neurological Sciences*, 34(2), pp. 213–219. doi:10.1016/0022-510X(77)90069-7.

Trompetto, C. *et al.* (2000) 'Motor recovery following stroke: a transcranial magnetic stimulation study.', *Clinical neurophysiology: official journal of the International Federation of Clinical Neurophysiology*, 111(10), pp. 1860–1867. doi:10.1016/s1388-2457(00)00419-3.

Turton, A. *et al.* (1995) 'Ipsilateral EMG responses to transcranial magnetic stimulation during recovery of arm and hand function after stroke', *Electroencephalography and Clinical Neurophysiology/ Electromyography and Motor Control*, 97(4), p. S192.

Turton, A. *et al.* (1996) 'Contralateral and ipsilateral EMG responses to transcranial magnetic stimulation during recovery of arm and hand function after stroke', *Electroencephalography and Clinical Neurophysiology/Electromyography and Motor Control*, 101(4), pp. 316–328. doi:https://doi.org/10.1016/0924-980X(96)95560-5.

UK Screening Committee (2003) *Criteria for appraising the viability, effectiveness and appropriateness of a screening programme - GOV.UK*. Available at: <https://www.gov.uk/government/publications/evidence-review-criteria-national-screening->

programmes/criteria-for-appraising-the-viability-effectiveness-and-appropriateness-of-a-screening-programme (Accessed: 29 April 2019).

Vetter, R.J. *et al.* (2004) 'Chronic neural recording using silicon-substrate microelectrode arrays implanted in cerebral cortex', *IEEE Transactions on Biomedical Engineering*, 51(6), pp. 896–904. doi:10.1109/TBME.2004.826680.

Walker (1996) 'Normal neuromuscular sonography', *Neurosonology*, pp. 397–405.

Walker, F.O. *et al.* (2004) 'Ultrasound of nerve and muscle', *Clinical Neurophysiology*, 115(3), pp. 495–507. doi:10.1016/j.clinph.2003.10.022.

Wassermann, E.M. *et al.* (1991) 'Effects of transcranial magnetic stimulation on ipsilateral muscles', *Neurology*, 41(11), pp. 1795–1799. doi:10.1212/wnl.41.11.1795.

Wassermann, E.M. *et al.* (1992) 'Noninvasive mapping of muscle representations in human motor cortex', *Electroencephalography and Clinical Neurophysiology/ Evoked Potentials*, 85(1), pp. 1–8. doi:10.1016/0168-5597(92)90094-R.

Wassermann, E.M. (2002) 'Variation in the response to transcranial magnetic brain stimulation in the general population', *Clinical Neurophysiology*, 113(7), pp. 1165–1171. doi:https://doi.org/10.1016/S1388-2457(02)00144-X.

Wassermann, E.M., Pascual-Leone, A. and Hallett, M. (1994) 'Cortical motor representation of the ipsilateral hand and arm', *Experimental Brain Research*, 100(1), pp. 121–132. doi:10.1007/BF00227284.

Werhahn, K.J. *et al.* (1994) 'The effect of magnetic coil orientation on the latency of surface EMG and single motor unit responses in the first dorsal interosseous muscle', *Electroencephalography and Clinical Neurophysiology/ Evoked Potentials*, 93(2), pp. 138–146. doi:10.1016/0168-5597(94)90077-9.

Whittaker, R.G. (2012) 'The fundamentals of electromyography', *Practical Neurology*, 12(3), pp. 187–194. doi:10.1136/practneurol-2011-000198.

Wiesendanger, M. (1981) 'The Pyramidal Tract', in Towe, A.L. and Luschei, E.S. (eds) *Motor Coordination*. Boston, MA: Springer US, pp. 401–491. doi:10.1007/978-1-4684-3884-0_8.

Willadt, S., Nash, M. and Slater, C. (2018) 'Age-related changes in the structure and function of mammalian neuromuscular junctions', *Annals of the New York Academy of Sciences*, 1412(1), pp. 41–53. doi:10.1111/nyas.13521.

Willadt, S., Nash, M. and Slater, C.R. (2016) 'Age-related fragmentation of the motor endplate is not associated with impaired neuromuscular transmission in the mouse diaphragm.', *Scientific reports*, 6, p. 24849. doi:10.1038/srep24849.

Willison, R.G. *et al.* (1980) 'Arrangement of muscle fibers of a single motor unit in mammalian muscles', *Muscle & Nerve*. Muscle Nerve, pp. 360–362. doi:10.1002/mus.880030414.

Wilson, V.J. and Peterson, B.W. (1981) 'Vestibulospinal and Reticulospinal Systems', in *Handbook of Physiology, vol. 2, The Nervous System*. The American Physiological Society, Bethesda, pp. 667–702. doi:10.1002/cphy.cp010214.

Wittstock, M. *et al.* (2020) 'Mirror Movements in Amyotrophic Lateral Sclerosis: A Combined Study Using Diffusion Tensor Imaging and Transcranial Magnetic Stimulation', *Frontiers in Neurology*, 11, p. 164. doi:10.3389/fneur.2020.00164.

Wittstock, M., Wolters, A. and Benecke, R. (2007) 'Transcallosal inhibition in amyotrophic lateral sclerosis', *Clinical Neurophysiology*, 118(2), pp. 301–307. doi:10.1016/j.clinph.2006.09.026.

Yuen, E.C. and Olney, R.K. (1997) 'Longitudinal study of fiber density and motor unit number estimate in patients with amyotrophic lateral sclerosis', *Neurology*, 49(2), p. 573 LP – 578. doi:10.1212/WNL.49.2.573.

Zaaimi, B. *et al.* (2012) 'Changes in descending motor pathway connectivity after corticospinal tract lesion in macaque monkey', *Brain*, 135(7), pp. 2277–2289. doi:10.1093/brain/aws115.

Zaaimi, B., Dean, L.R. and Baker, S.N. (2018) 'Different contributions of primary motor cortex, reticular formation, and spinal cord to fractionated muscle activation', *Journal of Neurophysiology*, 119(1), pp. 235–250. doi:10.1152/jn.00672.2017.

Zewdie, E. *et al.* (2017) 'Contralesional Corticomotor Neurophysiology in Hemiparetic Children With Perinatal Stroke: Developmental Plasticity and Clinical Function', *Neurorehabilitation and Neural Repair*, 31(3), pp. 261–271. doi:10.1177/1545968316680485.

Ziemann, U. *et al.* (1999) 'Dissociation of the pathways mediating ipsilateral and contralateral motor-evoked potentials in human hand and arm muscles', *The Journal of Physiology*, 518(3), pp. 895–906. doi:10.1111/j.1469-7793.1999.0895p.x.